AD_____

Award Number: DAMD17-00-1-0345

TITLE: Genetic Determinants of Inflammatory Breast Cancer

PRINCIPAL INVESTIGATOR: Sofia D. Merajver, M.D., Ph.D.

CONTRACTING ORGANIZATION: University of Michigan
Ann Arbor, Michigan 48109-1274

REPORT DATE: July 2004

TYPE OF REPORT: Final

PREPARED FOR: U.S. Army Medical Research and Materiel Command
Fort Detrick, Maryland 21702-5012

DISTRIBUTION STATEMENT: Approved for Public Release;
Distribution Unlimited

The views, opinions and/or findings contained in this report are those of the author(s) and should not be construed as an official Department of the Army position, policy or decision unless so designated by other documentation.

REPORT DOCUMENTATION PAGE

Form Approved
OMB No. 074-0188

1. AGENCY USE ONLY (Leave blank)	2. REPORT DATE	3. REPORT TYPE AND DATES COVERED
	July 2004	Final (15 Jun 00 - 14 Jun 04)

4. TITLE AND SUBTITLE
Genetic Determinants of Inflammatory Breast Cancer

5. FUNDING NUMBERS
DAMD17-00-1-0345

6. AUTHOR(S)
Sofia D. Merajver, M.D., Ph.D.

7. PERFORMING ORGANIZATION NAME(S) AND ADDRESS(ES)
University of Michigan
Ann Arbor, Michigan 48109-1274

E-Mail: qpan@med.umich.edu

8. PERFORMING ORGANIZATION REPORT NUMBER

9. SPONSORING / MONITORING AGENCY NAME(S) AND ADDRESS(ES)
U.S. Army Medical Research and Materiel Command
Fort Detrick, Maryland 21702-5012

10. SPONSORING / MONITORING AGENCY REPORT NUMBER

11. SUPPLEMENTARY NOTES

12a. DISTRIBUTION / AVAILABILITY STATEMENT
Approved for Public Release; Distribution Unlimited

12b. DISTRIBUTION CODE

13. ABSTRACT (Maximum 200 Words)

Primary inflammatory breast cancer (IBC) accounts for approximately 6% of new breast cancers annually. We hypothesized that a limited number of concordant genetic alterations give rise to the unique aggressive inflammatory phenotype of IBC. While working on the genetic determinants underlying the IBC phenotype, we found concordant and consistent alterations of two genes, RhoC GTPase and a novel IGF-binding protein (IGF-BP), in patients with IBC. RhoC was overexpressed in 90% of IBC samples examined compared to 30% of stage matched non-IBC tumors. LIBC was lost in 80% of the IBC samples and only 20% of non-IBC samples examined. Since RhoC and LIBC appear to act in concert in IBC, coupled to the preliminary evidence from other laboratories of genes from these families playing a role in pancreatic cancer (another highly aggressive adenocarcinoma), they are excellent candidate genes to begin to probe the genetic basis of the aggressive phenotype in IBC. We hypothesize that the phenotype of IBC is due to alterations in expression of RhoC and IGF-BP early in tumorigenesis. We will elucidate the signaling pathway downstream from RhoC GTPase and attempt to determine what effect RhoC and LIBC have on cellular motility and invasion.

14. SUBJECT TERMS
Motility, invasion, aggressive phenotype

15. NUMBER OF PAGES
58

16. PRICE CODE

17. SECURITY CLASSIFICATION OF REPORT	18. SECURITY CLASSIFICATION OF THIS PAGE	19. SECURITY CLASSIFICATION OF ABSTRACT	20. LIMITATION OF ABSTRACT
Unclassified	Unclassified	Unclassified	Unlimited

Table of Contents

Sofia D. Merajver, M.D., Ph.D.
Final Report for Award DAMD 17-00-1-0345

Introduction:

Inflammatory breast cancer (IBC) is the most lethal form of locally advanced breast cancer and accounts for approximately 6% of new breast cancer cases annually in the United States (1, 2). IBC has distinct clinical and pathological features. Patients present with erythema, skin nodules, dimpling of the skin (termed "peau d'orange"), all features that develop rapidly, typically progressing within 6 months (1-4). One salient feature of IBC that is observed in tissue sections is that cancer cells form emboli that spread through the dermal lymphatics. The dermatotropism of IBC is believed to be responsible for the clinical signs and symptoms and probably enables effective dissemination to distant sites (2). These observations lead us to conclude that IBC is highly invasive and it is capable of metastases from its inception. Indeed, at the time of diagnosis, the majority of patients have locoregional and/or distant metastatic disease (3, 4). In spite of new advances in breast cancer therapy including multimodality approaches, the 5-year disease-free survival rate is less than 45% (3, 4).

Until recently, no biologic markers defined the IBC phenotype. We hypothesized that a limited number of genetic alterations, occurring in rapid succession or concordantly, are responsible for the rapidly progressive and distinct clinical and pathologic features of IBC. Using a modified version of the differential display technique and *in situ* hybridization of human tumors, we identified two genes that are consistently and concordantly altered in human IBC when compared to stage-matched, non-IBC tumors: loss of WISP3 and over-expression of RhoC-GTPase (5).

WISP3 is member of the CCN family of proteins, which have important biological functions in normal physiology as well as in carcinogenesis (6-8). We found that WISP3 has growth and angiogenesis inhibitory functions in IBC *in vitro* and *in vivo* (9). RhoC-GTPase is a member of the Ras-superfamily of small guanosine triphosphatases (GTPases). Activation of Rho proteins leads to assembly of the actin-myosin contractile filaments into focal adhesion complexes that lead to cell polarity and facilitate motility (10-12). Our laboratory has characterized RhoC as a transforming oncogene for human mammary epithelial cells, whose overexpression results in a highly motile and invasive phenotype that recapitulates the IBC phenotype. Predicated on the high rate of concordance of RhoC and WISP3 changes in IBC, we hypothesize that these two genes cooperate to determine this highly metastatic, unique breast cancer phenotype.

This is an annual progress report for a project that aims at understanding the genetic determinants of inflammatory breast cancer (IBC). In particular, we aim to discern the relative role of the RhoC GTPase gene and WISP3 (formally named LIBC) in the specific phenotypic characteristics of inflammatory breast cancer. We have made progress in the last year, which is summarized below.

Body:

Task 1: To identify the signaling pathways involved in growth control affected by RhoC overexpression or mutation in inflammatory breast cancer.

Inflammatory breast cancer (IBC) is a distinct and aggressive form of locally advanced breast cancer. IBC is highly angiogenic, invasive, and metastatic at its inception. Previously, we identified specific genetic alterations of IBC that contribute to this highly invasive phenotype. RhoC GTPase was overexpressed in 90% of archival IBC tumor samples, but not in stage-matched, non-IBC tumors.

To study the role of RhoC GTPase in contributing to an IBC-like phenotype, we generated stable transfectants of human mammary epithelial cells overexpressing the RhoC gene. The HME-RhoC transfectants formed large colonies under anchorage-independent growth conditions, were more motile, and were invasive (**Appendix #1, Figures 2-4**). In conjunction with an increase in motility, overexpression of RhoC led to an increase in actin stress fiber and focal adhesion contact formation (**Appendix #1, Figure 5**). Levels of vascular endothelial growth factor (VEGF), basic fibroblast growth factor (bFGF), interleukin-6 (IL-6), and interleukin-8 (IL-8) were significantly higher in the conditioned media of the HME-RhoC transfectants than in the untransfected HME and HME-beta-galactosidase control media or the SUM149 IBC cell line (**Appendix #2, Figure 1**). Inhibition of RhoC function by introduction of C3 exotransferase decreased production of angiogenic factors by the HME-RhoC transfectants and the SUM149 IBC cell line, but did not affect the control cells (**Appendix #2, Figure 3**). Furthermore, orthotopic injection into immunocompromised mice led to tumor formation (**Appendix #1, Table 1**). These data indicate that RhoC GTPase is a transforming oncogene in human mammary epithelial cells and can lead to a highly angiogenic and invasive phenotype, akin to that seen in IBC.

To delineate the signaling pathways responsible for each aspect of the IBC phenotype, we used well-established inhibitors to the mitogen activated protein kinase (MAPK) and phosphatidylinositol-3 kinase (PI3K) pathways. We found that activation of the MAPK pathway was responsible for motility, invasion and production of angiogenic factors (**Appendix #3, Figures 2-5**). In contrast, growth under anchorage independent conditions was dependent on the PI3K pathway (**Appendix #3, Figures 2-5**). Farnesyl transferase inhibitors (FTIs) were previously shown to be effective in modulating tumor growth in Ras-transformed tumor cells. Recently, studies have focused on RhoB as a putative non-Ras target of FTI action. We assessed the effect of the FTI L-744,832 on RhoC-overexpressing IBC and RhoC-transfected human mammary epithelial (HME-RhoC) cells. Treatment of the SUM149 IBC cell line and HME-RhoC transfectants with the FTI L-744,832 led to reversion of the RhoC-induced phenotype, manifested by a significant decrease in anchorage-independent growth, motility, and invasion (**Appendix #4, Figures 1-4**). Although RhoC expression and activation were not affected, RhoB levels were increased by FTI treatment (**Appendix #4, Figure 3 and Table 1**). Transient transfection of geranylgeranylated RhoB (RhoB-GG) into the same cells reproduced the

effects of the FTI, thus suggesting that FTI-induced reversion of the RhoC phenotype may be mediated by an increase in RhoB-GG levels.

Task 2: To explore the role of RhoC and IGF-binding proteins in IGF-induced motility and invasion.

To begin to address the experimental questions in Task 2, we had to develop cell lines that have high RhoC expression and low LIBC (WISP3) expression. We decided to use immortalized mammary epithelial cells (HME) as our model cell line. Using an antisense approach, inhibition of WISP3 expression in HME cells resulted in a 3-fold increase in RhoC GTPase transcript levels (**Appendix #5, Figure 1**). The HME/high RhoC-low WISP3 cells exhibited increased cellular proliferation and anchorage independent growth in soft agar (**Appendix #5, Figure 2**). These high RhoC-low WISP3 clones produced significantly more colonies in soft agar when compared with the control cells, an average of 58% of the level of colonies formed by the SUM149 IBC cells. Moreover, these HME/high RhoC-low WISP3 cells also exhibited decreased production of VEGF in the conditioned medium (**Appendix #5, Figure 2**). These results revealed that WISP3 modulates RhoC expression in HME cells and in the IBC cell line SUM149, and provide further evidence in support that these two genes act in concert to give rise to the highly aggressive IBC phenotype.

We also investigate the relationship of WISP3 to the IGF signaling cascade. WISP3 was found to be secreted into the conditioned media and into the lumens of normal breast ducts (**Appendix #6, Figure 2**). Once secreted, WISP3 was able to decrease, directly or through induction of other molecule(s), the IGF-1-induced activation of the IGF-IR, and two of its main downstream signaling molecules, IRS1 and ERK-1/2, in SUM149 IBC cells (**Appendix #6, Figures 3-5**). Furthermore, WISP3 containing conditioned media decreased the growth rate of SUM149 cells (**Appendix #6, Figure 6**). This work sheds light into the mechanism of WISP3 function by demonstrating that it is secreted and that, once in the extracellular media, it induces a series of molecular events that leads to modulation of IGF-IR signaling pathways and cellular growth in IBC cells.

Key Research Accomplishments:

1. RhoC GTPase is a transforming oncogene in human mammary epithelial cells and can lead to a highly angiogenic and invasive cell phenotype.
2. MAPK signaling pathway is responsible for RhoC-mediated cell motility, invasion and production of angiogenic factors.
3. PI3K signaling pathway is responsible for RhoC-mediated anchorage independent colony formation.
4. FTI treatment leads to reversion of the RhoC-induced phenotype, manifested by a significant decrease in anchorage-independent growth, motility, and invasion

5. WISP3 was found to directly modulate RhoC GTPase expression in immortalized mammary epithelial cells.
6. Immortalized mammary epithelial cells with low WISP3 and high RhoC GTPase displayed neoplastic characteristics, specifically, an increase in cell proliferation, an increase in anchorage independent growth, and an increase in VEGF production.

Reportable Outcomes:

Publications

1. van Golen KL, Wu ZF, Qiao XT, Bao LW, and Merajver SD. RhoC GTPase, a novel transforming oncogene for human mammary epithelial cells that partially recapitulates the inflammatory breast cancer phenotype. Cancer Res., 60:5832-5838, 2000. **(Appendix 1)**
2. van Golen KL, Wu ZF, Qiao XT, Bao LW, and Merajver SD. RhoC GTPase overexpression modulates induction of angiogenic factors in breast cells. Neoplasia, 2:418-425, 2000. **(Appendix 2)**
3. van Golen KL, Bao LW, Pan Q, Miller FR, Wu ZF, and Merajver SD. Mitogen activated protein kinase pathway is involved in RhoC GTPase induced motility, invasion, and angiogenesis in inflammatory breast cancer. Clin. Exp. Metastasis, 19:301-311, 2002. **(Appendix 3)**
4. van Golen KL, Bao LW, DiVito MM, Wu ZF, Prendergast GC, and Merajver SD. Reversion of RhoC GTPase-induced inflammatory breast cancer phenotype by treatment with a farnesyl transferase inhibitor. Mol. Cancer Ther., 8:575-583, 2002. **(Appendix 4)**
5. Kleer CG, Zhang Y, Pan Q, Gallagher G, Wu M, Wu ZF, and Merajver SD. WISP3 and RhoC GTPase cooperate in the development of inflammatory breast cancer. Breast Cancer Res., 6:R110-115, 2004. **(Appendix 5)**
6. Kleer CG, Zhang Y, Pan Q, and Merajver SD. WISP3 is a secreted tumor suppressor protein that modulates IGF signaling in inflammatory breast cancer. Neoplasia, 6:179-185, 2004. **(Appendix 6)**

List of Personnel Supported From this Research Grant

1. Sofia D. Merajver, MD, PhD
2. Mei Wu, PhD

3. Zhi-Fen Wu, M.D.
4. Li-Wei Bao, M.D.
5. Robyn Hodges

Conclusions:

Inflammatory breast cancer (IBC) is the most lethal form of locally advanced breast cancer, with a 5-year disease free survival of less than 45%. Our work focused on determining the genetic alterations that result in this aggressive breast cancer phenotype. Our data indicate that RhoC GTPase is a transforming oncogene in human mammary epithelial cells and can lead to a highly angiogenic and invasive phenotype, akin to that seen in IBC. Moreover, our results reveal that WISP3 modulates RhoC expression in HME cells and in the IBC cell line SUM149, and provide further evidence in support that these two genes act in concert to give rise to the highly aggressive IBC phenotype.

References:

1. Jaiyesimi, I. A., Buzdar, A. U., and Hortobagyi, G. Inflammatory breast cancer: a review. J Clin Oncol, *10:* 1014-1024., 1992.
2. Lee, B. J. a. T., N.D. Inflammatory carcinoma of the breast: a report of twenty-eight cases from the breast clinic of Memorial Hospital. Surg Gynecol Obstet, *39:* 580-595, 1924.
3. Merajver, S. D., Weber, B. L., Cody, R., Zhang, D., Strawderman, M., Calzone, K. A., LeClaire, V., Levin, A., Irani, J., Halvie, M., August, D., Wicha, M., Lichter, A., and Pierce, L. J. Breast conservation and prolonged chemotherapy for locally advanced breast cancer: the University of Michigan experience. J Clin Oncol, *15:* 2873-2881., 1997.
4. Swain, S. M., Sorace, R. A., Bagley, C. S., Danforth, D. N., Jr., Bader, J., Wesley, M. N., Steinberg, S. M., and Lippman, M. E. Neoadjuvant chemotherapy in the combined modality approach of locally advanced nonmetastatic breast cancer. Cancer Res, *47:* 3889-3894., 1987.
5. van Golen, K. L., Davies, S., Wu, Z. F., Wang, Y., Bucana, C. D., Root, H., Chandrasekharappa, S., Strawderman, M., Ethier, S. P., and Merajver, S. D. A novel putative low-affinity insulin-like growth factor-binding protein, LIBC (lost in inflammatory breast cancer), and RhoC GTPase correlate with the inflammatory breast cancer phenotype. Clin Cancer Res, *5:* 2511-2519., 1999.
6. Perbal, B. NOV (nephroblastoma overexpressed) and the CCN family of genes: structural and functional issues. Mol Pathol, *54:* 57-79., 2001.
7. Pennica, D., Swanson, T. A., Welsh, J. W., Roy, M. A., Lawrence, D. A., Lee, J., Brush, J., Taneyhill, L. A., Deuel, B., Lew, M., Watanabe, C., Cohen, R. L., Melhem, M. F., Finley, G. G., Quirke, P., Goddard, A. D., Hillan, K. J., Gurney, A. L., Botstein, D., and Levine, A. J. WISP genes are members of the connective tissue growth factor family that are up-regulated in wnt-1-transformed cells and aberrantly expressed in human colon tumors. Proc Natl Acad Sci U S A, *95:* 14717-14722., 1998.
8. Hurvitz, J. R., Suwairi, W. M., Van Hul, W., El-Shanti, H., Superti-Furga, A., Roudier, J., Holderbaum, D., Pauli, R. M., Herd, J. K., Van Hul, E. V., Rezai-Delui, H., Legius, E., Le Merrer, M., Al-Alami, J., Bahabri, S. A., and Warman, M. L. Mutations in the CCN gene family member WISP3 cause progressive pseudorheumatoid dysplasia. Nat Genet, *23:* 94-98., 1999.
9. Kleer, C. G., Zhang, Y., Pan, Q., van Golen, K. L., Wu, Z. F., Livant, D., and Merajver, S. D. WISP3 is a novel tumor suppressor gene of inflammatory breast cancer. Oncogene, *21:* 3172-3180, 2002.
10. Kimura, K., Ito, M., Amano, M., Chihara, K., Fukata, Y., Nakafuku, M., Yamamori, B., Feng, J., Nakano, T., Okawa, K., Iwamatsu, A., and Kaibuchi, K. Regulation of myosin phosphatase by Rho and Rho-associated kinase (Rho-kinase). Science, *273:* 245-248, 1996.
11. Leung, T., Chen, X. Q., Manser, E., and Lim, L. The p160 RhoA-binding kinase ROK alpha is a member of a kinase family and is involved in the reorganization of the cytoskeleton. Mol Cell Biol, *16:* 5313-5327, 1996.

12. Nobes, C. D. and Hall, A. Rho, rac, and cdc42 GTPases regulate the assembly of multimolecular focal complexes associated with actin stress fibers, lamellipodia, and filopodia. Cell, *81:* 53-62, 1995.

[CANCER RESEARCH 60, 5832–5838, October 15, 2000]

RhoC GTPase, a Novel Transforming Oncogene for Human Mammary Epithelial Cells That Partially Recapitulates the Inflammatory Breast Cancer Phenotype[1]

Kenneth L. van Golen, Zhi-Fen Wu, Xiao Tan Qiao, Li Wei Bao, and Sofia D. Merajver[2]

Department of Internal Medicine, Division of Hematology and Oncology and Comprehensive Cancer Center, University of Michigan, Ann Arbor, Michigan 48109

ABSTRACT

Inflammatory breast cancer (IBC) is the most aggressive form of breast cancer and is phenotypically distinct from other forms of locally advanced breast cancer. In a previous study, we identified specific genetic alterations of IBC that could account for a highly invasive phenotype. RhoC GTPase was overexpressed in 90% of IBC archival tumor samples, but not in stage-matched, non-IBC tumors. To study the role of RhoC GTPase in contributing to an IBC-like phenotype, we generated stable transfectants of human mammary epithelial cells overexpressing the RhoC gene. The HME-RhoC transfectants formed large colonies under anchorage-independent growth conditions, were more motile, and were invasive. In conjunction with an increase in motility, overexpression of RhoC led to an increase in actin stress fiber and focal adhesion contact formation. Furthermore, orthotopic injection into immunocompromised mice led to tumor formation. Taken together, these data indicate that RhoC GTPase is a transforming oncogene in human mammary epithelial cells and can lead to a highly invasive phenotype, akin to that seen in IBC.

INTRODUCTION

Primary IBC[3] accounts for approximately 6% of new breast cancer cases annually in the United States (1). IBC is clinically well characterized by skin changes such as erythema, skin nodules, peau d'aurange, and nipple retraction (2, 3). IBC is also distinguished by a very rapid onset of characteristics of locally advanced breast cancer, typically within 6 months. Almost all tumors have lymph node metastases at the time of diagnosis, and approximately 36% have gross distant metastasis (2, 3). This number greatly increases 1 year after diagnosis, presumably due to the presence of occult metastases, suggesting that IBC cells acquire metastatic capabilities early in tumor formation. Not surprisingly, even with multimodality treatment, the 5-year disease-free survival is less than 45%, thus making IBC the most deadly form of locally advanced breast cancer (3).

Until recently, relatively little was known about the genetic mechanisms underlying the development and progression of IBC. In a previous study, our laboratory identified genes that strongly correlated with the aggressive and invasive IBC phenotype (4). In this study, we describe the potential role of one of those genes, RhoC GTPase, in modulating the invasive IBC phenotype.

RhoC GTPase is a member of the Ras superfamily of small GTPases. Activation of Rho proteins by soluble factors, such as serum or growth factors, leads to the assembly of actin-myosin contractile filaments and focal adhesion complexes (5, 6). "Cross-talk" interactions between the various members of the Ras superfamily lead to the dynamic reorganization of the cell cytoskeleton, resulting in polarity, the formation of lamellipodia, and adhesion during directed motility (7).

We hypothesized that, given these known functions of the Rho proteins, RhoC GTPase would confer to mammary epithelial cells specific features of enhanced invasiveness and tumorigenic potential. To test this hypothesis, we set out to determine whether overexpression of RhoC GTPase could alter the phenotype of nontransformed, immortalized HME cells. We generated stable HME-RhoC transfectants and tested them for any alterations in their phenotype. In contrast with either untransfected or HME-β-gal control, the HME-RhoC cells were able to form colonies under anchorage-independent growth conditions. Furthermore, these cells were highly invasive in a Matrigel invasion assay, exhibited enhanced motility in a random motility assay, and were tumorigenic in nude mice. These characteristics of the RhoC transfectants strikingly resemble *in vivo* behavior of IBC.

MATERIALS AND METHODS

Cell Lines. As described previously, cell lines were maintained under defined culture conditions for optimal growth in each case (8–10). Briefly, HME cells were immortalized with human papilloma virus E6/E7 (11) and grown in 5% FBS (Sigma Chemical Co., St. Louis, MO)-supplemented Ham's F-12 medium (JRH BioSciences, Lenexa, KS) containing insulin, hydrocortisone, epidermal growth factor, and cholera toxin (Sigma Chemical Co.). The SUM149 cell line was developed from a primary IBC tumor and grown in 5% FBS-supplemented Ham's F-12 medium containing insulin and hydrocortisone. The HME cells were characterized as being keratin 19 positive, ensuring that they are from the same differentiation lineage as the SUM149 IBC tumor cell line.

Transfection Experiments. Low passage (passage 10) immortalized HME cells were cotransfected with the PTP-2000-hygro vector and either pFLAG-RhoC GTPase, pFLAG-β-gal, or pFLAG-CMV-4 (Sigma Chemical Co.) alone using FuGene 6 transfection reagent (Roche-Boehringer Mannheim, Mannheim, Germany). Transfection efficiency was 22–85% as determined by β-gal staining of the pFLAG-β-gal-transfected cells using X-Gal reagent [1 mg/ml X-Gal, 4 mM potassium ferricyanide, 4 mM potassium ferrocyanide, 2 mM magnesium chloride-hexahydrate in PBS (pH 7.4); Life Technologies, Inc., Gaithersburg, MD] and 2% formaldehyde and 0.2% glutaraldehyde in cation-free PBS [(pH 7.4), Sigma Chemical Co.] for 16 h at 37°C. Stable transfectants were established by culturing the cells in the described medium supplemented with 100 μg/ml hygromycin (Life Technologies, Inc.) for 14–20 days. Expression of the transgene was determined by RT-PCR and immunoprecipitation followed by Western blot analysis.

Constructs. RhoC GTPase from the SUM149 cell line was amplified by RT-PCR and cloned using the pGEM-T Easy kit (Promega, Madison, WI). The full-length RhoC GTPase cDNA was sequenced and checked against the published sequence of any mutations. Using *Eco*RI (Roche-Boehringer Mannheim), the RhoC cDNA was excised and ligated into pFLAG-CMV-4 (Sigma Chemical Co.) and resequenced.

Expression Analysis of RhoC GTPase Transfectants. Total RNA was isolated from cells using Trizol reagent (Life Technologies, Inc.) according to the manufacturer's recommendations. One μg of total RNA was converted to cDNA using an avian myeloblastosis virus reverse transcription system (Promega). A 100-μg aliquot of the resulting cDNA was amplified in a double PCR with 25 ng each of pFLAG/GAPDH- or RhoC GTPase/GAPDH-specific primers. PCR products were separated on a 1.2% agarose gel and imaged on an Alpha Image 950 documentation system (Alpha Innotech, San Leandro, CA). Densitometry of images was performed using NIH Image version 1.62.

Received 3/1/00; accepted 8/18/00.

The costs of publication of this article were defrayed in part by the payment of page charges. This article must therefore be hereby marked *advertisement* in accordance with 18 U.S.C. Section 1734 solely to indicate this fact.

[1] Supported by NIH Grants R01 CA 77612 (to S. D. M.) and 5T32 CA09537-16, a grant (to S. D. M.) and a Postdoctoral Fellowship (to K. L. v. G.) from The Susan G. Komen Breast Cancer Foundation, and a grant from the Blodgett-Butterworth Research Foundation (to S. D. M.). K. L. v. G. and Z-F. W. contributed equally to this project and are considered co-first authors.

[2] To whom requests for reprints should be addressed, at Department of Internal Medicine, University of Michigan, 7217 CCGC, 1500 East Medical Center Drive, Ann Arbor, MI 48109-0948.

[3] The abbreviations used are: IBC, inflammatory breast cancer; HME, human mammary epithelial; FBS, fetal bovine serum; RT-PCR, reverse transcription-PCR; GAPDH, glyceraldehyde-3-phosphate dehydrogenase; MTT, 3-(4,5-dimethylthiazol-2-yl)-2,5-diphenyltetrazolium bromide; β-gal, β-galactosidase; MFP, mammary fat pad.

Proteins were harvested from cell cultures using radioimmunoprecipitation assay buffer (1× PBS, 1% NP40, 0.5% sodium deoxycholate, 0.1% SDS, 0.1 mg/ml phenylmethylsulfonyl fluoride, 1 mM sodium orthovanadate, and 0.3 mg/ml aprotinin; Sigma Chemical Co.). Whole cell lysates (100 μg) were precleared using normal mouse IgG and protein A/G-agarose (Santa Cruz Biotechnology Inc., Santa Cruz, CA). The cleared supernatants were incubated overnight with antibodies specific for the FLAG epitope (Eastman Kodak, Rochester, NY). Antibody-bound proteins were precipitated after the addition of protein A/G-agarose and washed four times with 1× PBS. Immunoprecipitates were resuspended in 20 μl of 2× Laemmli electrophoresis buffer, boiled for 3 min, and centrifuged briefly to pellet the free protein A/G-agarose. Samples were separated by SDS-PAGE on an 8% gel under nondenaturing conditions and transferred to a nitrocellulose membrane. Nonspecific binding was blocked by overnight incubation with 2% powdered milk (Kroger, Cincinnati, OH) in Tris-buffered saline with 0.05% Tween 20 (Sigma Chemical Co.). Anti-FLAG immunoprecipitate blots were incubated with the FLAG antibody. Protein bands were visualized by ECL (Amersham-Pharmacia Biotech, Piscataway, NJ).

Monolayer Growth Rate. Monolayer culture growth rate was determined as described previously (12) by conversion of MTT (Sigma Chemical Co.) to a water-insoluble formazan by viable cells. Three thousand cells in 200 μl of medium were plated in 96-well plates and grown under normal conditions. Cultures were assayed at 0, 1, 2, 3, 5, and 7 days by the addition of 40 μl of 5 mg/ml MTT and incubation for 1 h at 37°C. The MTT-containing medium was aspirated, and 100 μl of DMSO (Sigma Chemical Co.) were added to lyse the cells and solubilize the formazon. Absorbance values of the lysates were determined on a Dynatech MR 5000 microplate reader at 540 nm.

Anchorage-independent Growth in Soft Agar. A 2% stock of sterile, low melting point agarose was diluted 1:1 with 2× MEM. Further dilution to 0.6% agarose was made using 10% FBS-supplemented Ham's F-12 medium complete with growth factors, and 1 ml was added to each well of a 6-well plate as a base layer. The cell layer was then prepared by diluting agarose to 0.3% and 0.6% with 10^3 cells in 2.5% FBS-supplemented Ham's F-12 medium/1.5 ml/well. Colonies greater than or equal to 100 μM in diameter were counted after a 3-week incubation at 37°C in a 10% CO_2 incubator.

Invasion through a Matrigel-coated Filter. The invasion assay was performed as described previously, with minor modifications (12). A 10-μl aliquot of Matrigel (10 mg/ml) was spread onto a 6.5-mm Transwell filter with 8 μm pores (Costar, Corning, NY) and air dried in a laminar flow hood. Once dried, the filters were reconstituted with a few drops of serum-free medium. The lower chamber of the Transwell was filled with either serum-free or serum-containing media. Cells were harvested and resuspended in serum-free medium with 0.1% BSA at a concentration of 3.75×10^5 cells/ml, and 0.5 ml of cell suspension was added to the top chamber. The chambers were incubated for 24 h at 37°C in a 10% CO_2 incubator. The cell suspension was aspirated, and excess Matrigel was removed from the filter using a cotton swab. The filters were then cut away from the Transwell assembly and fixed with methanol, gel side down, to a glass microscope slide. The fixed filters were stained with H&E, and the cells in 20 random ×40 magnification fields counted. These cells were assumed to have invaded through the Matrigel/filter. The number of cells that had invaded the serum-free containing lower chambers was considered background, and this number was subtracted from the number of cells that had invaded in response to the serum-containing medium.

Random Motility Assay. Random motility was determined using a gold-colloid assay (13). Gold-colloid was layered onto glass coverslips and placed into 6-well plates. Cells were plated onto the coverslips and allowed to adhere for 1 h at 37°C in a CO_2 incubator (12,500 cells/3 ml in serum-free medium). To stimulate the cells, the serum-free medium was replaced with 5% FBS-containing Ham's F-12 medium supplemented with growth factors and allowed to incubate for 3 h at 37°C. The medium was aspirated, and the cells were fixed using 2% glutaraldehyde. The coverslips were then mounted onto glass microscope slides, and areas of clearing in the gold-colloid corresponding to phagokinetic cell tracks were counted.

Rhodamine-Phalloidin Staining of Actin Filaments. Visualization of actin filaments was accomplished by staining with a conjugated phallotoxin. Cells were grown on glass coverslips for 48 h and washed with PBS followed by fixation with 1:1 ice-cold acetone and methanol. After a 30-min incubation in PBS containing 1% BSA, 5 μl of methanolic rhodamine-phalloidin stock (Molecular Probes, Eugene, OR) were added to each coverslip and allowed to stain for 20 min at room temperature. After repeated washing with PBS, the coverslips were mounted onto glass microscope slides using Gel/Mount (Biomedia Co., Foster City, CA). Cells were visualized under an Olympus fluorescence microscope equipped with a 573 nm filter.

Orthotopic Injection into Nude Mice. Ten-week-old female NCR athymic nude mice were orthotopically injected with HME-, HME-β-gal-, or HME-RhoC GTPase-transfected cells. Injection into the MFP of 20 mice/group was performed as described previously (14). Briefly, cells were harvested by trypsinization, washed, and resuspended in HBSS at a concentration of 1.5×10^6 cells/0.2 ml. Mice were anesthetized using 10 mg/ml ketamine, 1 mg/ml xylazine, and 0.01 mg/ml glycopyrrolate, and an incision below the thoracic MFP was made. Using a 27-gauge needle, the cell suspension was injected directly into the exposed MFP, and the wound was closed with a single wound clip. Tumor growth measurements were taken weekly until tumors reached 2.5 cm in diameter. Mice were necropsied, and tumor tissues were dissected for histological analysis.

RESULTS

Expression of RhoC GTPase in Immortalized HME Cells Induces Anchorage-independent Growth but Does Not Alter the Monolayer Growth Rates. To study the effect of RhoC GTPase overexpression on the phenotype of HPV-immortalized HME cells, stable HME-RhoC GTPase-overexpressing transfectants were established. Quantitative RT-PCR using primers specific for the pFLAG-CMV vector and for RhoC GTPase verified expression levels of the RhoC transgene (Fig. 1*A*). Levels of RhoC GTPase expression were found to be 6–20-fold higher in RhoC GTPase transfectants when

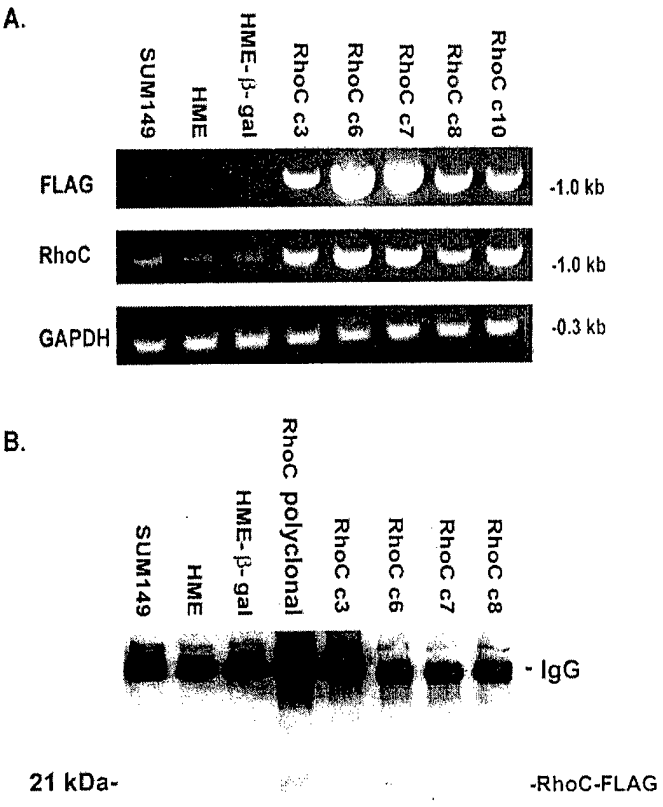

Fig. 1. Expression of pFLAG-RhoC in HME-RhoC clones. *A*, quantitative RT-PCR was performed on mRNA extracts using primers specific for the FLAG vector, the RhoC gene, and GAPDH (control). RhoC protein expression was confirmed by immunoprecipitation followed by immunoblotting. *B*, protein extracts were immunoprecipitated using antibodies for the FLAG epitope. The immunoprecipitated protein was then separated on a nonreducing gel, followed by immunoblotting with a FLAG antibody. Expression of the RhoC *trans*-gene and protein was confirmed in all HME-RhoC clones. Levels of expression were similar to those detected in the SUM149 IBC cell line and patient samples in a previous study.

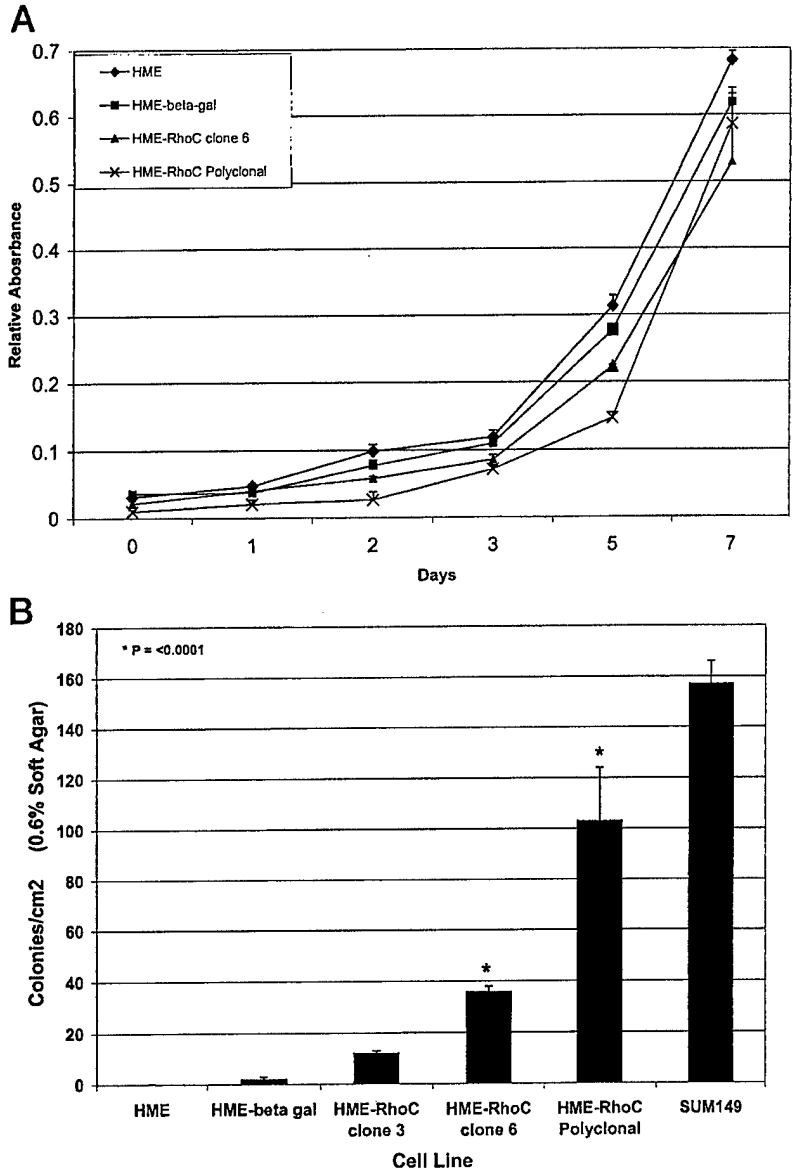

Fig. 2. Monolayer growth (*A*) of the HME-RhoC cells was not significantly different from that of untransfected HME or HME-β-gal control cells. When compared for their ability to grow under anchorage-independent conditions in 0.6% soft agar, the HME-RhoC cells produced significantly more colonies than the control HME cell lines (*B*). The number of colonies formed by the HME-RhoC cells was similar to the number of colonies formed by the SUM149 IBC cell line.

compared with the untransfected or HME-β-gal control-transfected HME cells. This level of expression is comparable with that of the SUM149 IBC cell line, which was found to have an 8-fold higher expression of *RhoC* as compared with normal HME cell lines and non-IBC breast cancer cell lines as determined by Northern blot analysis (4). Also, this level of expression was comparable to archival IBC tumor specimens, which were previously found to have 5–12-fold higher levels of *RhoC* expression compared with the surrounding normal tissue as determined by *in situ* hybridization (4). Expression of the FLAG-tagged RhoC GTPase protein was confirmed by immunoprecipitation with an anti-FLAG antibody followed by immunoblotting with the same antibody (Fig. 1*B*).

Because the Rho proteins can affect activation of transcription (15), we studied the monolayer growth rate of eight clones of the HME-RhoC transfectants. As shown in Fig. 2*A*, no significant changes in the monolayer growth rates were observed for any of the HME-RhoC transfectant clones or the mixed polyclonal population, as compared with the control cell lines using the MTT assay. Furthermore, regardless of quantitative differences in the level of RhoC transgene expression, no difference in growth rate was observed between the various clones and the polyclonal population.

When tested for their ability grow under anchorage-independent conditions, which is a strong indicator of malignant transformation, the HME-RhoC transfectants formed 6–176-fold more colonies in 0.6% soft agar than the control cell lines. As shown in Fig. 2*B*, the number of colonies greater than 100 μm in size formed by individual HME-RhoC clones ranged from 6–176 colonies/well in comparison to the HME-β-gal cells, which had a range of 0–6 colonies/well. This increase in anchorage-independent growth directly correlated with levels of expression of the RhoC transgene. The polyclonal population had the highest level of colony formation, and this recapitulated the behavior of the SUM149 IBC cell line in soft agar. The SUM149 cell line expressed RhoC GTPase at 8-fold higher levels than the HMEs. In the same assay, using the less stringent condition of 0.3% soft agar, the average HME-RhoC transfectant colony size was greater than 600 μm.

Overexpression of RhoC GTPase Produces a Motile and Invasive Phenotype in Immortalized HME Cells through Formation of Actin Stress Fibers and Focal Adhesion Points. The term IBC was coined in 1924 to describe the appearance of the skin overlaying the affected breast (16). This term is somewhat of a misnomer because IBC is not characterized by significant infiltration of inflammatory cells. The inflamed appearance of the skin is due to edema caused by

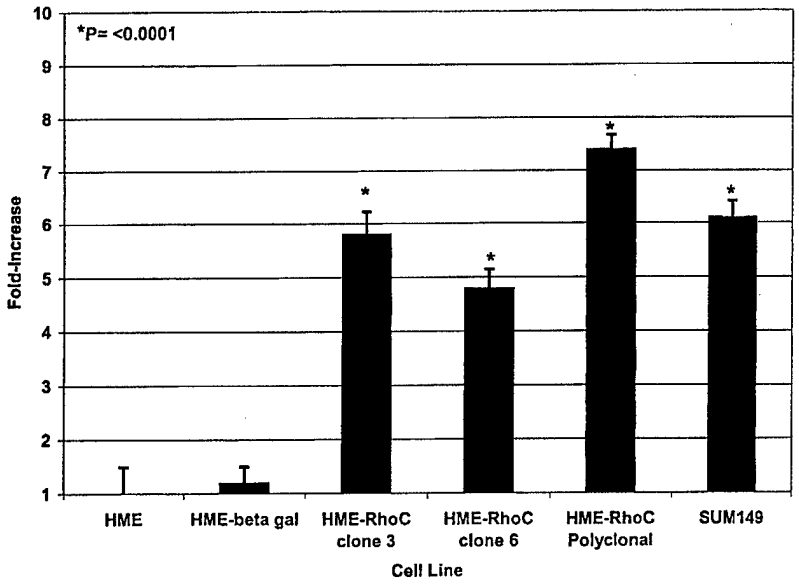

Fig. 3. Results of a Matrigel invasion assay. Cells in serum-free medium were seeded into the top half of a blind-well chamber onto a Matrigel-coated filter. Serum-containing medium was placed into the lower half of the chamber as a chemoattractant. The number of invading cells was counted 24 h later. Results are given as the fold increase in invasion over the that seen in untransfected HME cells. The HME-RhoC cells were, on average, 5-fold more invasive than the untransfected and HME-β-gal control cells. The invasive capabilities of the HME-RhoC cells were similar to those of the SUM149 IBC cell line.

invasion into and obstruction of the dermal lymphatics by tumor emboli (3).

Rho proteins are most noted for their ability to control polarity, protrusion, and adhesion during cell motility by rearranging the actin cytoskeleton (6). Given the clinical observations, coupled with the finding that RhoC GTPase is overexpressed in patient tumor samples (4), we sought to ascertain whether RhoC GTPase overexpression could generate highly invasive and motile HME cells.

Using a modified blind-well chamber model, we measured the amount of migration of cells across a porous membrane coated with the extracellular matrix conglomerate Matrigel in response to a chemoattractant. In this assay, all cell lines tested were invasive to varying degrees after 24 h. The data in Fig. 3 are expressed as the fold increase in invasion observed over the invasion level of the untransfected HME cell line. The HME-β-gal control-transfected cell line was 1.5-fold more invasive than the untransfected cells, whereas the HME-RhoC transfectants were, on average, 5-fold more invasive than either the untransfected or HME-β-gal cell lines. In comparison, the SUM149 primary IBC cell line was 4-fold more invasive than the control (untransfected and β-gal) HME cell lines. As was observed previously in the anchorage-independent growth assays, the ability to invade directly correlated with the level of RhoC GTPase expression of the HME-RhoC transfectant clones. Invasion rates from 1–19-fold over the control cell lines were observed, depending on the RhoC transgene expression levels. These data demonstrate that expression of RhoC GTPase directly correlates with the ability of the cells to invade, with a clear threshold effect dependent on RhoC expression level.

Similar results were obtained when the cells were assessed for their ability to move in response to stimulation during a random motility assay. Fig. 4*A* depicts representative photomicrographs of a gold-colloid random motility assay comparing HME-β-gal and HME-RhoC transfectants. In this assay, cells are layered onto a gold-colloid, on which motile cells produce tracks that can then be quantitated. The data depicted in Fig. 4*B* are represented as a percentage of the total number of cells of each clone that moved in response to serum activation over a 3-h period. In this assay, we found that more than 90% of the HME-RhoC cells were highly motile in response to serum stimulation. This was true for the different HME-RhoC GTPase clones. In comparison, only 10% of the HME-β-gal control-transfected HME cells were motile under the same conditions. Furthermore, in this assay, none of the untransfected HME cells were motile.

Rho proteins are reported to form actin stress fibers and focal adhesion points, whereas rac and Cdc42 are involved in lamellipodia and filopodia formation (17). The dynamic balance of formation and reformation of these structures leads to cellular motility. Recent evidence has implicated Rho in the control of lamellipodia through activation of Rho effector proteins (18). To test whether RhoC GTPase was effecting the motility of the HME transfectants through the formation of stress fibers and focal adhesions, we stained the cells with a rhodamine-tagged phallotoxin that targets actin structures and compared the patterns with those of the HME controls (untransfected and β-gal HME cells). As seen in Fig. 5, *B* and *C*, focal adhesion points and actin stress fibers are clearly visible and abundant in the HME-RhoC transfectants. The same was true for the SUM149 IBC cell line (data not shown). These prominent structures were not seen in the untransfected HME cells (data not shown) or in HME-β-gal control-transfected cells (Fig. 5*A*). The HME-RhoC clone 3 cell highlighted in Fig. 5*B* clearly shows actin stress fiber formation emanating from a focal adhesion point and leading to a discernible lamellipodial extension. Taken together, these features imply much greater motility and ability to effect cytoskeletal reorganization in the RhoC transfectants than control HMEs.

Malignant Transformation of HME Cells by RhoC GTPase. The HME-RhoC GTPase transfectants were assessed for their ability to form tumors in athymic nude mice. The SUM149 IBC cell line, untransfected HME, HME-β-gal, and the polyclonal population of the HME-RhoC GTPase transfectants were each injected into the MFP of female nude mice. As shown in Table 1, none of the untransfected HME cells or HME-β-gal cells formed tumors in nude mice. Untransfected HME cells have never been known to form tumors in nude mice. In contrast, both the SUM149 IBC cell line and the RhoC GTPase HME cells grew tumors in nude mice, in 86% (17 of 20) and 25% (5 of 20) of cases, respectively. The incidence of tumor growth by the SUM149 cell line is comparable with the SUM190 cell line, the only other known available IBC cell line (data not shown). These data indicate that overexpression of RhoC GTPase is weakly sufficient for malignant transformation of immortalized HME cells and that other genetic abnormalities in the IBC cell lines derived from established tumors contribute to the full-blown malignant phenotype.

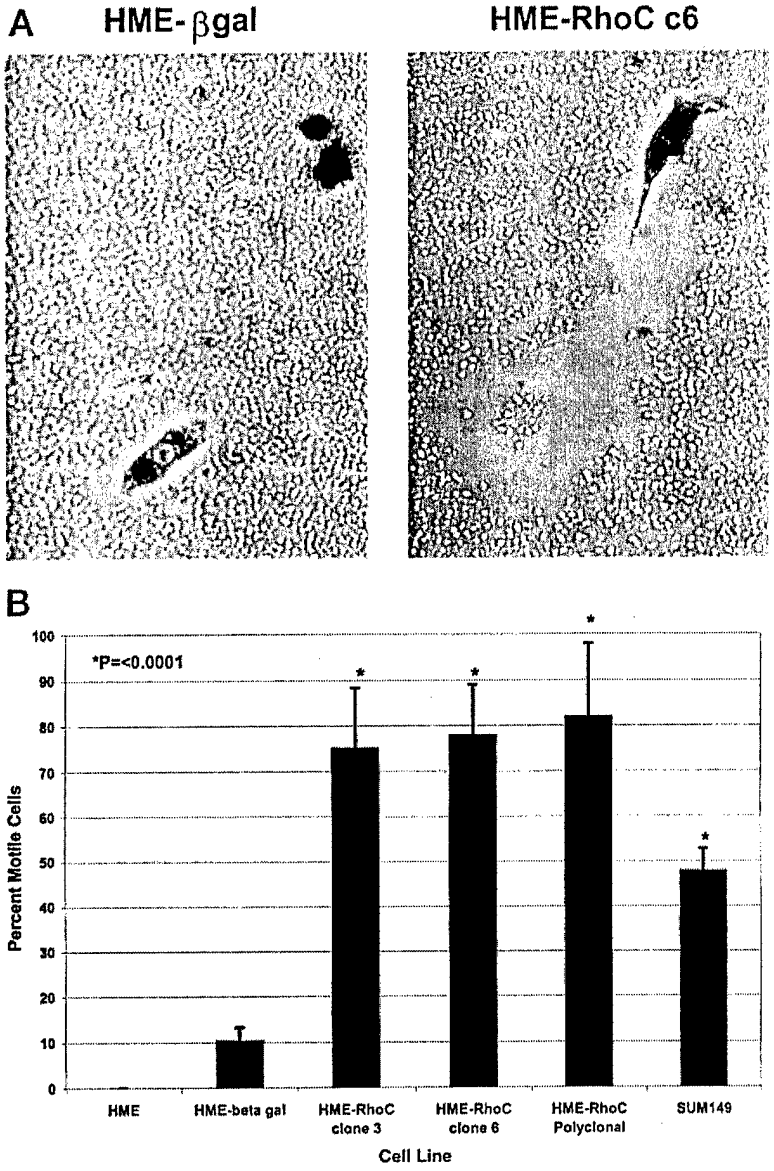

Fig. 4. *A*, representative photomicrographs of HME-β-gal control cells and HME-RhoC cells in a gold-colloid random motility assay. Cells in serum-free medium were seeded onto gold-colloid layered coverslips and allowed to adhere for 1 h. To stimulated motility, the serum-free medium was replaced with 5% serum-containing medium. Motile cells were counted 3 h after stimulation. The percentage of motile cells is given in *B*. The HME-RhoC cells were significantly more motile than the control HME cells and were even more motile than the SUM149 parent cell line.

DISCUSSION

Differential display and more recently, gene arrays, are leading to the isolation of many genes with altered patterns of expression in cancer. The task of sorting out their specific role and relative importance in the cancer phenotype is, in general, exceedingly complex. In the case of IBC, however, our previous work indicated that RhoC GTPase overexpression is specifically correlated with this phenotype in contrast to slow-growing locally advanced breast cancers. By exploiting insight from the clinical behavior of IBC, we focused on sorting out the specific contributions of RhoC GTPase to the IBC phenotype. In deciding how to go about defining the role of RhoC GTPase in IBC, we also considered the known functions of the Rho family members.

The mammalian Rho GTPase family can be divided in six different groups with the following members: (*a*) Rho (RhoA, RhoB, and RhoC); (*b*) Rac (RhoG and Rac1–3); (*c*) Cdc42 (Cdc42Hs, G25K, and TC10); (*d*) Rnd (Rho6, Rho7, and RhoE); (*e*) RhoD; and (*f*) TTF (19). RhoA, RhoB, and RhoC share a high degree of homology with one another, with RhoA and RhoC being the most homologous (20). Studies performed on Swiss 3T3 cells have helped to define the role that each of the Rho GTPase family members plays in controlling cytoskeletal reorganization (21). Rho controls actin stress fiber and focal adhesion contact formation, whereas rac and Cdc42 are responsible for the formation of lamellipodia and filopodia, respectively (17). Several upstream pathways that activate Rho as well as the downstream targets of activated Rho have been identified (15, 22–25). The ability of Rho to form stress fibers and focal adhesions is due to the phosphorylation and activation of two of these targets, Rho-kinase/ROK/ROCK (24, 26, 27) and the myosin-binding subunit of myosin phosphatase (18, 28). Phoshorylation of myosin-binding subunit by Rho inhibits myosin phosphatase, whereas activated Rho-kinase directly phosphorylates the myosin light chain. The phosphorylation of myosin light chain regulates the formation of stress fibers and focal adhesion contacts. Rho-kinase can also phosphorylate adducin, which leads to cell membrane ruffling and cell motility (29). It is also becoming clear that the various members of the Rho family (Rho, rac, and Cdc42) are able to undergo molecular "cross-talk," creating dynamic molecular interactions leading to cell motility (30, 31).

There is increasing evidence that the effects of Rho family mem-

Fig. 5. Rhodamine-tagged phallotoxin staining of actin filaments in (*A*) HME-β-gal control cells and (*B* and *C*) HME-RhoC transfectants. *A* and *B*, ×20; *C*, ×40. Diffuse actin staining is seen in the HME-β-gal control cells, whereas distinct actin stress fibers and focal adhesion contacts are seen in the HME-RhoC transfectants.

bers are, in fact, cell type specific and can extend beyond the actin cytoskeleton (reviewed in Ref. 6). For example, in keratinocytes, activated Rho and rac are responsible for cadherin-based adherens junctions (32). However, the opposite is true in Madin-Darby canine kidney epithelial cells, in which activated Rho and rac decrease cadherin expression (33). These observations demonstrate that expression of activated Rho GTPase can affect the expression of molecules, such as cadherins, that are integral in signal transduction pathways, thereby influencing transcription of other downstream genes (34, 35). Transcription of other genes, including those influencing motility, can also be regulated directly through activation of the mitogen-activated protein kinase subfamilies c-Jun NH_2-terminal kinase (35), and p38 kinase (36).

Our initial finding that RhoC was a key molecule in an invasive cancer such as IBC was consistent with observations of other groups in different tumor types (37). Suwa *et al.* (37) established a correlation between RhoC GTPase overexpression and the progression and prognosis of aggressive ductal adenocarcinoma of the pancreas. Other studies have demonstrated that activated Rho is an integral component for mediating cell motility required for producing intrahepatic metastasis of hepatocellular carcinoma (39).

Overexpression of RhoC GTPase in immortalized HME cells produced a striking phenotypic change that, for the most part, recapitulates that of the SUM149 IBC cell line. The extent of the phenotypic change appears to correlate with the level of RhoC expression in the various HME-RhoC clones. However, the highest expressers do not completely recapitulate the SUM149 cell line, suggesting that other genetic alterations in the IBC cell line contribute to the full-blown malignant phenotype of the IBC cell. Growth under anchorage-independent conditions was greatly enhanced in the RhoC transfectants. Almost all of the control untransfected or β-gal-transfected HME cells either underwent apoptosis (as determined by morphological changes) or were cytostatic under the same conditions. In comparison with the control cells, the RhoC transfectants produced up to 100-fold more colonies, which approached 63% of the level of colony formation of the SUM149 IBC cell line. Similarly, the effect of RhoC on both random and directed motility reproduced that of the SUM149 phenotype. As seen with anchorage-independent growth, the level of expression of RhoC GTPase influenced the level of bulk motility. As expected, there appears to be a threshold effect at the cellular level; even at lower (but still increased) expression levels, stress fiber and focal adhesion contact formation are seen. Further work in our laboratory[4] indicates that RhoC overexpression modulates the angiogenic potential of the transfectants.

Finally, RhoC-HME cells produced tumors in nude mice. As expected, however, the uptake was considerably lower than that of wild-type SUM149. This is likely due to the absence of many other genetic events that contribute to tumor growth in the RhoC-HME transfectants. To quantitatively reproduce the *in vivo* tumorigenic phenotype of the SUM149 cell line, other genes, such as *Ras*, *p53*, or antiapoptotic genes may need to be altered as well. Therefore, overexpression of *RhoC GTPase* represents a single but important component of HME transformation.

The set of experiments that test the potential oncogenicity of a gene vary according to cell type and study. However, in general, they comprise a battery of assays that test *in vitro*- and *in vivo*-specific qualities of the phenotypic behavior (40, 41). The experiments we chose for this work were guided by the specific IBC phenotypic characteristics of the human tumors and the IBC parent cell line (SUM149) as well as by the putative function of the Rho proteins. For this particular system, we conclude that all of our experiments credential RhoC GTPase as an oncogene in breast cancer, which, to a significant extent, recapitulates the invasive behavior of our IBC model system. In addition, given the specific role that RhoC plays in the invasive phenotype of IBC, interfering with its function suggests a new therapeutic target in a particularly challenging form of breast cancer. As the upstream and downstream signaling pathways are explored, these too may present new targets for therapeutic intervention.

Table 1 *Tumor take for various cell lines*

Cell line	No. of mice with tumor	Tumor take (%)
HME	0/20	0
HME-β-gal	0/20	0
HME-RhoC	5/20	25
SUM149	17/20	86

REFERENCES

1. Levine, P. H., Steinhorn, S. C., and Ries, I. G. Inflammatory breast cancer. The experience of the Surveillance, Epidemiology, and End Results (SEER) program. J. Natl. Cancer Inst., *74:* 291–297, 1985.
2. Jaiyesimi, I., Buzdar, A., and Hortobagyi, G. Inflammatory breast cancer: a review. J. Clin. Oncol., *10:* 1014–1024, 1992.
3. Beahrs, O., Henson, D., and Hutter, R. Manual for Staging of Cancer (3rd ed), pp. 145–150. 1988.
4. van Golen, K. L., Davies, S., Wu, Z. F., Wang, Y., Bucana, C. D., Root, H., Chandrasekharappa, S., Strawderman, M., Ethier, S. P., and Merajver, S. D. A novel putative low-affinity insulin-like growth factor-binding protein, LIBC (lost in inflammatory breast cancer), and RhoC GTPase correlate with the inflammatory breast cancer phenotype. Clin. Cancer Res., *5:* 2511–2519, 1999.
5. Ridley, A. Membrane ruffling and signal transduction. Bioessays, *16:* 321–327, 1994.
6. Hall, A. Rho GTPases and the actin cytoskeleton. Science (Washington DC), *279:* 509–514, 1998.
7. Nobes, C. D., and Hall, A. Rho GTPases control polarity, protrusion, and adhesion during cell movement. J. Cell Biol., *144:* 1235–1244, 1998.

[4] Unpublished observations.

8. Ethier, S. P., Kokeny, K. E., Ridings, J. W., and Dilts, C. A. erbB family receptor expression and growth regulation in a newly isolated human breast cancer cell line. Cancer Res., *56:* 899–907, 1996.
9. Ethier, S. P. Human breast cancer cell lines as models of growth regulation and disease progression. J. Mammary Gland Biol. Neoplasia, *1:* 111–121, 1996.
10. Sartor, C., Dziubinski, M., Yu, C., Jove, R., and Ethier, S. P. Role of epidermal growth factor receptor and STAT-3 activation in autonomous proliferation of SUM-102PT human breast cancer. cells. Cancer Res., *57:* 978–987, 1997.
11. Band, V., Zajchowski, D., Kulesa, V., and Sager, R. Human papilloma virus DNAs immortalize normal epithelial cells and reduce their growth factor requirements. Proc. Natl. Acad. Sci. USA, *87:* 463–467, 1990.
12. van Golen, K. L., Risin, S., Staroselsky, A., Berger, D., Tainsky, M. A., Pathak, S., and Price, J. E. Predominance of the metastatic phenotype in hybrids formed by fusion of mouse and human melanoma clones. Clin. Exp. Metastasis, *14:* 95–106, 1996.
13. Albrecht-Buehler, G. Phagokinetic tracks of 3T3 cells. Cell, *11:* 395–404, 1977.
14. Price, J. E., and Zhang, R. D. Studies of human breast cancer metastasis using nude mice. Cancer Metastasis Rev., *8:* 285–291, 1989.
15. Clark, E. A., King, W. G., Brugge, J. S., Symons, M., and Hynes, R. O. Integrin-mediated signals regulated by members of the Rho family GTPases. J. Cell Biol., *142:* 573–586, 1998.
16. Nobes, C. D., and Hall, A. Rho, rac, and cdc42 GTPases regulate the assembly of multimolecular focal complexes associated with actin stress fibers, lamellipodia and filopodia. Cell, *81:* 53–62, 1995.
17. Kimura, K., Ito, M., Amano, M., Chihara, K., Fukata, Y., Nakafuku, M., Yamamori, B., Feng, J., Nakano, T., Okawa, K., Iwamatsu, A., and Kaibuchi, K. Regulation of myosin phosphatase by Rho and Rho-associated kinase (Rho-kinase). Science (Washington DC), *273:* 245–248, 1996.
18. Apenstrom, P. Effectors for the Rho GTPases. Curr. Opin. Cell Biol., *11:* 95–102, 1999.
19. Prendergast, G. C., Khosravi-Far, R., Solski, P. A., Kurzawa, H., Lebowitz, P. F., and Der, C. J. Critical role of Rho in cell transformation by oncogenic Ras. Oncogene, *10:* 2289–2296, 1995.
20. Kozma, R., Ahmed, S., Best, A., and Lim, L. The ras-related protein cdc42 Hs and bradykinin promote formation of peripheral actin microspikes and filapodia in Swiss 3T3 fibroblasts. Mol. Cell. Biol., *15:* 1942–1952, 1995.
21. Kjoller, L., and Hall, A. Signaling to Rho GTPases. Exp. Cell Res., *253:* 166–179, 1999.
22. Fujisawa, K., Madule, P., Ishizaki, T., Watanabe, G., Bito, H., Saito, Y., Hall, A., and Narumiya, S. Different regions of Rho determine Rho-selective binding of different classes of Rho target molecules. J. Biol. Chem., *273:* 18943–18949, 1998.
23. Maekawa, M., Ishizaki, T., Boku, S., Watanabe, N., Fujita, A., Iwamatsu, A., Obinata, T., Ohashi, K., Mizuno, K., and Narumiya, S. Signaling from Rho to the actin cytoskeleton through protein kinases and LIM-kinase. Science (Washington DC), *285:* 895–898, 1999.
24. Fukata, Y., Oshiro, N., Kinoshita, N., Kawano, Y., Matsuoka, Y., Bennet, V., Matsuura, Y., and Kaibuchi, K. Phosphorylation of adducin by Rho-kinase plays a crucial role in cell motility. J. Cell Biol., *145:* 347–361, 1999.
25. Amano, M., Chihara, K., Kimura, K., Fukata, Y., Nakamura, N., Matsuura, Y., and Kaibuchi, K. Formation of actin stress fibers and focal adhesions enhanced by Rho-kinase. Science (Washington DC), *275:* 1308–1311, 1997.
26. Leung, T., Chen, X. Q., Manser, E., and Lim, L. The p160 RhoA-binding kinase ROK α is a member of a kinase family and is involved in the reorganization of the cytoskeleton. Mol. Cell. Biol., *16:* 5313–5327, 1996.
27. Amano, M., Ito, M., Kimura, K., Fukata, Y., Chihara, K., Nakano, T., Matsuura, Y., and Kaibuchi, K. Phosphorylation and activation of myosin by Rho-associated kinase (Rho-kinase). J. Biol. Chem., *271:* 20246–20249, 1996.
28. Koch, A. E., Kunkel, S. L., Burrows, J. C., Evanoff, H. L., Haines, G. K., Pope, R. M., and Strieter, R. M. Synovial tissue macrophage as a source of the chemotactic cytokine IL-8. J. Immunol., *147:* 2187–2195, 1991.
29. Small, J. V., Kaverina, I., Krylyshkina, O., and Rottner, K. Cytoskeleton cross-talk during cell motility. FEBS Lett., *452:* 96–99, 1999.
30. Sander, E. E., ten Klooster, J. P., van Delft, S., van der Kammen, R. A., and Collard, J. G. Rac downregulates Rho activity: reciprocal balance between both GTPases determines cellular morphology and migratory behavior. J. Cell Biol., *147:* 1009–1021, 1999.
31. Braga, V. M., Del Maschio, A., Machesky, L. M., and Dejana, E. Regulation of cadherin function by Rho and Rac; modulation by junction maturation and cellular context. Mol. Cell. Biol., *10:* 9–22, 1999.
32. Ridley, A. J., Comoglio, P. M., and Hall, A. Regulation of scatter factor/hepatocyte growth factor responses by Ras, Rac, and Rho in MDCK cells. Mol. Cell. Biol., *15:* 1110–1122, 1995.
33. Coso, O., Chiariello, M., Yu, J. C., Teramoto, H., Crespo, P., Xu, N., Miki, T., and Gutkind, J. S. The small GTP-binding proteins Rac1 and Cdc42 regulate the activity of the JNK/SAPK signaling pathway. Cell, *81:* 1137–1146, 1995.
34. Teramoto, H., Crespo, P., Coso, O., Igishi, T., Xu, N., and Gutkind, J. S. The small GTP binding protein Rho activates c-Jun N-terminal kinases/stress-activated protein kinases in human kidney 293T cells. J. Biol. Chem., *271:* 25731–25734, 1996.
35. Vadlamudi, R., Adam, L., Talukder, A., Mendelsohn, J., and Kumar, R. Serine phosphorylation of paxillin by heregulin-β1: role of p38 mitogen activated protein kinase. Oncogene, *18:* 7253–7264, 1999.
36. del Peso, L., Hernandez-Alcoceba, R., Embade, N., Carnero, A., Esteve, P., Paje, C., and Lacal, J. Rho proteins induce metastatic properties *in vivo*. Oncogene, *15:* 3047–3057, 1997.
37. Suwa, H., Ohshio, G., Imamura, T., Watanabe, G., Arii, S., Imamura, M., Narumiya, S., Hiai, H., and Fukumoto, M. Overexpression of the *rhoC* gene correlates with progression of ductal adenocarcinoma of the pancreas. Br. J. Cancer, *77:* 147–152, 1998.
38. Genda, T., Sakamoto, M., Ichida, T., Asakura, H., Kojiro, M., Narumiya, S., and Hirohashi, S. Cell motility mediated by rho and Rho-associated protein kinase plays a critical role in intrahepatic metastasis of human hepatocellular carcinoma. Hepatology, *30:* 1027–1036, 1999.
39. Land, H., Parada, L. F., and Weinberg, R. A. Tumorigenic conversion of primary embryo fibroblasts requires at least two cooperating oncogenes. Nature (Lond.), *304:* 596–602, 1983.
40. Weinberg, R. A. The action of oncogenes in the cytoplasm and nucleus. Science (Washington DC), *230:* 770–776, 1985.
41. Bernstein, S. C., and Weinberg, R. A. Expression of the metastatic phenotype in cells transfected with human metastatic tumor DNA. Proc. Natl. Acad. Sci. USA, *82:* 1726–1730, 1985.

BRIEF ARTICLE

Neoplasia • Vol. 2, No. 5, September–October 2000, pp. 418–425 418

www.nature.com/neo

RhoC GTPase Overexpression Modulates Induction of Angiogenic Factors in Breast Cells[1]

Kenneth L. van Golen, Zhi-Fen Wu*, XiaoTan Qiao*, LiWei Bao* and Sofia D. Merajver*†*

*Department of Internal Medicine, Division of Hematology and Oncology; †The University of Michigan Comprehensive Cancer Center, Ann Arbor, MI 48109

Abstract

Inflammatory breast cancer (IBC) is a distinct and aggressive form of locally advanced breast cancer. IBC is highly angiogenic, invasive, and metastatic at its inception. Previously, we identified specific genetic alterations of IBC that contribute to this highly invasive phenotype. *RhoC GTPase* was overexpressed in 90% of archival IBC tumor samples, but not in stage-matched, non-IBC tumors. To study the role of *RhoC GTPase* in contributing to an IBC-like phenotype, we generated stable transfectants of human mammary epithelial cells overexpressing the *RhoC* gene, and studied the effect of *RhoC GTPase* overexpression on the modulation of angiogenesis in IBC. Levels of vascular endothelial growth factor (VEGF), basic fibroblast growth factor (bFGF), interleukin-6 (IL-6), and interleukin-8 (IL-8) were significantly higher in the conditioned media of the HME-RhoC transfectants than in the untransfected HME and HME-β-galactosidase control media, similar to the SUM149 IBC cell line. Inhibition of *RhoC* function by introduction of C3 exotransferase decreased production of angiogenic factors by the HME-RhoC transfectants and the SUM149 IBC cell line, but did not affect the control cells. These data support the conclusion that overexpression of *RhoC GTPase* is specifically and directly implicated in the control of the production of angiogenic factors by IBC cells. *Neoplasia* (2000) **2,** 418–425.

Keywords: inflammatory breast cancer, human mammary epithelial cells, *RhoC GTPase*, angiogenesis, angiogenic factors.

Introduction

Primary inflammatory breast cancer (IBC) accounts for approximately 6% of new breast cancer cases annually in the United States [1]. IBC is characterized by a very rapid course, progressing within 6 months to cause the clinical manifestations of erythmea, skin nodules, peau d'aurange, and nipple retraction due to tumor infiltration of lymphatic and connective tissue [2,3]. IBC tumors are highly angiogenic and at the time of diagnosis nearly all patients have nodal metastasis, whereas approximately 36% have gross distant metastases [2,3]. This number greatly increases 1 year after diagnosis, presumably due to the progression of occult metastases, suggesting that IBC cells acquire metastatic capabilities early in tumor formation. Not surprisingly, even with multimodality treatment, the 5-year disease-free survival is less than 45%, making IBC the most deadly form of locally advanced breast cancer [3].

Until recently, relatively little was known about the genetic mechanisms underlying the development and progression of IBC. In a previous study, our laboratory identified genes that strongly correlate with the aggressive and invasive IBC phenotype [4]. *RhoC GTPase* is overexpressed in 90% of archival IBC tumors, but not in stage-matched non-IBC tumors. Our laboratory has also demonstrated that *RhoC GTPase* is a transforming oncogene of human mammary epithelial cell [5]. RhoC is a member of the Ras superfamily of small GTP-binding proteins, which play a crucial role in the control of actin cytoskeletal reorganization and DNA transcription [6–8]. Another oncogene, *ras*, has been shown to induce the production of angiogenic cytokines such as vascular endothelial growth factor (VEGF) [9,10]. Recent evidence suggests that overexpression of *RhoA*, a member of the Rho family that is 95% homologous to *RhoC*, can induce angiogenesis in human prostate cancer as well as interleukin-8 (IL-8) in human endothelial cells [11].

To study the effect of *RhoC GTPase* overexpression on the modulation of angiogenic factors in human mammary epithelial cells, stable human mammary epithelial (HME)-RhoC transfectants were established as previously described [5]. We found that production of active VEGF, basic fibroblast growth factor (bFGF), IL-6 and IL-8, were significantly increased in the HME-RhoC cells compared with the controls and were comparable to the SUM149 IBC cell line, which also overexpresses *RhoC GTPase*. The production of these factors was specifically inhibited by the introduction of an inhibitor of Rho activity, C3 exotransferase, into HME-RhoC cells.

Abbreviations: IBC, inflammatory breast cancer; HME, human mammary epithelial cell; VEGF, vascular endothelial growth factor; bFGF, basic fibroblast growth factor; IL, interleukin

Address all correspondence to: Sofia D. Merajver, Department of Internal Medicine, University of Michigan, 7217 CCGC, 1500 East Medical Center Drive, Ann Arbor, MI 48109-0948. E-mail: smerajve@umich.edu

[1]This work was supported by National Institutes of Health (NIH) R01 CA 77612-(S.D.M.), and NIH 5T32 CA09537-16, DOD-DAMD17-OD-1-0345 (S.D.M. and K.v.G.), and by Susan G. Komen Foundation Postdoctoral Fellowship (K.v.G.) and grant (S.D.M.).

Received 6 September 2000; Accepted 3 October 2000.

Materials and Methods

Cell Lines

Cell lines were maintained under defined culture conditions for optimal growth in each case as previously described [12–14]. Briefly, human mammary epithelial (HME) cells were immortalized with human papilloma virus E6/E7 [15] and grown in 5% FBS (Sigma Chemical Co., St. Louis, MO) supplemented Ham's F-12 medium (JRH BioSciences, Lenexa, KS) containing insulin, hydrocortisone, epidermal growth factor, and cholera toxin (Sigma). HME cells were transfected with either β-galactosidase or RhoC GTPase [5]. Stable HME-β-gal and HME-RhoC cells were maintained in the medium described above supplemented with 100 μg/ml hygromycin (LifeScience Technologies). The SUM149 cell line was developed from a primary IBC tumor and grown in 5% FBS supplemented Ham's F-12 medium containing insulin and hydrocortisone. The HME cells were characterized as being keratin-19 positive, ensuring that they are from the same differentiation lineage as the SUM149 IBC tumor cell line [4].

Cytokine ELISA Assays

Levels of soluble cytokines were determined from cell-conditioned media. Cells were incubated in normal growth medium for 4 days. The cell-conditioned media was harvested, centrifuged for 5 minutes at 2500 rpm, and divided into 1-ml aliquots. The Quantikine hVEGF and human bFbF immunoassays (R&D Systems, Minneapolis, MN) were used to measure protein levels of the 165 amino acid species of VEGF and of bFGF. ELISA was performed per the manufacture recommendations. ELISAs for IL-6, IL-8, and IL-12 were performed by the University of Maryland Cytokine Core Laboratory (www.cytokinelab.com).

Quantitative RT-PCR of Cytokines

Levels of cytokine mRNA was determined by quantitative RT-PCR. Briefly, total RNA was harvested from cells using Trizol reagent (Life Technologies, Gaithersburg, MD) per the recommendations of the manufacturer. One microgram of total RNA was reverse transcribed to cDNA using the AMV reverse transcription kit (Promega, Madison, WI). Aliquots of cDNA totaling 50 ng were amplified by PCR using primers specific for either IL-6, IL-8, bFGF, or VEGF (10 ng/μl final concentration) and β-actin (1 ng/μl final concentration). PCR products were separated on a 1.2% agarose gel and imaged on an Alpha Image 950 documentation system (Alpha Innotech, San Leandro, CA). Densitometry of images was performed using NIH Image (version 1.62).

Rat Aortic Ring Assay

The rat aortic ring assay was used to measure the functional potency of angiogenic factors [16]. Briefly, the aorta was removed from a freshly sacrificed Sprague-Dawley rat and rinsed in ice-cold Hank's buffered saline solution (HBSS) containing penicillin and streptomycin (Life Technologies). Segmental rings, approximately 1 mm in width, were cut from the aorta and embedded in a 50 μl aliquot of 10 mg/ml Matrigel in six-well plates. The rat aortic rings were incubated overnight at 37°C in 2 ml of serum-free medium. The serum-free medium was then exchanged for 2 ml of the same cell-conditioned medium that was used for cytokine determination. Rat aortic ring segments were incubated for 4 days at 37°C, and then analyzed by phase-contrast microscopy for microvessel growth.

C3 Exotransferase Inhibition of RhoC GTPase Activity

The HME-β-gal, HME-RhoC, and SUM149 cells were transiently transfected with pEF-myc C3 transferase using FuGene 6 transfection reagent (Roche-Boehringer Mannheim, Mannheim, Germany). Cells were incubated for 2 days at 37°C, at which time cell-conditioned media and protein were harvested. Expression of C3 transferase was confirmed by Western blot analysis using an antibody to the c-myc-epitope tag. Control cells were transfected with pFLAG-β-galactosidase or FuGene 6 alone.

Active C3 exoenzyme was introduced into cells using a method based on liposome encapsulation and membrane fusion, which we have termed lipoporation. Briefly, cells were grown in six-well plates until reaching a confluence of 40% to 50% and the medium replaced with fresh medium. Three micrograms of human recombinant C3 exotransferase (Cytoskeleton Inc., Denver, CO) was combined with FuGene 6 transfection reagent (Roche-Boehringer Mannheim) and added to the cultures. As controls either an equal quantity of human recombinant tubulin or FuGene 6 alone were added to cell cultures. The cells were incubated for 2 days at 37°C, at which time cell-conditioned medium was harvested, for cytokine assays. Presence of the intracellular C3 exoenzyme was confirmed by visualizing the rhodamine-tagged protein using fluorescent microscopy. The efficiency and activity of both the transfected and lipoporated C3 exoenzyme were confirmed by a quantitative ADP-ribosylation assay [17].

ADP-Ribosylation Assay

The efficiency of *in vivo* ADP-ribosylation of *RhoC GTPase* by C3 exotransferase was determined as previously described [17]. Active C3 exotransferase was efficiently introduced into HME-β-gal, HME-RhoC, and SUM149, as described above. Cells were collected 48 hours later, washed in medium, and pelleted. The cells were lysed in 20 mM Hepes pH 8.0 (Sigma) by three repeated freeze/thaw cycles. Cell lysates (10 μg) were combined with 50 ng/ml C3 exotransferase and 5×10^6 cpm [^{32}P]NAD (Amersham) in ADP-ribosylation buffer (20 mM Hepes, pH 8.0, 1 mM $MgCl_2$, 1 mM AMP, and thymidine, Sigma) and incubated for 30 minutes at 37°C. TCA-precipitable material was then recovered and radioactivity was counted on a Packard scintillation counter.

Labeling of C3 Exotoxin

Cellular internalization of C3 exotoxin was visualized by fluorescence microscopy. C3 exotoxin was labeled using the

FluorReporter Rhodamine Red-X Protein Labeling Kit (Molecular Probes Inc., Eugene, OR). HME-β-gal, HME-RhoC, and SUM149 (100,000 cells/chamber) were plated into the chambers of Lab-Tek slides (Nalgene Nunc International, Naperville, IL). C3 exotoxin was introduced into cells as described above and cells were visualized 48 hours later using an Olympus fluorescent microscope equipped with a 573 nm filter.

Results

IBC is highly angiogenic, giving rise to profusely vascularized tumors at the primary and metastatic sites, including the skin overlying the breast (reviewed in Ref. [18]). Previous observations by our laboratory have demonstrated that IBC tumors and IBC cell lines produce high levels of angiogenic factors such as VEGF and bFGF (unpublished results). To determine if overexpression of *RhoC GTPase* could lead to increased production of angiogenic cytokines in mammary epithelial cells, we performed ELISAs on cell-conditioned media from the untransfected HME, HME-β-galactosidase control transfectants, HME-RhoC transfectants, and the wild-type SUM149 IBC cell lines. Cell-conditioned media were tested for the presence of the pro-angiogenic cytokines VEGF, bFGF, IL-6, IL-8, and the anti-angiogenic cytokine IL-12. Results were similar for all of the individual HME-RhoC clones tested (data not shown); thus, for brevity, only data from the polyclonal population is represented in this manuscript. The HME-RhoC polyclonal transfectants produced 10-fold more VEGF and bFGF, and five-fold more IL-6 and IL-8 than the untransfected HME and HME-β-gal control transfected cell lines. Compared with the SUM149 IBC cells, the HME-RhoC cells produced approximately 90% of the level of VEGF, twice the levels of IL-6 and IL-8, and equivalent levels of bFGF (Figure 1). IL-12 production was minimal in all cell lines tested (data not shown), suggesting that IL-12 is not an important angiogenic inhibitor in this system. To determine if the increased production of angiogenic factors correlated with an increase in cytokine message, we performed quantitative RT-PCR on mRNA from the untransfected HME, HME-β-gal control transfectants, HME-RhoC transfectants, and the wild-type SUM149 IBC cell lines. As determined by quantitative RT-PCR, the mRNA levels of IL-6, IL-8, bFGF, and VEGF was 2- to 10-fold higher in the *RhoC* transfectants and SUM149 IBC cell line compared with the control cell lines (data not shown). These data suggest that the increased cytokine levels were due in part to increased transcription of these genes.

The functional activity of the angiogenic cytokines was determined using the rat aortic ring assay (Figure 2). A fresh 1 mm segment of rat aorta was embedded in Matrigel and incubated with cell-conditioned medium for 4 days. Negligible microvessel growth was observed from the rings incubated with conditioned media from the untransfected HME (*panel A*) or HME-β-gal control (*panel B*). In contrast, prominent microvessel growth was observed for cell-conditioned medium from the HME-RhoC (*panel C*) and the SUM149 IBC (*panel D*) cell lines. The control

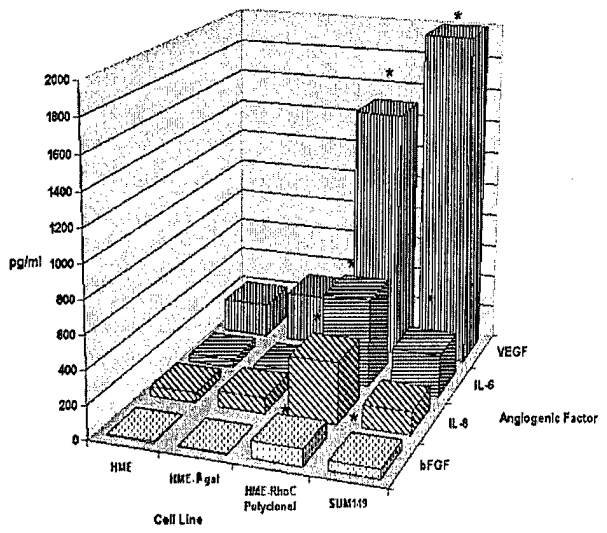

Figure 1. *Comparison of levels of angiogenic factors by HME-RhoC transfectants, SUM149 IBC cell line and the HME-β-gal control cell line as determined by ELISA. The HME-RhoC cells produced significantly higher levels of angiogenic factors compared with the HME-β-gal control cell line, nearly recapitulating the levels produced by the SUM149 IBC cell line. Significant differences ($p<0.001$) between the control cells and the HME-RhoC cells are denoted by an asterisk (*) with standard deviations within 10% of the reported values.*

samples incubated in growth medium alone did not stimulate microvessel growth in this system (data not shown).

To determine whether the production of angiogenic factors elicited by *RhoC GTPase* was directly related to its activity, we used C3 exotransferase to inhibit *RhoC* function. Specific inhibition of *RhoC GTPase* activity by C3 exotransferase led to decreased production of angiogenic factors. The HME, HME-β-gal control, HME-RhoC, and SUM149 IBC cells were transiently transfected with a c-myc-tagged C3 exotransferase expression construct and assayed 48 hours later for production of VEGF, bFGF, IL-6, and IL-8. As shown in Figure 3*A*, VEGF production was unchanged in the HME-β-gal controls transiently transfected with C3 exotransferase. In contrast, there was a 4.9- and 1.8-fold decrease in VEGF production by the HME-RhoC and SUM149 cells inhibited with C3, respectively. Expression of C3 exotransferase decreased the production of VEGF by the HME-RhoC and SUM149 cells to a level equivalent to that of the control cells. The levels of bFGF were decreased 37% and 34% in the HME-RhoC and SUM149 cells expressing C3 exotransferase, respectively. The levels of IL-6 production were reduced by 42% and 25% in the HME-RhoC and SUM149 cells, respectively, whereas production of these cytokines in the HME-β-gal control remained unchanged. Production of IL-8 was reduced 2.1- and 1.3-fold in the HME-RhoC and SUM149 cell lines by C3 inhibition.

The activity of the C3 exotransferase was confirmed by measuring the efficiency of *in vivo* ADP-ribosylation. As shown in Figure 3*B*, compared with their non–C3-expressing counterparts, all the C3-expressing cell lines had a

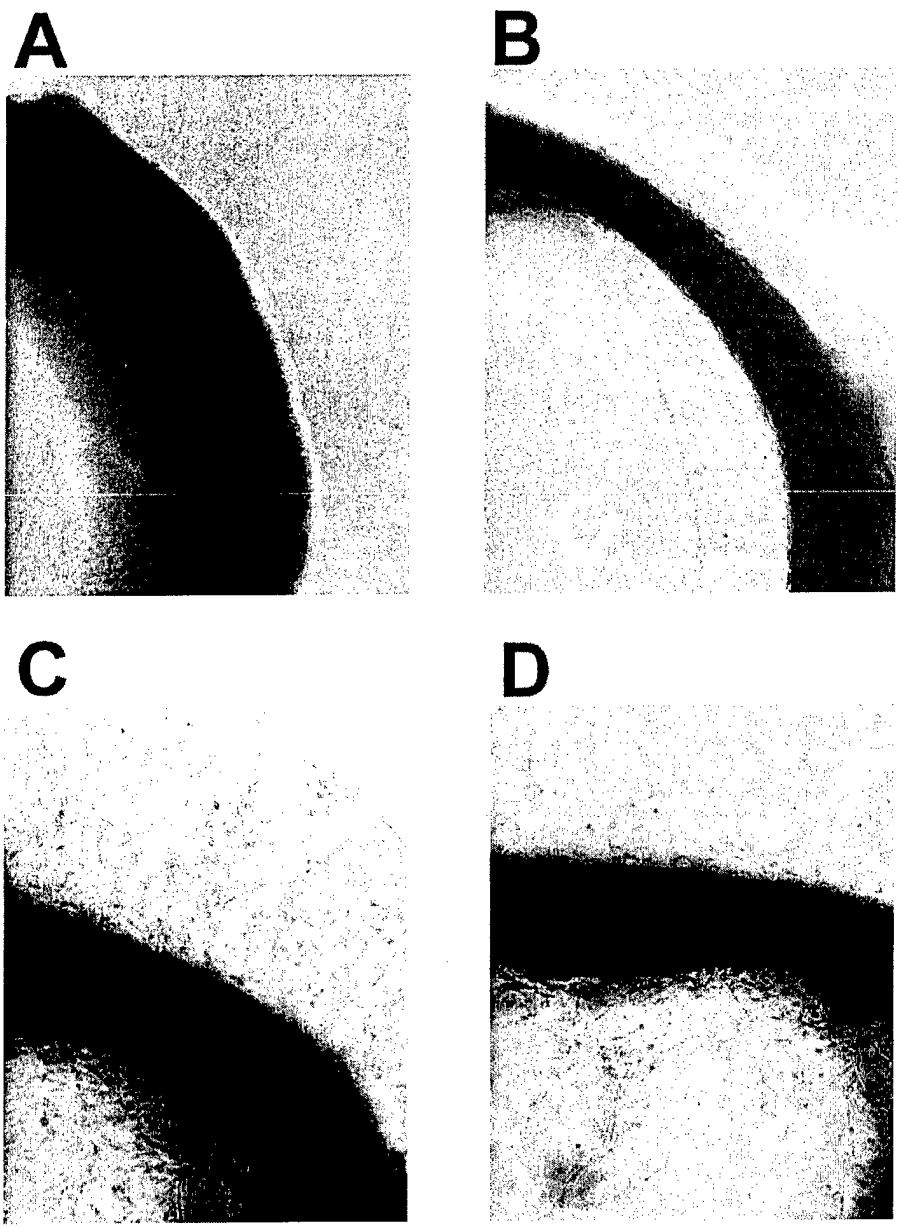

Figure 2. *Results of a rat aortic ring assay for functional angiogenic factors produced by untransfected HME (panel A), HME-β-gal control transfectants (panel B), HME-RhoC transfectants (panel C) and the SUM149 IBC cell line (panel D). Segments of rat aorta were embedded in Matrigel and cultured in the corresponding cell-conditioned media for 4 days and then observed for microvessel outgrowth. Conditioned media from the control cell lines (panels A and B) did not induce microvessel outgrowth. However, conditioned medium from the HME-RhoC transfectants (panel C) produced similar levels of new vessel growth as the SUM149 IBC cell line (panel D).*

significant reduction in the levels of available sites that could be ADP-ribosylated in the *in vitro* assay. Specifically, the C3-expressing HME-RhoC and SUM149 cells had a two-fold decrease in the number of ADP-ribosylated sites compared to the nontransfected controls. These data indicate that at least half of the RhoC proteins have been ADP-ribosylated *in vivo*, and therefore inhibited by C3 exotransferase.

To confirm these results by another approach, *RhoC GTPase* function was inhibited by direct introduction of C3 exotransferase protein into the cells. Equivalent results were observed when active recombinant C3 exotransferase protein was introduced into the cells using a lipoporation technique. The recombinant C3 protein was rhodamine-labeled and, as demonstrated in Figure 4, the presence of the protein in the cell was confirmed by fluorescent microscopy 48 hours later. VEGF production was significantly reduced in both the HME-RhoC and SUM149 cells, upon introduction of active C3 exotransferase. As shown in Figure 3*A*, HME-RhoC cells treated with C3 exoenzyme had a 5.8-fold decrease in VEGF production, whereas the SUM149 cells had a 1.9-fold decrease. A 2.8- and 3.0-fold decrease in bFGF production was observed in the HME-RhoC and SUM149 cells, respectively. Levels of IL-6

production were also moderately affected by C3 treatment. IL-6 levels were decreased by 37% and 53% in the HME-RhoC and SUM149 cell lines, respectively. Treatment of the HME-β-gal control cells with C3 exoenzyme did not effect the production of VEGF or IL-6. As before, introduction of C3 exotransferase reduced the levels of IL-8 production by 2.4- and 1.3-fold for the HME-RhoC and SUM149 cell lines, respectively. These results were also confirmed by a third method namely, RhoC inhibition using C3 exotoxin purified from *Clostridium botulinum* (data not shown). As demonstrated in the C3 exotransferase plasmid transfection experiment, there was a two-fold decrease in the number of ADP-ribosylated sites in all the C3-treated cell lines (Figure 3*B*). Therefore, at least half of the active Rho proteins were inhibited by the introduction of active C3 transferase.

Taken together these data indicate that *RhoC GTPase* overexpression can directly lead to the increased production of the pro-angiogenic factors VEGF, bFGF, IL-6 and IL-8. Specific inhibition of RhoC by C3 exotransferase significantly reduced the production of VEGF, bFGF, and IL-8. However, production of IL-6 was only moderately affected by the C3 exoenzyme.

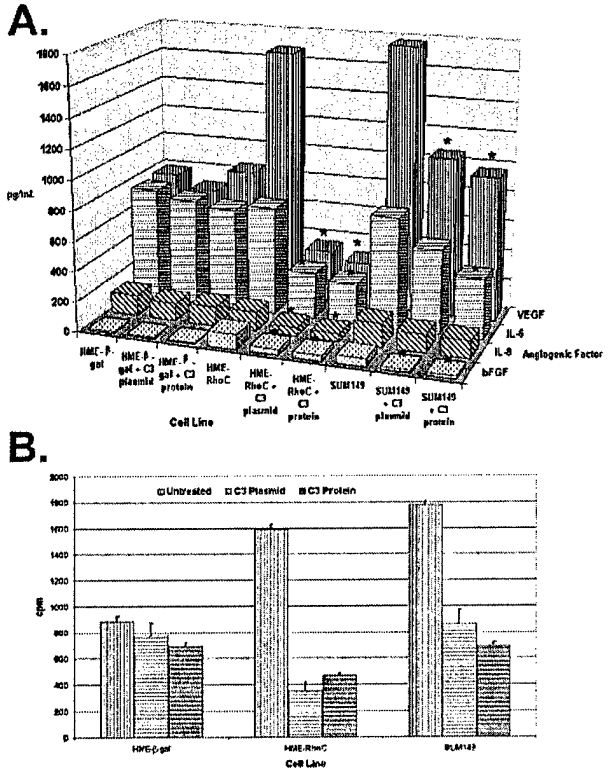

Figure 3. *Panel A demonstrates the effect on production of angiogenic factors by inhibition of RhoC GTPase with C3 exotransferase. Similar levels of inhibition were accomplished by expressing a C3 exotransferase construct or introducing the active protein directly into the cells. Significant differences ($p<0.05$) between the untreated and C3 exotransferase treated cells are denoted by an asterisk (*) with standard deviations within 10% of the reported values. Panel B demonstrates the results of an in vitro ADP-ribosylation study to determine the in vivo efficiency of C3 exotransferase inhibition of Rho activity. The assay was performed as outlined in the Materials and Methods section. The potential ADP-ribosylated sites in both the HME-RhoC and SUM149 cell lines were significantly reduced after C3 treatment, thus indicating efficient in vivo inhibition of RhoC GTPase.*

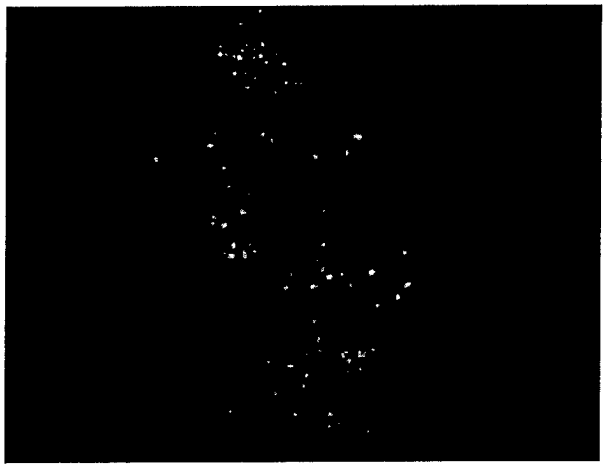

Figure 4. *Rhodamine-labeled C3 exotransferase was introduced into cells using a lipid mediated transfer method (see Materials and Methods section). The presence and efficiency of C3 protein transfer was determined by visualizing cells under a fluorescent microscope.*

Discussion

Despite recent advances in multimodality treatments, the prognosis for patients with IBC is guarded, leading to poor overall survival and to significant impairment of local control of the disease in the breast and chest wall. This is primarily due to the ability of the tumor to grow quickly and disseminate to distant organs where metastatic cells can establish secondary tumors. Both of these properties are facilitated by and dependent on neovascularization, which provide both nutrients for the primary tumor and a means for metastatic cells to access the circulation [19,20].

Angiogenesis in IBC is dependent on the active production of several potent pro-angiogenic factors and cytokines and the inhibition of anti-angiogenic cytokines [21–23]. Two well-described pro-angiogenic factors that are active in IBC are VEGF and bFGF. These two angiogenic factors can act synergistically to induce angiogenesis [24,25]. Production of VEGF and bFGF has been demonstrated for a variety of tumors such as melanoma, prostate, and lung cancer [26–28]. Previous unpublished studies in our laboratory have demonstrated that IBC cell lines and tumors produce large quantities of VEGF and bFGF. Other laboratories have demonstrated that VEGF expression and production is increased early in preinvasive breast cancers, whereas bFGF is increased in invasive breast tumors in general [29]. The relationship between oncogenic transformation and angiogenesis has been explored in several studies.

Exposure of NIH3T3 cells to TPA, IL-1β, PDGF, or TGF-β can induce expression of VEGF mRNA [30–33]. As these mechanisms use the same signal transduction pathways as *ras*, other groups have investigated and demonstrated upregulation of VEGF by mutant and/or overexpressed oncogenes such as H- and K-*ras*, v-*raf* and v-*src* [34–37]. It is believed that activation of the MAP kinase pathway leads

to the induction of the AP-1 transcription factor, which could bind to four potential AP-1 consensus sites in the human VEGF gene [38,39]. Another hypothesis is that induction of VEGF expression could occur through the phosphatidylinositol 3-kinase pathway, as has been demonstrated in endothelial cell models [40]. An increasing body of evidence suggests that the mode of VEGF induction (i.e., MAPK vs PI3K) by activated H-*ras* is a cell-type specific process, with cells of epithelial origin signaling more commonly through the MAP kinase pathway whereas those of fibroblastic origin utilizing the PI3K pathway [10].

The *Rho* genes, which were originally cloned on the basis of their homology to *ras*, also use the same signal transduction pathways to induce gene transcription (reviewed in Ref. [41]). However, it was not previously known whether the Rho proteins modulate the production of angiogenic factors in cancer cells. In this study, we demonstrate strikingly high levels of VEGF production by HME cells overexpressing *RhoC GTPase* and not by HME-β-gal controls. The HME-RhoC cells had a five-fold increase in VEGF production over the control transfected cells, nearly recapitulating the VEGF levels produced by the SUM149 IBC cell line. Furthermore, VEGF levels were reduced to a level equivalent to the control cells when the HME-RhoC cells were treated with recombinant human C3 exotransferase, a specific inhibitor of Rho activity (reviewed in Ref. [42]). Similar results were seen for the SUM149 cell line, which also overexpresses *RhoC GTPase*, when treated with the C3 exoenzyme. In contrast to the *RhoC* overexpressing cells, the HME-β-gal controls were unaffected by C3 treatment. Although the C3 exotransferase is not a specific inhibitor of *RhoC* itself, it may therefore be inhibiting more than one Rho molecule or more than one process. However, because both the HME-β-gal and the HME-RhoC transfectants are genotypically identical except for the expression of *RhoC GTPase*, we can confidently state that inhibition of angiogenic factor production is due to inhibition of RhoC GTPase. Taken together, these results not only demonstrate that the specific GTPase function of *RhoC* is required for the increased production of VEGF and bFGF, but that *RhoC* overexpression is specifically responsible for this effect. This latter conclusion derives from the lack of effect of C3 exotransferase on VEGF and bFGF production in HME-β-gal controls that express *RhoA*, *RhoB*, and other members of the Rho family, at normal levels.

A recent study has demonstrated that acidic FGF is transcriptionally regulated by ras, rac, and cdc42 [43]. Ras and rac were shown to activate the bFGF promoter, although it is not known whether bFGF transcription was increased. Our data clearly indicate that *RhoC GTPase* overexpressing cells produce more bFGF than the corresponding controls. Similar to the results obtained for VEGF, production of bFGF by these cells was diminished, although not entirely eliminated, by treatment with C3 exotransferase. This suggests that the basal production of bFGF may be RhoC independent in IBC.

IL-6 is an inflammatory cytokine that has become known as an indirect effector of angiogenesis because it can induce VEGF expression [44]. Whether *RhoC* overexpression can directly induce IL-6 production has yet to be addressed. Although the data in this study demonstrate that expression levels of IL-6 are higher in both the HME-RhoC and SUM149 IBC cells as compared with normal and HME-β-gal control cells, the increase in expression may not be a direct effect, but due to induction of expression by bFGF. Other studies suggest that bFGF, acting in an autocrine and paracrine fashion, can induce IL-6 expression through the p38-MAP kinase pathway [45]. Levels of IL-6 were moderately reduced when the cells were treated with C3 exotransferase, suggesting that the presence of bFGF could be inducing IL-6 expression independent of *RhoC* activity. It is therefore unknown at this time whether induction of IL-6 is directly linked to *RhoC* expression. However, it is clear from these data that VEGF expression is induced by *RhoC*, at least in part, independently of IL-6.

It has been suggested that Rho proteins and the p38-MAP kinase pathway modulate the expression of IL-8 [11,46]. IL-8 expression has profound biologic consequences: it is a potent angiogenic, mitogenic, and chemotactic factor, as has been shown for several tumor types, particularly melanoma, breast, prostate, bladder, and lung cancers [47–51]. Furthermore, IL-8 can increase the growth rate of both tumor and endothelial cells, and although its role in the establishment of metastases is unclear, it can increase both tumor cell growth rates and metastatic potential in nude mice [52]. In this study, we demonstrate a 10-fold increase in IL-8 expression by the HME-RhoC cells over the control-transfected cells, and a two-fold increase over the SUM149 IBC cell lines. IL-8 production was significantly reduced in the HME-RhoC transfectants by treatment with C3 exotransferase. However, these levels are not significantly decreased by inhibition of *RhoC* by C3 exotransferase in the SUM149 IBC cell line. IL-8 production in these cells may be driven by another factor that signals to the nucleus in the presence of *RhoC* overexpression, with bFGF being one possible candidate.

Conclusion

We have demonstrated increased expression of VEGF, bFGF, IL-6, and IL-8 in HME-RhoC stable transfectants compared with HME control transfectants. These levels recapitulated those of the wild-type SUM149 IBC cell line, which also overexpresses *RhoC GTPase*, thus demonstrating a key role for *RhoC* overexpression in modulation of angiogenesis by mammary epithelial cells. Further studies are needed to understand in detail the molecular basis for the modulation of production of the individual angiogenic factors by *RhoC GTPase*.

References

[1] Levine PH, Steinhorn SC, and Ries IG (1985). Inflammatory breast cancer. The experience of the surveillance, epidemiology, and end results (SEER) program. *J Natl Cancer Inst* **74**, 291–297.

[2] Jaiyesimi I, Buzdar A, and Hortobagyi G (1992). Inflammatory breast cancer: a review. *J Clin Oncol* **10**, 1014–1024.

[3] Beahrs O, Henson D, and Hutter R (1988). *Manual for Staging of Cancer* (3rd ed). pp. 145–150.

[4] van Golen KL, Davies S, Wu ZF, Wang Y, Bucana CD, Root H, Chandrasekharappa S, Strawderman M, Ethier SP, and Merajver SD (1999). A novel putative low-affinity insulin-like growth factor-binding protein, LIBC (lost in inflammatory breast cancer), and *RhoC GTPase* correlate with the inflammatory breast cancer phenotype. *Clin Cancer Res* **5**, 2511–2519.

[5] van Golen KL, Wu ZF, Qiao XT, Bao LW, and Merajver SD (2000). *RhoC GTPase*, a novel transforming oncogene for human mammary epithelial cells that partially recapitulates the inflammatory breast cancer phenotype. *Cancer Res* **60**, 5832–5838.

[6] Ridley AJ, and Hall A (1992). The small GTP-binding protein rho regulates the assembly of focal adhesions and actin stress fibers in response to growth factors. *Cell* **70**, 389–399.

[7] Nobes CD, and Hall A (1999). Rho GTPases control polarity, protrusion, and adhesion during cell movement. *J Cell Biol* **144**, 1235–1244.

[8] Nobes CD, and Hall A (1995). Rho, rac, and cdc42 GTPases regulate the assembly of multimolecular focal complexes associated with actin stress fibers, lamellipodia and filopodia. *Cell* **81**, 62.

[9] Okada F, Rak JW, St.Croix B, Lieubeau B, Kaya M, Roncari L, Shirasawa S, Sasazuki T, and Kerbel RS (1998). Impact of oncogenes in tumor angiogenesis: mutant ki-ras up-regulation of vascular endothelial growth factor/vascular permeability factor is necessary, but not sufficient for tumorigenicity of human colorectal carcinoma cells. *Proc Natl Acad Sci USA* **95**, 3609–3614.

[10] Rak J, Mitsuhashi Y, Sheehan C, Tamir A, Viloria-Petit A, Filmus J, Mansour SJ, Ahn NG, and Kerbel RS (2000). Oncogenes and tumor angiogenesis: differential modes of vascular endothelial growth factor up-regulation in ras-transformed epithelial cells and fibroblasts. *Cancer Res* **60**, 490–498.

[11] Hippenstiel S, Soeth S, Kellas B, Fuhrmann O, Seybold J, Krull M, Eichel-Streiber C, Goebeler M, Ludwig S, and Suttorp N (2000). Rho proteins and the p38-MAPK pathway are important mediators for LPS-induced interleukin-8 expression in human endothelial cells. *Blood* **95**, 3044–3051.

[12] Ethier SP, Kokeny KE, Ridings JW, and Dilts CA (1996). erbB family receptor expression and growth regulation in a newly isolated human breast cancer cell line. *Cancer Res* **56**, 899–907.

[13] Ethier SP (1996). Human breast cancer cell lines as models of growth regulation and disease progression. *J Mammary Gland Biol Neoplasia* **1**, 111–121.

[14] Sartor C, Dziubinski M, Yu CL, Jove R, and Ethier SP (1997). Role of epidermal growth factor receptor and STAT-3 activation in autonomous proliferation of *SUM*-102PT human breast cancer cells. *Cancer Res* **57**, 978–987.

[15] Band V, Zajchowski D, Kulesa V, and Sager R (1990). *Human* papilloma virus DNAs *immortalize* normal *epithelial cells* and reduce their growth factor requirements. *Proc Natl Acad Sci USA* **87**, 463–467.

[16] Nicosia RF, and Ottinetti A (1990). Growth of microvessels in serum-free matrix culture of rat aorta. A quantitative assay of angiogenesis *in vitro*. *Lab Invest* **63**, 115–122.

[17] Stasia MJ, and Vignais PV (1995). In JM Abelson and MI Simon (Eds). *Methods in Enzymology*. Academic Press, New York. Vol. 256. pp. 324–327.

[18] Kleer CG, van Golen KL, and Merajver SD (2000). Inflammatory breast cancer: clinical syndrome and molecular determinants. Submitted to *Breast Cancer Res* **2**, 423–429.

[19] Weidner N, Semple JP, Welch WR, and Folkman J (1991). Tumor angiogenesis and metastasis-correlation in invasive breast carcinoma. *N Engl J Med* **324**, 1–8.

[20] Fidler IJ, Kumar R, Bielenberg DR, and Ellis LM (1998). Molecular determinants of angiogenesis in cancer metastasis. *Cancer J Sci Am* **4**, S58–S66.

[21] Folkman J (1994). Angiogenesis and breast cancer. *J Clin Oncol* **12**, 441–443.

[22] Folkman J (1985). Angiogenesis and its inhibitors. In V DeVita, S Hellman and S Rosenberg (Eds). *Important Advances in Oncology*. J.B. Lippincott, Philadelphia, PA. pp. 42–62.

[23] Folkman J (1995). Angiogenesis inhibitors generated by tumors. *Mol Med* **1**, 120–122.

[24] Asahara T, Bauters C, Zheng LP, Takeshita S, Bunting S, Ferrara N, Symes JF, and Isner JM (1995). Synergistic effect of vascular endothelial growth factor and basic fibroblast growth factor on angiogenesis *in vivo*. *Circulation* **92**, II365–II371.

[25] Pepper MS, Ferrara N, Orci L, and Montesano R (1992). Potent synergism between vascular endothelial growth factor and basic fibroblast growth factor in the induction of angiogenesis *in vitro*. *Biochem Biophys Res Commun* **189**, 824–831.

[26] Harper ME, Glynne-Jones E, Goddard L, Mathews P, and Nicholson RI (1998). Expression of androgen receptor and growth factors in premalignant lesions of the prostate. *J Pathol* **186**, 169–177.

[27] Volm M, Koomagi R, Mattern J, and Stammler G (1997). Angiogenic growth factors and their receptors in non-small cell lung carcinomas and their relationships to drug response *in vitro*. *Anticancer Res* **17**, 99–103.

[28] Danielsen T, and Rofstad EK (1998). VEGF, BFGF and EGF in the angiogenesis of human melanoma xenografts. *Int J Cancer* **76**, 836–841.

[29] Heffelfinger SC, Miller MA, Yassin R, and Gear R (1999). Angiogenic growth factors in preinvasive breast disease. *Clin Cancer Res* **5**, 2867–2876.

[30] Wang D, Huang HJ, Kazlauskas A, and Cavenee WK (1999). Induction of vascular endothelial growth factor expression in endothelial cells by platelet-derived growth factor through the activation of phosphatidylinositol 3-kinase. *Cancer Res* **59**, 1464–1472.

[31] Li J, Perrella MA, Tsai JC, Yet SF, Hsieh CM, Yoshizumi M, Patterson C, Endege WO, Zhou F, and Lee ME (1995). Induction of vascular endothelial growth factor gene expression by interleukin-1 beta in rat aortic smooth muscle cells. *J Biol Chem* **270**, 308–312.

[32] Finkenzeller G, Marme D, Weich HA, and Hug H (1992). Platelet-derived growth factor-induced transcription of the vascular endothelial growth factor gene is mediated by protein kinase C. *Cancer Res* **52**, 4821–4823.

[33] Pertovaara L, Kaipainen A, Mustonen T, Orpana A, Ferrara N, Saksela O, and Alitalo K (1994). Vascular endothelial growth factor is induced in response to transforming growth factor-beta in fibroblastic and epithelial cells. *J Biol Chem* **269**, 6271–6274.

[34] Grugel S, Finkenzeller G, Weindel K, Barleon B, and Marme D (1995). Both v-Ha-Ras and v-Raf stimulate expression of the vascular endothelial growth factor in NIH 3T3 cells. *J Biol Chem* **270**, 25915–25919.

[35] Konishi T, Huang CL, Adachi M, Taki T, Inufusa H, Kodama K, Kohno N, and Miyake M (2000). The K-ras gene regulates vascular endothelial growth factor gene expression in non-small cell lung cancers. *Int J Oncol* **16**, 501–511.

[36] Mukhopadhyay D, Tsiokas L, and Sukhatme VP (1995). Wild-type p53 and v-Src exert opposing influences on human vascular endothelial growth factor gene expression. *Cancer Res* **55**, 6161–6165.

[37] Rak J, Mitsuhashi Y, Bayko L, Filmus J, Shirasawa S, Sasazuki T, and Kerbel RS (1995). Mutant ras oncogenes upregulate VEGF/VPF expression: implications for induction and inhibition of tumor angiogenesis. *Cancer Res* **55**, 4575–4580.

[38] Milanini J, Vinals F, Pouyssegur J, and Pages G (1998). p42/p44 MAP kinase module plays a key role in the transcriptional regulation of the vascular endothelial growth factor gene in fibroblasts. *J Biol Chem* **273**, 18165–18172.

[39] Damert A, Ikeda E, and Risau W (1997). Activator-protein-1 binding potentiates the hypoxia-inducible factor-1-mediated hypoxia-induced transcriptional activation of vascular-endothelial growth factor expression in C6 glioma cells. *Biochem J* **327** (Pt 2), 419–423.

[40] Jiang BH, Zheng JZ, Aoki M, and Vogt PK (2000). Phosphatidylinositol 3-kinase signaling mediates angiogenesis and expression of vascular endothelial growth factor in endothelial cells. *Proc Natl Acad Sci USA* **97**, 1749–1753.

[41] Lim L, Manser E, Leung T, and Hall C (1996). Regulation of phosphorylation pathways by p21 GTPases. The p21 Ras-related Rho subfamily and its role in phosphorylation signaling pathways. *Eur J Biochem* **242**, 171–185.

[42] Aktories K (1997). Rho proteins: targets for bacterial toxins. *Trends Microbiol* **5**, 282–288.

[43] Chotani MA, Touhalisky K, and Chiu IM (2000). The small GTPases Ras, Rac and Cdc42 transcriptionally regulate expression of human fibroblast growth factor 1. *J Biol Chem* **275**, 30432–30438.

[44] Cohen T, Nahari D, Cerem LW, Neufeld G, and Levi BZ (1996). Interleukin 6 induces the expression of vascular endothelial growth factor. *J Biol Chem* **271**, 736–741.

[45] Kozawa O, Tokuda H, Matsuno H, and Uematsu T (1999). Involvement of p38 mitogen-activated protein kinase in basic fibroblast

growth factor-induced interleukin-6 synthesis in osteoblasts. *J Cell Biochem* **74**, 479–485.

[46] Warny M, Keates AC, Keates S, Castagliuolo I, Zacks JK, Aboudola S, Qamar A, Pothoulakis C, LaMont JT, and Kelly CP (2000). p38 MAP kinase activation by *Clostridium difficile* toxin A mediates monocyte necrosis, IL-8 production, and enteritis. *J Clin Invest* **105**, 1147–1156.

[47] Rodeck U, Becker D, and Herlyn M (1991). Basic fibroblast growth factor in human melanoma. *Cancer Cells* **3**, 308–311.

[48] Speirs V, and Atkin SL (1999). Production of VEGF and expression of the VEGF receptors Flt-1 and KDR in primary cultures of epithelial and stromal cells derived from breast tumours. *Br J Cancer* **80**, 898–9030.

[49] Inoue K, Slaton JW, Eve BY, Kim SJ, Perrotte P, Balbay MD, Yano S, Bar-Eli M, Radinsky R, Pettaway CA, and Dinney CP (2000). Interleukin 8 expression regulates tumorigenicity and metastases in androgen-independent prostate cancer [in process citation]. *Clin Cancer Res* **6**, 2104–2119.

[50] Miller LJ, Kurtzman SH, Wang Y, Anderson KH, Lindquist RR, and Kreutzer DL (1998). Expression of interleukin-8 receptors on tumor cells and vascular endothelial cells in human breast cancer tissue. *Anticancer Res* **18**, 77–81.

[51] Mizuno K, Sone S, Orino E, Mukaida N, Matsushima K, and Ogura T (1994). Spontaneous production of interleukin-8 by human lung cancer cells and its augmentation by tumor necrosis factor alpha and interleukin-1 at protein and mRNA levels. *Oncology* **51**, 467–471.

[52] Bar-Eli M (1999). Role of interleukin-8 in tumor growth and metastasis of human melanoma. *Pathobiology* **67**, 12–18.

Clinical & Experimental Metastasis **19:** 301–311, 2002.

Mitogen activated protein kinase pathway is involved in RhoC GTPase induced motility, invasion and angiogenesis in inflammatory breast cancer

Kenneth L. van Golen[1], Li Wei Bao[1], Quintin Pan[1], Fred R. Miller[2], Zhi Fen Wu[1] & Sofia D. Merajver[1]
[1]*Department of Internal Medicine, University of Michigan Comprehensive Cancer Center, Ann Arbor, Michigan, USA;*
[2]*Breast Cancer Program, Barbara Ann Karmanos Cancer Institute, Detroit, Michigan, USA*

Received 24 August 2001; accepted in revised form 4 December 2001

Key words: angiogenic factors, C3 exotransferase, human mammary epithelial (HME) cells, inflammatory breast cancer (IBC), inhibitors, invasion, mitogen activated protein kinase (MAPK), motility, phosphatidylinositol-3 kinase (PI3K), RhoC GTPase

Abstract

Inflammatory breast cancer (IBC) is the most lethal form of locally advanced breast cancer known. IBC carries a guarded prognosis primarily due to rapid onset of disease, typically within six months, and the propensity of tumor emboli to invade the dermal lymphatics and spread systemically. Although the clinical manifestations of IBC have been well documented, until recently little was known about the genetic mechanisms underlying the disease. In a comprehensive study aimed at identifying the molecular mechanisms responsible for the unique IBC phenotype, our laboratory identified overexpression of RhoC GTPase in over 90% of IBC tumors in contrast to 36% of stage-matched non-IBC tumors. We also demonstrated that overexpression of RhoC GTPase in human mammary epithelial (HME) cells nearly recapitulated the IBC phenotype with regards to invasion, motility and angiogenesis. In the current study we sought to delineate which signaling pathways were responsible for each aspect of the IBC phenotype. Using well-established inhibitors to the mitogen activated protein kinase (MAPK) and phosphatidylinositol-3 kinase (PI3K) pathways. We found that activation of the MAPK pathway was responsible for motility, invasion and production of angiogenic factors. In contrast, growth under anchorage independent conditions was dependent on the PI3K pathway.

Abbreviations: ELISA – enzyme linked immunoabsorbant assay; FBS – fetal bovine serum; FGF2 – basic fibroblast growth factor; FGF-BP – fibroblast growth factor binding protein; HME – human mammary epithelial; IBC – inflammatory breast cancer; IGFBP-rP – insulin-like growth factor binding protein related protein; IL – interleukin, LABC – locally advanced breast cancer; MAPK – mitogen activated protein kinase; MEM – minimal essential medium; MTT – 3-[4,5-Dimethylthiazol-2-yl]-2,5-diphenyltetrazolium bromide; PI3K – phosphatidylinositol-3 kinase; TCA – tricholoracetic acid; VEGF – vascular endothelial growth factor

Introduction

Inflammatory breast cancer (IBC) is a phenotypically distinct form of locally advanced breast cancer (LABC) that has a propensity to invade, grow and spread in the dermal lymphatics of the skin overlying the breast [1–3]. It is the ability of the tumor emboli to invade and block the dermal lymphatics that leads to its poor prognosis [1–4].

Although the clinical manifestations of IBC have been well documented in the literature, until recently little was known about the molecular mechanisms involved in conferring the unique IBC phenotype. In an effort to identify genetic alterations involved in determining the IBC phenotype, our laboratory isolated two genes that were consistently and concordantly altered in IBC compared with stage-matched non-IBC tumors [5]. RhoC GTPase, was found to be over-expressed in 90% of IBC tumors versus 36% of the stage-matched controls.

RhoC GTPase is a member of the Ras-superfamily of small GTP binding proteins and is primarily responsible for re-organization of the actin cytoskeleton leading to the formation of lamellipodia and fillipodia resulting in cellular motility [6–13]. Transfection of the RhoC homologue, RhoB, into Ras-transformed NIH3T3 cells leads to increased focus formation suggesting a role for the Rho proteins as a transforming oncogene or as a metastasis gene [14]. Similarly, our laboratory has demonstrated that RhoC transfected HME cells become highly motile and invasive, grow under anchorage independent conditions, produce angiogenic factors, and are tumorigenic and metastatic when orthotopically implanted into nude mice [15–17].

Correspondence to: Sofia D. Merajver, MD, PhD, Department of Internal Medicine, University of Michigan Comprehensive Cancer Center, 7217 CCGC, 1500 East Medical Center Drive, Ann Arbor, MI 48109-0948, USA. Tel: +1-734-764-2248; Fax: +1-734-615-2719; E-mail: smerajve@umich.edu

These *in vitro* data have additional clinical significance as RhoC overexpression is associated with the transition to metastatic disease in other cancers [18–20]. It has been proposed that Rho proteins act through and potentiate signaling via the c-Jun kinase/stress activated protein kinase (JNK/SAPK) and mitogen activated protein kinase (MAPK) pathway (reviewed by Takai et al. [21]). Evidence from other laboratories suggest that Rho proteins can signal through both the MAPK pathway as well as the phosphoinositol-3 kinase (PI3K) pathway, while cdc42 and Rac1 are associated with the JNK/SAPK pathway [22–25]. Furthermore, it has been demonstrated that in certain cell types, the MAPK pathway is involved in signaling and the production of angiogenic factors while the PI3K pathway is involved in growth and survival [26–33].

In the present study we set out to determine the major pathways involved in RhoC signaling in IBC. Specifically, we attempted to determine which pathways and cascades were involved in conferring specific aspects of the RhoC-induced phenotype. Many of the published studies that describe the signal transduction pathways involved in Rho signaling were performed in transfected NIH3T3 cells, thus our study focused on the RhoC signaling pathways specific to IBC and HME cells. We treated HME-RhoC stable transfectants, control HME-β-galactosidase (HME-β-gal) transfectants or the SUM149 IBC cell line with C3 exotransferase (a specific inhibitor of Rho proteins), a variety of MAPK inhibitors, or a PI3K inhibitor and assayed them for specific biological functions. The inhibitors were used at concentrations that would inhibit signal transduction without affecting cellular viablility. We found that the PI3K pathway was involved in anchorage independent growth and survival, while multiple arms of the MAPK pathway were involved in motility and invasion, and that p38 is a downstream modulator in the production of angiogenic factors. These data provide significant new insight as to how overexpression of RhoC can lead to a variety of phenotypic effects in breast cells.

Materials and methods

Cell culture

Cell lines were maintained under defined culture conditions for optimal growth in each case [34–36]. Briefly, human mammary epithelial (HME) cells were immortalized with human papilloma virus E6/E7 [37] and grown in 5% fetal bovine serum (FBS; Sigma Chemical Co., St. Louis, Missouri) supplemented Ham's F-12 medium (JRH BioSciences, Lenexa, Kansas) containing insulin, hydrocortisone, epidermal growth factor, and cholera toxin (Sigma Chemical Co.). Stable HME transfectants containing either the human wild-type RhoC GTPase or control β-galactosidase genes were produced and maintained in the described medium supplemented with 100 μg/ml hygromycin (LifeScience Technologies) as previously published [15–17]. The SUM149 cell line was developed from a primary IBC tumor and grown in 5% FBS supplemented Ham's F-12 medium containing insulin and hydrocortizone. The HME cells were characterized as being keratin 19 positive, ensuring that they are from the same differentiation lineage as the SUM149 IBC tumor cell line [5].

Cells actively growing in culture were treated with MAPK inhibitors, 2.0 μM PD98059, 1.5 μM U0126, 1.5 μM SKF86002, or 1.5 μM SB220025 (all obtained from Calbiochem, San Diego, California) 24 h prior to assays and treated everyday with fresh inhibitor until the end of the assay. Treatment of cells with 2.5 μM LY294002 (Calbiochem), a PI3K inhibitor, was performed in the same manner as described for the MAPK inhibitors. These concentrations were below the IC_{50} of the compounds to avoid direct cell toxicity to allow for meaningful biological assays.

Western blot analysis

Proteins were harvested from cell cultures using RIPA buffer (1× PBS, 1% Nonidet P-40, 0.5% sodium deoxycholate, 0.1% SDS, 0.1 mg/ml PMSF, 1 mM sodium orthovanadate and 0.3 mg/ml aprotinin; Sigma Chemical Co.). Ten μg aliquots were mixed with Laemelli buffer, heat denatured for 3 min, separated by SDS-PAGE, and transferred to nitrocellulose. Non-specific binding was blocked by overnight incubation with 2% powdered milk in tris-buffered saline with 0.05% Tween-20 (Sigma Chemical Co.). Immobilized proteins were probed using antibodies specific for total MAPK proteins, the membranes were then stripped and reprobed for the phosphorylated form of the MAPK protein. Specifically, p38/pp38, pJNK/ppJNK, and pErk/ppErk (Cell Signaling Technologies, Beverly, Massachusettes). Protein bands were visualized by ECL (Amersham-Pharmacia Biotech, Piscataway, New Jersey).

C3 exotransferase treatment

Active C3 exoenzyme was introduced into the HME, HME-β-gal, HME-RhoC, and SUM149 cells using a method based on liposome encapsulation and membrane fusion, which we have termed lipoporation [16]. Briefly, cells were grown in 6-well plates until reaching a confluence of 40–50% and the medium replaced with fresh medium. Three micrograms of human recombinant C3 exotransferase (Cytoskeleton Inc., Denver, Colorado) was combine with FuGene^{TM} 6 transfection reagent (Roche-Boehringer Mannheim) and added to the cultures. As controls either an equal quantity of human recombinant tubulin or FuGene^{TM} 6 alone were added to cell cultures. The cells were incubated for 2 days at 37 °C, at which time cell-conditioned medium was harvested. Presence of the intracellular C3 exoenzyme was confirmed by visualizing the rhodamine-tagged protein using fluorescent microscopy. The efficiency and activity of both the transfected and lipoporated C3 exoenzyme were confirmed by a quantitative ADP-ribosylation assay [38].

The efficiency of *in vivo* ADP-ribosylation of RhoC GTPase by C3 exotransferase was determined as previously described [16]. Active C3 exotransferase was efficiently introduced into HME-β-gal, HME-RhoC, and SUM149, as described above. Cells were collected 48 h later, washed

in medium, and pelleted. The cells were lysed in 20 mM HEPES pH 8.0 (Sigma Chemical Co.) by 3 repeated freeze/thaw cycles. Cell lysates (10 μg) were combined with 50 ng/ml C3 exotransferase and 5×10^6 cpm (with a specific activity of 1×10^6 cpm/μl) [^{32}P]NAD (Amersham) in ADP-ribosylation buffer (20 mM HEPES, pH 8.0, 1 mM $MgCl_2$, 1 mM AMP and thymadine, Sigma Chemical Co.), and incubated for 30 min at 37 °C. TCA-percipitable material was then recovered and radioactivity was counted on a Packard scintillation counter.

Growth assays

Monolayer culture growth rate was determined as previously described [39] by conversion of MTT (3-[4,5-dimethylthiazol-2-yl]-2,5-diphenyltetrazolium bromide; Sigma Chemical Co.) to a water insoluble formazon by viable cells. Three thousand cells in 200 μl medium were plated in 96-well plates and grown under normal conditions. Cultures were assayed at 0, 1, 2, 3, 5 and 7 days by the addition of 40 μl 5 mg/ml MTT and incubating for 1 h at 37 °C. The time points of the assay were chosen to sufficiently discern any effect that the inhibitors may have on cell viability, which may affect the outcomes of the phenotypic experiments. The MTT containing medium was aspirated and 100 μl DMSO (Sigma Chemical Co.) added to lyse the cells and solublize the formazon. Absorbance values of the lysates were determined on a Dynatech MR 5000 microplate reader at 540 nm.

For anchorage independent growth assays, a 2% stock of sterile low-melt agarose was diluted 1:1 with 2× MEM. Further dilution to 0.6% agarose was made using 10% FBS supplemented Ham's F-12 medium complete with growth factors, and 1 ml was added to each well of a six-well plate as a base-layer. The cell layer was then prepared by diluting agarose to 0.3% and 0.6% with 10^3 cells in 2.5% FBS supplemented Ham's F-12/1.5 ml/well. Colonies greater than or equal to 100 μ in diameter were counted after a 3-week incubation at 37 °C in a 10% CO_2 incubator.

Random motility assay

Random motility was determined using a gold-colloid assay [40]. Gold-colloid (Sigma Chemical Co.) was layered onto glass coverslips and placed into 6-well plates. Cells were plated onto the coverslips and allowed to adhere for 1 h at 37 °C in a CO_2 incubator (12500 cells/3 ml in serum-free medium). To stimulate the cells, the serum-free medium was replaced with 5% FBS containing Ham's F-12 supplemented with growth factors and allowed to incubate for 3 h at 37 °C. The medium was aspirated and the cells fixed using 2% gluteraldehyde (Sigma Chemical Co.). The coverslips were then mounted onto glass microscope slides and areas of clearing in the gold-colloid corresponding to phagokinetic cell tracks counted.

Invasion assay

The invasion assay was performed as previously described with minor modification [39]. A 10 μl aliquot of 10 mg/ml Matrigel (Becton Dickenson, Bedford, Massachusetts) was spread onto a 6.5 mm Transwell filter with 8 μm pores (Costar, Corning, New York) and air dried in a laminar flow hood. Once dried, the filters were reconstituted with a few drops of serum-free medium. The lower chamber of the Transwell was filled with either serum-free or serum containing media. Cells were harvested and resuspended in serum-free medium with 0.1% BSA at a concentration of 3.75×10^5 cells/ml and 0.5 ml was added to the top chamber. The chambers were incubated for 24 h at 37 °C in a 10% CO_2 incubator. The cell suspension was aspirated and excess Matrigel removed from the filter using a cotton swab. The filters were then cut away from the Transwell assembly and fixed with methanol, gel side down, to a glass microscope slide. The fixed filters were stained with hematoxylin and eosin, and the cells on the entire filter were counted at a 40×-magnification individually by two investiagtors. These cells were assumed to have invaded through the Matrigel and filter. The number of cells that had invaded in the serum-free containing lower chambers was considered background and this number was subtracted from the number of cells that had invaded in response to the serum-containing medium.

Quantitation of vascular endothelial growth factor

Levels of soluble cytokines and chemokines were determined from cell-conditioned media. Cells were incubated in normal growth medium for four days. The cell-conditioned media was harvested, centrifuged for 5 min at 2,500 rpm and divided into 1 ml aliquots. The Quantikine human vascular endothelial growth factor (hVEGF; R&D Systems, Minneapolis, Minnesota) were used to measure protein levels of the 165 amino acid species of hVEGF. The enzyme linked immunoabsorbant assay (ELISA) was performed per the manufacturers recommendations.

Results

C3 exotransferase inhibition of RhoC GTPase

In a previous study we demonstrated that inhibition of RhoC GTPase activity by C3 exotransferase treatment led to decreased production of angiogenic factors [16, 17]. In order to demonstrate that the other phenotypic changes seen in the HME-RhoC transfectants are indeed due to RhoC expression, we treated the cells with C3 exotransferase. C3 exotransferase is not a specific inhibitor of RhoC *per se*, but a specific inhibitor of Rho proteins (reviewed in [41]). C3 has been demonstrated to have an affinity for RhoC and affects the formation of actin filaments *in vivo* [42]. Given that the untransfected HME, the HME-β-galactosidase control transfectants, and the HME-RhoC transfected cells were all derived from the same culture, they are likely to share the same distribution of Rho proteins, except for RhoC. Therefore, main changes of phenotype produced by C3 treatment would be ascribed to C3 induced changes in RhoC GTPase activity.

Table 1. Comparison of monolayer population doubling time and anchorage independent growth of untreated and C3 treated HME, HME transfectants and SUM149 IBC cell lines. Despite treatment of the cells with C3, monolayer population doubling time was not affected. In contrast, the ability of the RhoC expressing HME and SUM149 cells to grow under anchorage independent conditions was significantly reduced (* $P = 0.01$, ** $P = 0.001$).

	Population doubling time (hours)		Anchorage independent growth (number of cholonies)	
	Untreated	C3 Treated	Untreated	C3 Treated
HME	34 h	36 h	0 ± 0	0 ± 0.1
HME-β-gal	35 h	34 h	5 ± 0.8	17 ± 7.5
HME-RhoC	33 h	36 h	102 ± 5.4	40 ± 13.6**
SUM149	39 h	39 h	75 ± 4.9	47 ± 3.3*

Active C3 exotransferase was introduced into the cells using a liposome mediated method termed lipoporation [16]. As shown in Table 1, the population doubling time of all the cell lines tested was not significantly affected by C3 treatment. However, the ability of the HME-RhoC transfectants and the SUM149 IBC cell line to grow under anchorage independent conditions, a hallmark of malignant transformation, was significantly reduced. In contrast, C3 treatment of the HME untransfected or the HME-β-gal control did not result in any changes in their ability to grow in soft agar. The monolayer growth rate was not influenced by transfection or RhoC expression, as the HME-RhoC transfectants did not differ from the untransfected or control transfected HME counterparts, or by C3 treatment so, these data suggest that RhoC confers the ability to HME-RhoC cells to grow under anchorage independent conditions.

As demonstrated in Figure 1A, C3 treatment significantly reduced HME-RhoC and SUM149 IBC motility in a random colloidal gold assay. The HME-β-galactosidase control transfectants were unaffected by C3 treatment. Similarly, the ability of the HME-RhoC and SUM149 cells to invade a Matrigel coated filter in response to a chemoattractant was significantly reduced after C3 treatment (Figure 1B).

The activity of the C3 exotransferase was confirmed by measuring the efficiency of *in vivo* ADP-ribosylation. As shown in Figure 1C, in comparison with their non-C3 treated counterparts, all the C3 treated cell lines had a significant reduction in the levels of available sites that could be ADP-ribosylated in the *in vitro* assay. Specifically, the C3-treated HME-RhoC and SUM149 cells had a 2-fold decrease in the number of ADP-ribosylated sites compared to the non-transfected controls. These data indicate that at least half of the Rho proteins have been ADP-ribosylated *in vivo*, and therefore inhibited by C3 exotransferase. Taken together, these data demonstrate that expression and activity of RhoC GTPase is responsible for conferring the ability to grow under anchorage independent conditions, and the production of a motile and invasive cell.

Inhibition of anchorage independent growth by the LY294002 PI3K inhibitor

To determine whether the PI3K or the MAPK pathways were involved in RhoC signaling, the cells were treated with either LY294002 (a potent PI3K inhibitor) or PD98059 (a general MAPK inhibitor that blocks all arms of the MAPK pathway). To avoid confounding effects due to direct cytotoxicity, we chose concentrations of the inhibitors that inhibited signal transduction but were not cytotoxic. The cells were treated 48 h prior to plating in 0.6% soft agar and fresh medium containing each of the inhibitors was layered onto the soft agar daily. The MCF10AT c1 cell line, with a constituitvely active Ras was used as a positive control [43]. The ability of the HME-RhoC and SUM149 cells to form colonies in 0.6% soft agar was significantly reduced by treatment with the PI3K inhibitor (Figure 2). In contrast, treatment with the general MAPK inhibitor PD98059 had little effect on the colony number. The reduction in colony formation was not due to a significant change in the population doubling time of the cells treated with LY294002, as determined by an MTT monolayer growth assay performed on cells treated long-term with the inhibitors (data not shown). These data indicate the PI3K pathway, and not the MAPK pathway is involved in RhoC conferring the ability of the cells to survive and form colonies under anchorage independent conditions.

MAPK status in cell lines after inhibitor treatment

In order to determine which arms of the MAPK pathway were involved in the different aspects of the RhoC-induced phenotype, the cells were treated with a variety of MAPK inhibitors that affect different points of the pathway. The general MAPK inhibitor PD98059 effects the MAPK pathway at 2 distinct, points; (1) MEKK-1 (which activates p38 and MEK1 & 2, and therefore ERK1 & 2), and (2) directly at MEK1 & 2. The inhibitor U0126 specifically inhibits MEK1 & 2 activation. The inhibitors SKF86002 and SB22025 are inhibitors of p38 activation and of p38 itself, respectively. As demonstrated in Figure 3, all cell lines expressed p38, ERK (p42/p44), and JNK/SAPK. However, none of the untreated cell lines (A) expressed activated phospho-JNK/SAPK, sug-

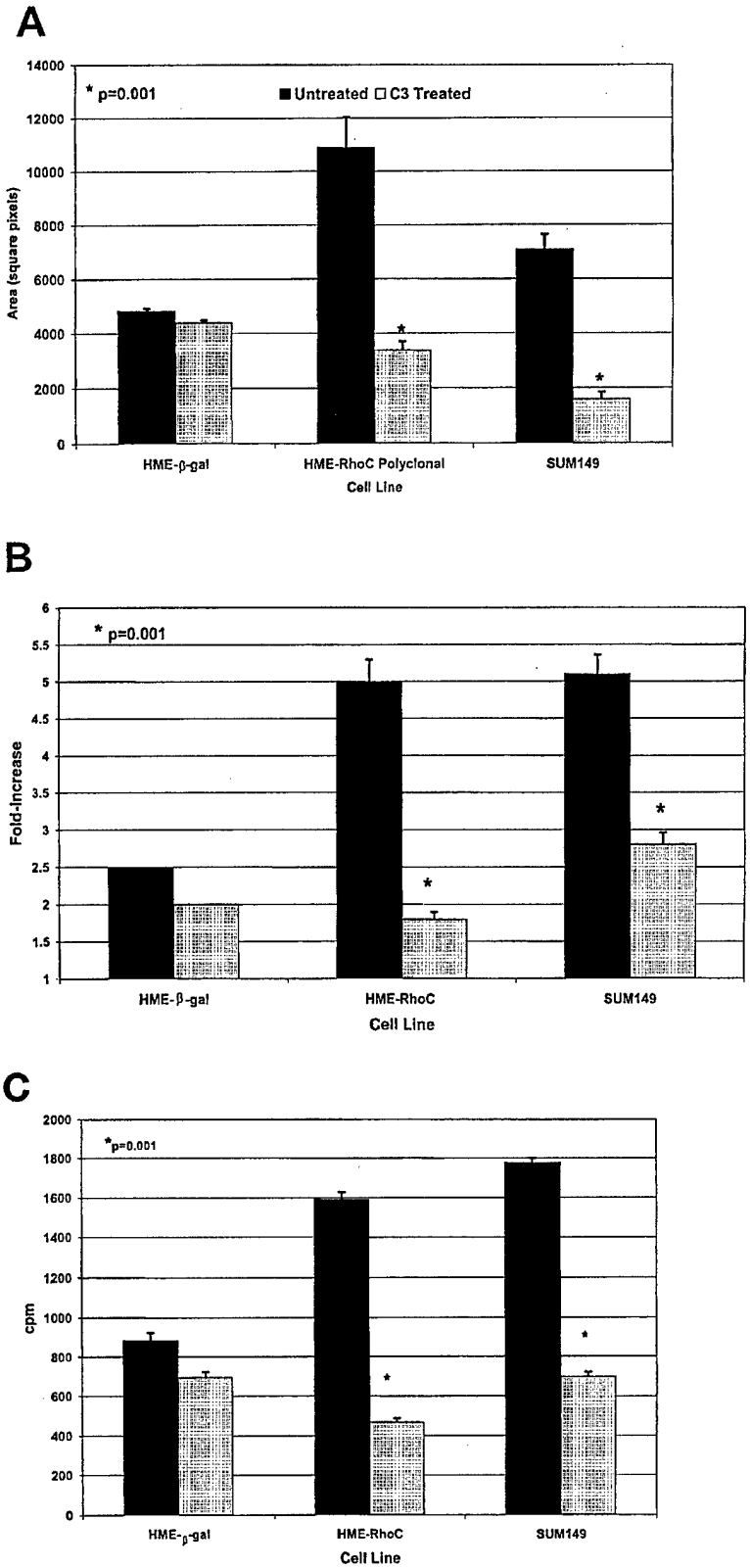

Figure 1. Comparison of the average area of migration in a colloidal gold motility assay by control HME-β-gal and RhoC overexpressing mammary cells after treatment with C3 exotransferase. Treatment of cells with C3 exoenzyme significantly reduced the motile ability of the RhoC overexpressing cells HME-RhoC and SUM149. Similarly, as demonstrated in panel B, the invasive capabilities of the RhoC overexpressing cells were also significantly reduced after C3 treatment as determined in a Matrigel invasion assay. To determine the extent of Rho inhibition by C3 exotransferase, an *in vitro* ADP-ribosylation assay was performed (panel C). The number of ADP-ribosylated targets was greatly reduced in the HME-RhoC and SUM149 cells, thus indicating that C3 exotransferase treatment had effectively blocked the Rho targets within those cells.

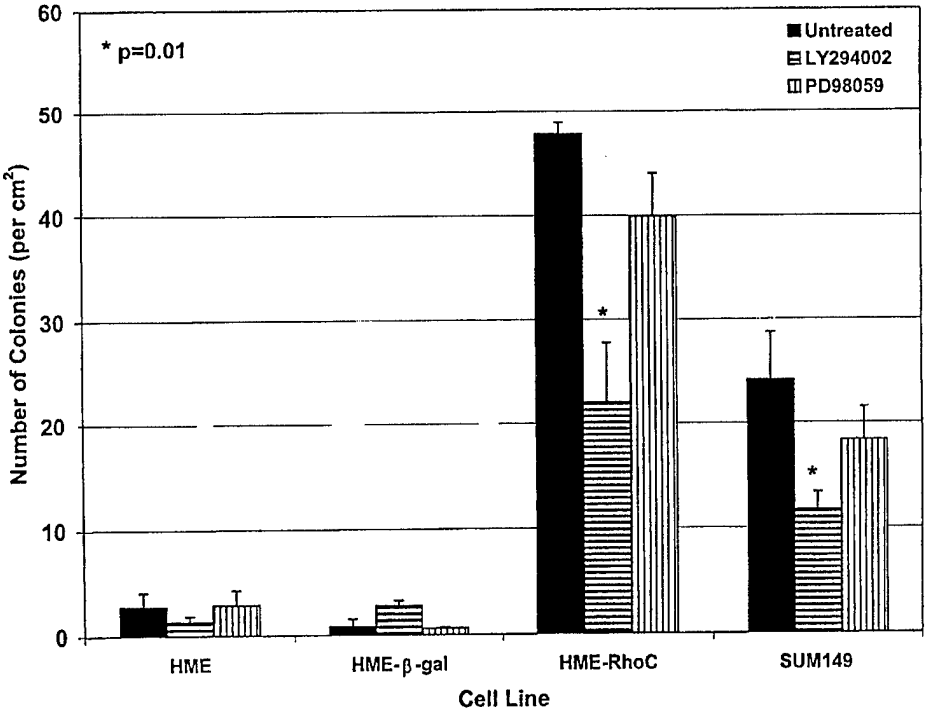

Figure 2. Anchorage independent growth in 0.6% soft agar after treatment with either the PI3K inhibitor LY294002 or the general MAPK inhibitor PD98059. The ability of the RhoC overexpressing cells HME-RhoC and SUM149 was significantly reduced after treatment with the LY294002, but not with PD98059. These data suggests that RhoC-mediated anchorage independent growth, is signaled through the PI3K and not the MAPK pathway in these mammary cells.

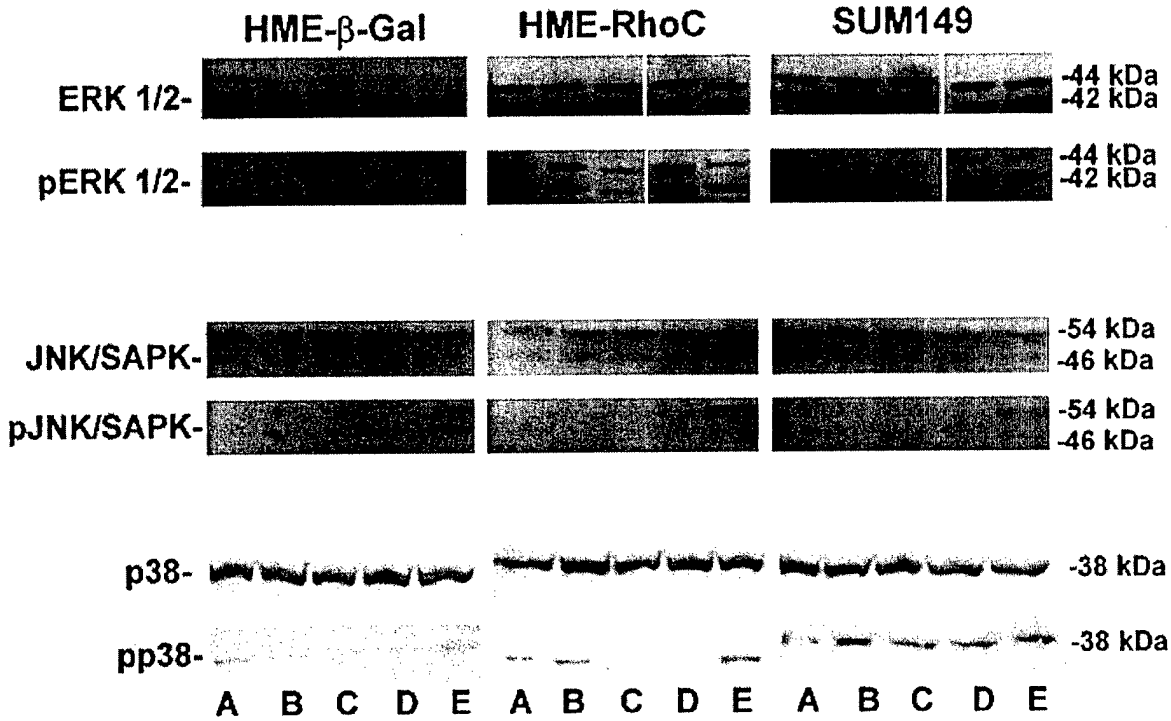

Figure 3. Western blot analysis of basal and phosphorylated (activated) levels of different arms of the MAPK pathway before (A) and after inhibitor treatment with SKF86002 (B), PD98059 (C), U0126 (D), or C3 exotransferase (E). All the cell lines tested expressed ERK (p42/p44), JNK/SAPK, and p38. However, none of the untreated cell lines (A) expressed activated phospho-JNK/SAPK, suggesting that only pp38 and phospho-ERK are involved in RhoC signal transduction. Each set of Western blots looking at p38, JNK/SAPK and ERK were performed separately on the same cell lysates. Each individual blot in the set (i.e. total protein *versus* the phosphorylated form of that protein) was the same blot stripped and re-probed.

gesting that only pp38 and phospho-ERK are involved in RhoC signal transduction. Each set of Western blots looking at p38, JNK/SAPK and ERK were performed separately on the same cell lysates. Each individual blot in the set (i.e., total protein versus the phosphorylated form of that protein) was the same blot stripped and re-probed. Each set of Western blots looking at p38, JNK/SAPK and ERK were performed separately on the same cell lysates. Each set of Western blots compares total protein *versus* the phosphorylated form of that protein of the same blot. Treatment of the cells for 24 h with SKF86002 (B), PD98059 (C), U0126 (D), or C3 exotransferase (E), led to a decrease in the levels of the active phosphorylated form of the target protein(s), while the basal levels remained unchanged. Interestingly, C3 treatment of the cells lead to increased phosphorylation of JNK/SAPK.

Effect of inhibition of MAPK on motility and invasion

Because of the postulated relationship between Rho-induced motility and Ras activation of the MAPK pathway, we set out to understand how are the MAPK signaling cascades are involved in Rho-modulated motility and invasion. To accomplish this we treated the cells with the various MAPK inhibitors described above. The cells were treated with the MAPK inhibitors 48 h prior to assessing motility and invasion. No significant decrease in population doubling time was observed for the cells treated with inhibitors, as determined over a seven-day assay (data not shown).

As demonstrated in Figure 4A, all of the MAPK inhibitors had a significant ($P = 0.01$) effect on the motility of the HME-RhoC and SUM149 cell lines. The areas of the phagokinetic tracks were reduced to nearly the level of the HME-β-gal control cell line, which was unaffected by any of the MAPK inhibitors. Since all of the MAPK inhibitors had an effect on the motility of the cells, this suggested that multiple arms of the MAPK pathway are involved in RhoC mediated motility. Motility of the MCF10AT c1 positive control cell line that has a constituatively active Ras was also affected by all four of the MAPK inhibitors, although the motility of these cells is much reduced compared to the HME-RhoC and SUM149 cells.

Next, we concentrated on the cells ability to invade through a Matrigel coated filter (Figure 4B). The invasive capabilities of the cells are described as fold-increase in invasion over untransfected HME controls. Treatment with all four of the MAPK inhibitors reduced the invasive capabilities of the HME-RhoC and SUM149 cell lines. The HME-β-gal control cells were not significantly affected, by the other MAPK inhibitors. The invasive capabilities of the MCF10AT c1 cells were the same as the HME-β-gal control cells, and were likewise unaffected by the MAPK inhibitors. When cells were treated with a combination of the LY294002 and PD98059 inhibitors, the level of inhibition was similar to that of the PD98059 inhibitor alone (data not shown), suggesting that the PI3K pathway is not involved in either motility or invasion.

Taken together, these data suggest that RhoC induced motility and invasion is mediated to a significant extent by the p38 and ERK arms of the MAPK pathway. This is shared with Ras alone induced motility, but active Ras is not sufficient to produce an invasive phenotype in the MCF10A cells. In all these experiments the concentrations of inhibitors used did not effect cell doubling times or cell viability.

VEGF production after inhibition of the MAPK pathway

In a previous study, we demonstrated that RhoC overexpression leads to increased production of angiogenic factors, particularly vascular endothelial growth factor (VEGF) [16, 17]. Since VEGF production was significantly increased in RhoC expressing breast cells, and considering its importance in as an angiogenic factor, VEGF expression was the logical endpoint to study after inhibitor treatment. Treatment of the mammary cells with the different MAPK inhibitors resulted in decreased VEGF production by the HME-RhoC and SUM149 IBC cell lines (Figure 5). The greatest reduction in VEGF production was seen when the cells were treated with the inhibitor SB22025, which prevents p38 activation. Treatment with the inhibitor SKF86002, an inhibitor of phosho-p38 activity, resulted in the second greatest decrease in VEGF production. Taken together, these data suggest that activation of the p38 arm of the MAPK pathway is responsible for production of VEGF simultaneously by RhoC overexpression.

Discussion

The highly invasive and metastatic phenotype of IBC is one of the hallmarks of its unique clinical manifestations and the major cause of the poor outcome of many patients who are diagnosed with IBC. In a previous set of studies, our laboratory identified RhoC GTPase to be overexpressed in IBC and responsible for anchorage independent growth, cellular motility and invasion, and production of angiogenic factors.

In the current study, we begin to delineate the signaling pathways responsible for each aspect of the RhoC-mediated phenotype. We hypothesized that for RhoC GTPase to achieve diverse phenotypic attributes, cell signaling must take place through several signal transduction pathways. We utilized specific inhibitors of different points of the PI3K and MAPK pathways, an approach which has proven successful in similar previous studies [44, 45].

The MAPK pathway has been previously implicated in Ras and RhoA signaling, while the JNK/SAPK pathway has been shown to be mediated by Rac1 and cdc42 signaling, and all have been shown to use the PI3K pathway (reviewed in [46, 47]). These pathways, depending on cell type, have been attributed to participate in growth/survival and motility (reviewed in [29]). However, the signal transduction pathway(s) utilized by RhoC during growth, motility and invasion has not been described in any cell type. In the current study we examined RhoC signal transduction in the SUM149 IBC and HME-RhoC breast cell lines. Because RhoC appears to be a major determinant of a clinically well-defined mammary cancer metastatic phenotype it is es-

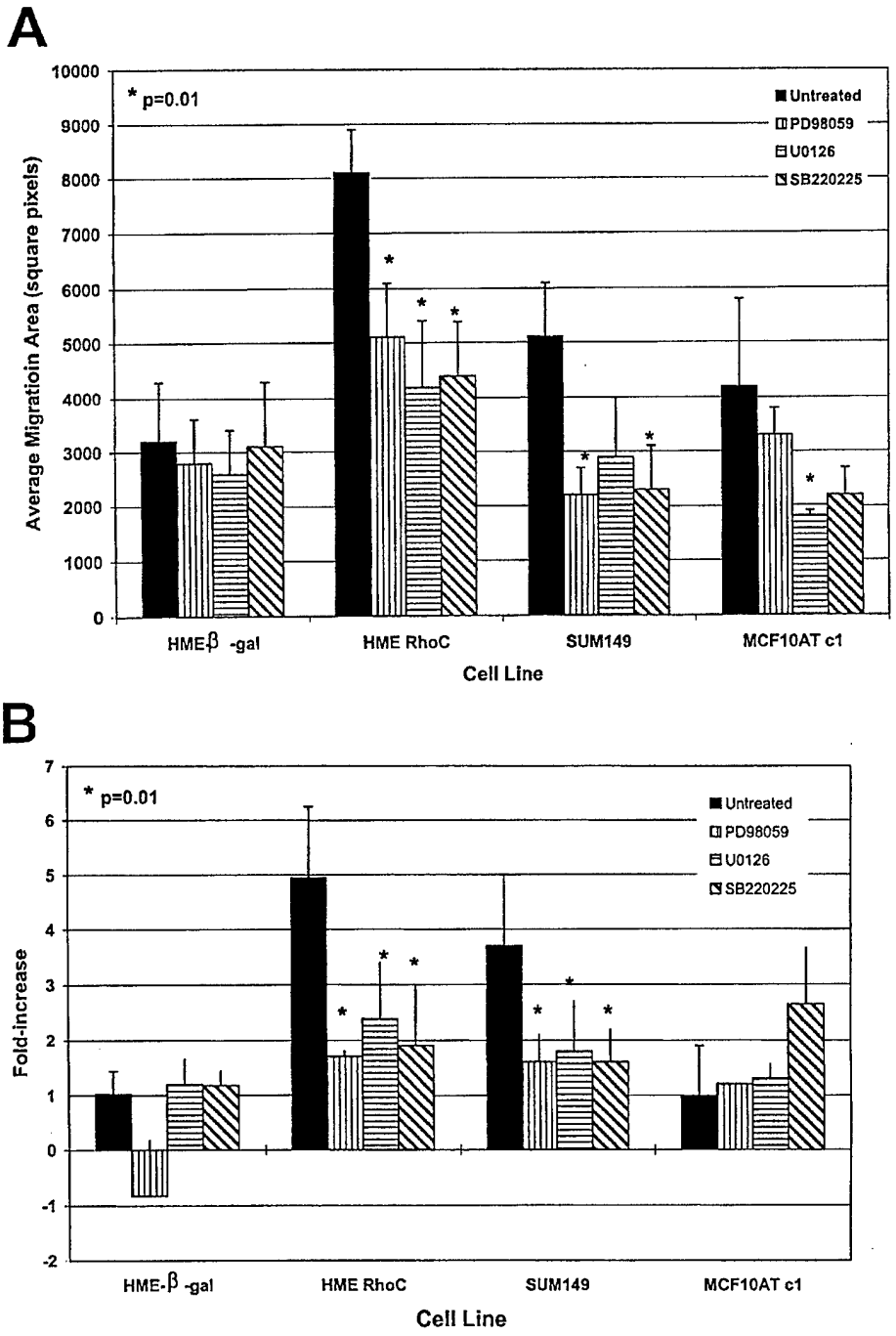

Figure 4. Effects on motility and invasion of RhoC overexpressing cells after treatment with PD98059, U0126 or the p38 inhibitor SB220225. Panel A demonstrates a significant decrease in the motility of the RhoC overexpressing HME-RhoC and SUM149 cells treated with the various MAPK inhibitors. Similarly, the ability of these cells to invade through a Matrigel coated filter was also significantly reduced after treatment with the MAPK inhibitors (panel B). These data suggest that RhoC mediated motility and invasion is mediated through the MAPK pathway, to a large extent through activated p38.

pecially relevant to understand how RhoC elicits multiple actions in breast tissue.

Using MAPK and PI3K inhibitors at concentrations below cytotoxic and cytostatic levels, we have determined that the PI3K pathway is involved in the ability of RhoC overexpressing cells to grow under anchorage independent conditions without effecting monolayer growth. We also determined that signaling through the MAPK pathway is involved in motility, invasion and the production of angiogenic factors. Specifically, we found that the ERK and p38 arms of the MAPK signaling complex are involved in motility and invasion, as no one inhibitor of the individual arms com-

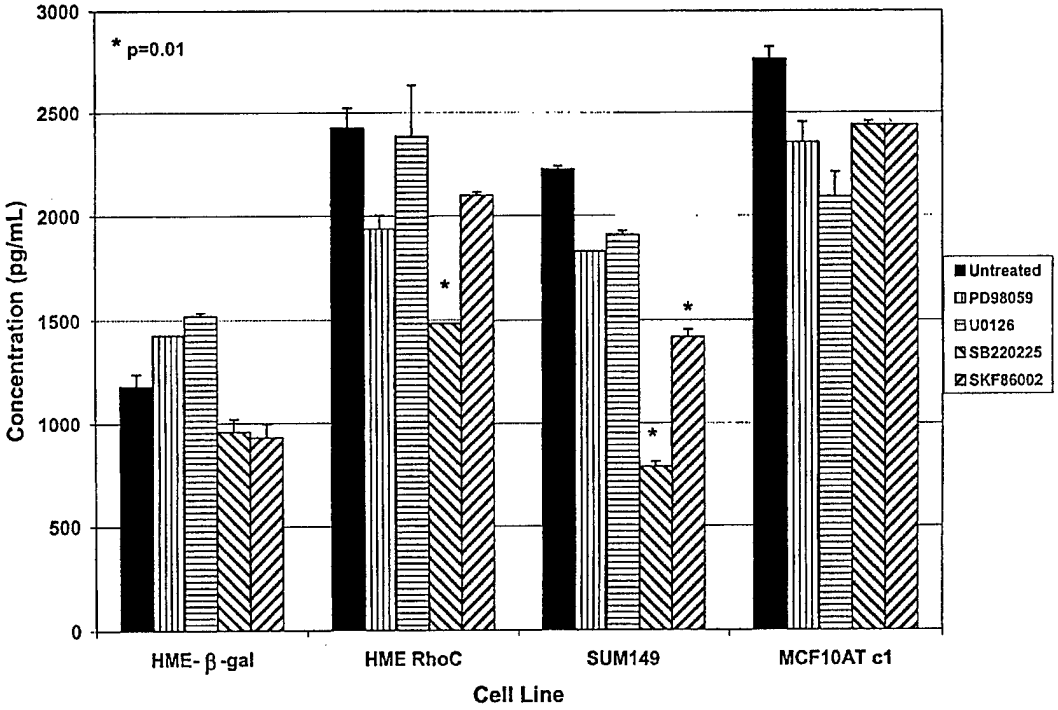

Figure 5. The effect of MAPK inhibitors on the production and secretion of the pro-angiogenic molecule vascular endothelial growth factor (VEGF). Production of VEGF by the HME-RhoC and SUM149 cell lines were significantly reduced when the cells were treated with the p38 inhibitors SB220225 or SKF86002. Taken together, these data suggest that activation of the p38 arm of the MAPK pathway is responsible for production of VEGF simultaneously by RhoC overexpression.

pletely blocked motility of the HME-RhoC or SUM149 IBC cell lines. In addition, although it is expressed, we know that JNK/SAPK does not appear to be involved given that it is not phosphorylated or active in any of the breast lines (IBC or HME) studied.

Previous experiments have demonstrated that the various signal transduction pathways have diverse effects in different cell types activated by a variety of stimuli. For example in Schwann cells, PI3K activation by Rac1 leading to lamellipodia formation and motility has been shown to occur upon stimulation by insulin-like growth factor-I [25]. Whereas stimulation of adipocytes with insulin leads activation of the PI3K pathway and Rho-mediated glucose uptake [48]. In support of our data, Amundadottir and Leder [49] demonstrated that regardless of the oncogene involved in transformation, the PI3K pathway was involved in conferring anchorage independent growth to transformed mammary epithelial cells. They also demonstrated that anchorage independent growth of mammary cells transformed by Her2/neu, v-Ha-ras, and c-myc, could not be inhibited by treatment with the MAPK inhibitor PD98059. Thus consistent with our study of RhoC-expressing cells, it appears that the PI3K pathway is exclusively involved in conferring anchorage independent growth, without involving the MAPK pathway.

Several studies have demonstrated that activation of the MAPK pathway can lead to cell migration and invasion of fibroblasts, keratinocytes and endothelial cells [50–52]. Further, it has been well documented that the Rho proteins can activate the MAPK cascade stimulating various aspects of cellular motility [29, 53–55]. Rac1 and cdc42 have been shown to signal gene transcription through JNK/SAPK and RhoA through p38, or when bound to fibronectin, ERK 1 & 2 [22, 53, 56, 57]. Akin to RhoA, we have made similar observations for RhoC, having demonstrated activation of both p38 and ERK, but not JNK/SAPK, in IBC and transfected HME cells. During motility, a dynamic interplay between Rac1, cdc42 and Rho must occur to form lamellipodia, fillipodia, focal adhesions, and stress fibers [7, 58, 59]. 'Cross-talk' between these molecules results in reciprocal activation of Rho with Rac1 and cdc42 [59–61]. Therefore, each arm of the MAPK pathway may be involved in motility and invasion during some point of the process.

In a previous study we demonstrated that levels of VEGF was significantly elevated due to RhoC overexpression [16]. In support, other laboratories have demonstrated that expression of angiogenic factors is mediated by the p38 MAPK cascade [26–28]. An increasing body of evidence suggests that the mode of VEGF induction (i.e., MAPK vs. PI3K) by activated H-*ras* is a cell-type specific process, with cells of epithelial origin signaling more commonly through the MAPK pathway and those cells of mesodermal origin utilizing the PI3K pathway [62]. Stimulation of a variety of breast cancer cell lines with heregulin results in activation of p38 and subsequent upregulation of VEGF expression and secretion [28]. Similarly, epidermal growth factor stimulation of squamous cell carcinoma cell lines, results in activation of both p38 and ERK, which in turn, leads to expression

of fibroblast growth factor-binding protein (FGF-BP), a potent angiogenic modulator [26]. Furthermore, it has been suggested that Rho proteins and the p38-MAP kinase pathway modulate IL-8 expression [63, 64]. IL-8 expression has profound biological consequences: it is a potent angiogenic, mitogenic and chemotactic factor in several malignancies including breast and prostate cancer [65–69]. Still others have suggested that FGF2, acting in an autocrine and paracrine fashion, can induce IL-6 expression through p38. In future studies we will determine whether IL-6, IL-8, and FGF2 production is also modulated by the p38 pathway in RhoC overexpressing mammary cells.

In conclusion, we have begun to identify the different signal transduction pathways involved in RhoC GTPase driven phenotypes associated with highly metastatic inflammatory breast cancer. We specifically demonstrated that anchorage independent growth is mediated via the PI3K pathway. Induction of motility and invasion are mediated through activation of the ERK and p38 arms of the MAPK pathway, and the production of VEGF is mediated primarily by p38 activation. This study provides new insight into the signal transduction pathways of an aggressive disease mediated by overexpression and activation of RhoC GTPase and suggests new potential targets for therapeutic interventions focused on the biological actions of RhoC.

Acknowledgements

This work was supported by the National Cancer Institute grant R01 CA 77612 (S.D.M.), DAMD 17-00-1-0345, from The Department of Defense, U.S. Army Breast Cancer Program (S.D.M.) and 5T32 CA 09537 and a post-doctoral fellowship (to K.L.v.G.) from the Susan G. Komen Breast Cancer Foundation. We would like to thank Ms L. Robbins for help in preparation of this manuscript.

References

1. Levine PH, Steinhorn SC, Ries LG et al. Inflammatory breast cancer: The experience of the surveillance, epidemiology, and end results (SEER) program. J Natl Cancer Inst 1985; 74: 291–7.
2. Jaiyesimi I, Buzdar A, Hortobagyi G. Inflammatory breast cancer: A review. J Clin Oncol 1992; 10: 1014–24.
3. Beahrs O, Henson D, Hutter R (eds). Manual for Staging of Cancer. Philadelphia: Lippincott 1988; 145–50.
4. Kleer cg, van Golen KL, Merajver SD. Molecular biology of breast cancer metastasis. Inflammatory breast cancer: Clinical syndrome and molecular determinants. Breast Cancer Res 2000; 2: 423–9.
5. van Golen KL, Davies S, Wu ZF et al. A novel putative low-affinity insulin-like growth factor-binding protein, LIBC (lost in inflammatory breast cancer), and RhoC GTPase correlate with the inflammatory breast cancer phenotype. Clin Cancer Res 1999; 5: 2511–9.
6. Ridley A. Membrane ruffling and signal transduction. Bioessays 1994; 16: 321–7.
7. Hall A. Rho GTPases and the actin cytoskeleton. Science 1998; 279: 509–14.
8. Ridley AJ. The GTP-binding protein Rho. Int J Biochem Cell Biol 1997; 29: 1225–9.
9. Esteve P, Embade N, Perona R et al. Rho-regulated signals induce apoptosis *in vitro* and *in vivo* by a p53-independent, but Bcl2 dependent pathway. Oncogene 1998; 17: 1855–69.
10. Hall A. Small GTP-binding proteins and the regulation of the cytoskeleton. Annu Rev Cell Biol 1994; 10: 31–54.
11. Apenstrom P. Effectors for the Rho GTPases. Curr Opin Cell Biol 1999; 11: 95–102.
12. Nobes CD, Hall A. Rho, rac, and cdc42 GTPases regulate the assembly of multimolecular focal complexes associated with actin stress fibers, lamellipodia and filopodia. Cell 1995; 81: 53–62.
13. Helvie MA, Wilson TE, Roubidoux MA et al. Mammographic appearance of recurrent breast carcinoma in six patients with TRAM flap breast reconstructions. Radiology 1998; 209: 711–5.
14. Jimenez B, Arenda M, Esteve P et al. Induction of apoptosis in NIH3T3 cells after serum deprivation by overexpression of *rho*-p21, a GTPase protein of the *ras* superfamily. Oncogene 1995; 10: 811–6.
15. van Golen KL, Wu ZF, Qiao XT et al. RhoC GTPase, a novel transforming oncogene for human mammary epithelial cells that partially recapitulates the inflammatory breast cancer phenotype. Cancer Res 2000; 60: 5832–8.
16. van Golen KL, Wu ZF, Qiao XT et al. RhoC GTPase overexpression modulates induction of angiogenic factors in breast cells. Neoplasia 2000; 2: 418–25.
17. van Golen KL, Wu ZF, Bao LW et al. RhoC GTPase induces a motile and invasive phenotype in inflammatory breast cancer. Clin Exp Metastasis 1999; 17: 745 (Abstract #2.7).
18. Suwa H, Ohshio G, Imamura T et al. Overexpression of the *rhoC* gene correlates with progression of ductal adenocarcinoma of the pancreas. Br J Cancer 1998; 77: 147–52.
19. Genda T, Sakamoto M, Ichida T et al. Cell Motility mediated by rho and Rho-associated protein kinase plays a critical role in intrahepatic metastasis of human hepatocellular carcinoma. Hepatology 1999; 30: 1027–36.
20. Clark EA, Golub TR, Lander ES et al. Genomic analysis of metastasis reveals an essential role for RhoC. Nature 2000; 406: 532–5.
21. Takai Y, Sasaki T, Matozaki T. Small GTP-binding proteins. Physiol Rev 2001; 81: 153–208.
22. Danen EH, Sonneveld P, Sonnenberg A et al. Dual stimulation of Ras/mitogen-activated protein kinase and RhoA by cell adhesion to fibronectin supports growth factor-stimulated cell cycle progression. J Cell Biol 2000; 151: 1413–22.
23. Vojtek AB, Cooper JA. Rho family members: Activators of MAP kinase cascades. Cell 1995; 82: 527–9.
24. Arozarena I, Aaronson DS, Matallanas D et al. The Rho family GTPase Cdc42 regulates the activation of Ras/MAP kinase by the exchange factor Ras-GRF. J Biol Chem 2000; 275: 26441–8.
25. Cheng HL, Steinway ML, Russell JW et al. GTPases and phosphatidylinositol 3-kinase are critical for insulin-like growth factor-I-mediated Schwann cell motility. J Biol Chem 2000; 275: 27197–204.
26. Harris VK, Coticchia CM, Kagan BL et al. Induction of the angiogenic modulator fibroblast growth factor-binding protein by epidermal growth factor is mediated through both MEK/ERK and p38 signal transduction pathways. J Biol Chem 2000; 275: 10802–11.
27. Sodhi A, Montaner S, Patel V et al. The Kaposi's sarcoma-associated herpes virus G protein-coupled receptor up-regulates vascular endothelial growth factor expression and secretion through mitogen-activated protein kinase and p38 pathways acting on hypoxia-inducible factor 1α. Cancer Res 2000; 60: 4873–80.
28. Xiong S, Grijalva R, Zhang L et al. Up-regulation of vascular endothelial growth factor in breast cancer cells by the heregulin-beta1-activated p38 signaling pathway enhances endothelial cell migration. Cancer Res 2001; 61: 1727–32.
29. Parise LV, Lee J, Juliano RL. New aspects of integrin signaling in cancer. Semin Cancer Biol 2000; 10: 407–14.
30. Downward J. Mechanisms and consequences of activation of protein kinase B/Akt. Curr Opin Cell Biol 1998; 10: 262–7.
31. Khwaja A, Rodriguez-Viciana P, Wennstrom S et al. Matrix adhesion and Ras transformation both activate a phosphoinositide 3-OH kinase and protein kinase B/Akt cellular survival pathway. EMBO J 1997; 16: 2783–93.
32. Ilic D, Almeida EA, Schlaepfer DD et al. Extracellular matrix survival signals transduced by focal adhesion kinase suppress p53-mediated apoptosis. J Cell Biol 1998; 143: 547–60.
33. Tamura M, Gu J, Danen EH et al. PTEN interactions with focal adhesion kinase and suppression of the extracellular matrix-dependent phosphatidylinositol 3-kinase/Akt cell survival pathway. J Biol Chem 1999; 274: 20693–703.

34. Ethier SP, Kokeny KE, Ridings JW et al. erbB family receptor expression and growth regulation in a newly isolated human breast cancer cell line. Cancer Res 1996; 56: 899–907.
35. Ethier SP. Human breast cancer cell lines as models of growth regulation and disease progression. J Mammary Gland Biol Neoplasia 1996; 1: 111–21.
36. Sartor CI, Dziubinski ML, Yu CL et al. Role of epidermal growth factor receptor and STAT-3 activation in autonomous proliferation of SUM-102PT human breast cancer cells. Cancer Res 1997; 57: 978–87.
37. Band V, Zajchowski D, Kulesa V et al. Human papilloma virus DNAs immortalize normal human mammary epithelial cells and reduce their growth factor requirements. Proc Natl Acad Sci USA 1990; 87: 463–7.
38. Stasia MJ, Vignais PV. In Abelson JM, Simon MI (eds): Methods in Enzymology. New York: Academic Press 1995; 324–7.
39. van Golen KL, Risin S, Staroselsky A et al. Predominance of the metastatic phenotype in hybrids formed by fusion of mouse and human melanoma clones. Clin Exp Metastasis 1996; 14: 95–106.
40. Albrecht-Buehler G. The phagokinetic tracks of 3T3 cells. Cell 1977; 11: 395–404.
41. Aktories K. Rho proteins: targets for bacterial toxins. Trends Microbiol 1997; 5: 282–8.
42. Chardin P, Boquet P, Madaule P et al. The mammalian G protein rhoC is ADP-ribosylated by Clostridium botulinum exoenzyme C3 and affects actin microfilaments in Vero cells. EMBO J 1989; 8(4): 1087–92.
43. Santner SJ, Dawson PJ, Tait L et al. Malignant MCF10CA1 cell lines derived from premalignant human breast epithelial MCF10AT cells. Breast Cancer Res Treat 2001; 65: 101–10.
44. Dunn SE, Torres JV, Oh JS et al. Up-regulation of urokinase-type plasminogen activator by insulin-like growth factor-I depends upon phosphatidylinositol-3 kinase and mitogen-activated protein kinase kinase. Cancer Res 2001; 61: 1367–74.
45. Cuenda A, Alessi DR. Use of kinase inhibitors to dissect signaling pathways. Methods Mol Biol 2000; 99: 161–75.
46. Wymann MP, Pirola L. Structure and function of phosphoinositide 3-kinases. Biochim Biophys Acta 1998; 1436: 127–50.
47. Lopez-Ilasaca M. Signaling from G-protein-coupled receptors to mitogen-activated protein (MAP)-kinase cascades. Biochem Pharmacol 1998; 56: 269–77.
48. Karnam P, Standaert ML, Galloway L et al. Activation and translocation of Rho (and ADP ribosylation factor) by insulin in rat adipocytes. Apparent involvement of phosphatidylinositol 3-kinase. J Biol Chem 1997; 272: 6136–40.
49. Amundadottir LT, Leder P. Signal transduction pathways activated and required for mammary carcinogenesis in response to specific oncogenes. Oncogene 1998; 16: 737–46.
50. Yujiri T, Ware M, Widmann C et al. MEK kinase 1 gene disruption alters cell migration and c-Jun NH2- terminal kinase regulation but does not cause a measurable defect in NF- kappa B activation. Proc Natl Acad Sci USA 2000; 97: 7272–7.
51. Zeigler ME, Chi Y, Schmidt T et al. Role of ERK and JNK pathways in regulating cell motility and matrix metalloproteinase 9 production in growth factor-stimulated human epidermal keratinocytes. J Cell Physiol 1999; 180: 271–84.
52. Matsumoto T, Yokote K, Tamura K et al. Platelet-derived growth factor activates p38 mitogen-activated protein kinase through a Ras-dependent pathway that is important for actin reorganization and cell migration. J Biol Chem 1999; 274: 13954–60.
53. Minden A, Lin A, Claret FX et al. Selective activation of the JNK signaling cascade and c-Jun transcriptional activity by the small GTPases Rac and Cdc42Hs. Cell 1995; 81: 1147–57.
54. Santibanez JF, Iglesias M, Frontelo P et al. Involvement of the Ras/MAPK signaling pathway in the modulation of urokinase production and cellular invasiveness by transforming growth factor-beta(1) in transformed keratinocytes. Biochem Biophys Res Commun 2000; 273: 521–7.
55. Royal I, Lamarche-Vane N, Lamorte L et al. Activation of cdc42, rac, PAK, and rho-kinase in response to hepatocyte growth factor differentially regulates epithelial cell colony spreading and dissociation. Mol Biol Cell 2000; 11: 1709–25.
56. Coso O, Chiariello M, Yu JC et al. The small GTP-binding proteins proteins Rac1 and Cdc42 regulate the activity of the JNK/SAPK signaling pathway. Cell 1995; 81: 1137–46.
57. Marinissen MJ, Chiariello M, Gutkind JS. Regulation of gene expression by the small GTPase Rho through the ERK6 (p38 gamma) MAP kinase pathway. Genes Dev 2001; 15: 535–53.
58. Small JV, Kaverina I, Krylyshkina O et al. Cytoskeleton cross-talk during cell motility. FEBS Lett 1999; 452: 96–9.
59. Bishop AL, Hall A. Rho GTPases and their effector proteins. Biochem J 2000; 348 (2): 241–55.
60. Ridley AJ, Paterson H, Johnston C et al. The small GTP-binding protein rac regulates growth-factor induced membrance ruffling. Cell 1992; 70: 401–10.
61. Zondag GCM, Evers EE, ten Klooster JP et al. Oncogenic Ras downregulates Rac activity, which leads to increased Rho activity and epithelial-mesenchymal transition. J Cell Biol 2000; 149: 775–82.
62. Rak J, Mitsuhashi Y, Sheehan C et al. Oncogenes and tumor angiogenesis: differential modes of vascular endothelial growth factor upregulation in *ras*-transformed epithelial cells and fibroblasts. Cancer Res 2000; 60: 490–8.
63. Warny M, Keates AC, Keates S et al. p38 MAP kinase activation by Clostridium difficile toxin A mediates monocyte necrosis, IL-8 production, and enteritis. J Clin Invest 2000; 105: 1147–56.
64. Hippenstiel S, Soeth S, Kellas B et al. Rho proteins and the p38-MAPK pathway are important mediators for LPS-induced interleukin-8 expression in human endothelial cells. Blood 2000; 95: 3044–51.
65. Rodeck U, Becker D, Herlyn M. Basic fibroblast growth factor in human melanoma. Cancer Cells 1991; 3: 308–11.
66. Speirs V, Atkin SL. Production of VEGF and expression of the VEGF receptors Flt-1 and KDR in primary cultures of epithelial and stromal cells derived from breast tumours. Br J Cancer 1999; 80: 898–903.
67. Inoue K, Slaton JW, Eve BY et al. Interleukin 8 expression regulates tumorigenicity and metastases in androgen-independent prostate cancer. Clin Cancer Res 2000; 6: 2104–19.
68. Miller LJ, Kurtzman SH, Wang Y et al. Expression of interleukin-8 receptors on tumor cells and vascular endothelial cells in human breast cancer tissue. Anticancer Res 1998; 18: 77–81.
69. Mizuno K, Sone S, Orino E et al. Spontaneous production of interleukin-8 by human lung cancer cells and its augmentation by tumor necrosis factor alpha and interleukin-1 at protein and mRNA levels. Oncology 1994; 51: 467–71.

Vol. 1, 575–583, June 2002

Reversion of RhoC GTPase-induced Inflammatory Breast Cancer Phenotype by Treatment with a Farnesyl Transferase Inhibitor[1]

Kenneth L. van Golen, LiWei Bao, Melinda M. DiVito, ZhiFen Wu, George C. Prendergast, and Sofia D. Merajver[2]

Department of Internal Medicine, Division of Hematology/Oncology [K. L. v. G., L. B., M. M. D., Z. W., S. D. M.], and Comprehensive Cancer Center [K. L. v. G., L. B., Z. W., S. D. M.], University of Michigan, Ann Arbor, Michigan 48109; The Wistar Institute, Philadelphia, Pennsylvania 19104 [G. C. P.]; and Glenolden Laboratory, The DuPont Pharmaceuticals Company, Wilmington, Delaware 19898 [G. C. P.]

Abstract

Inflammatory breast carcinoma (IBC) is a highly aggressive form of locally advanced breast cancer that has the ability to invade and block the dermal lymphatics of the skin overlying the breast. In a previous series of studies, our laboratory identified overexpression of RhoC GTPase in >90% of IBCs (K. L. van Golen *et al.*, Clin. Cancer Res., *5:* 2511–2519, 1999) and defined *RhoC* as a mammary oncogene involved in conferring the metastatic phenotype (K. L. van Golen *et al.*, Cancer Res., *60:* 5832–5838, 2000). RhoC GTPase is involved in cytoskeletal reorganization during cellular motility. Farnesyl transferase inhibitors (FTIs) were previously shown to be effective in modulating tumor growth in Ras-transformed tumor cells. Recently, studies have focused on RhoB as a putative non-Ras target of FTI action. In the present study, we assessed the effect of the FTI L-744,832 on RhoC-overexpressing IBC and RhoC-transfected human mammary epithelial (HME-RhoC) cells. Treatment of the SUM149 IBC cell line and HME-RhoC transfectants with the FTI L-744,832 led to reversion of the RhoC-induced phenotype, manifested by a significant decrease in anchorage-independent growth, motility, and invasion. Although RhoC expression and activation were not affected, RhoB levels were increased by FTI treatment. Transient transfection of geranylgeranylated RhoB (RhoB-GG) into the same cells reproduced the effects of the FTI, thus suggesting that FTI-induced reversion of the RhoC phenotype may be mediated by an increase in RhoB-GG levels. These data provide direct evidence that FTIs may find use in the clinic when directed against RhoC-overexpressing tumors and suggest appropriate biological markers to evaluate during FTI treatment.

Introduction

The term IBC[3] was first coined in 1924 by Drs. Lee and Tannenbaum to describe a phenotypically distinct form of locally advanced breast cancer (LABC) (1, 2). IBC is a fast-growing, highly invasive, and metastatic form of LABC, which is clinically characterized by primary skin changes (1–4). These primary skin changes are the result of blockage of the dermal lymphatics of the skin overlying the breast resulting in edema, *peau d' aurange,* and nipple retraction (1–4). At the time of diagnosis, nearly all tumors have spread to the regional lymph nodes and on close inspection, more than one-third of patients have gross distant metastases (1–4). Despite aggressive multimodality treatments, the 5-year disease-free survival rate for women with IBC is <45%, making IBC the deadliest form of breast cancer (1–4).

During investigation of the genetic mechanisms responsible for the unique IBC phenotype, our laboratory identified overexpression of RhoC GTPase in >90% of IBCs (5). RhoC GTPase is a member of the Ras-homology family of small GTP-binding proteins and is responsible for cytoskeletal reorganization during cellular motility (6–10). RhoC belongs to a highly homologous subfamily comprised of RhoA, RhoB, and RhoC (11). Although these family members have >90% sequence homology to one another, their roles in the cell are distinct (11). To determine the contribution of RhoC GTPase overexpression to the IBC phenotype, we generated stable RhoC-overexpressing HME cell lines (HME-RhoC) (12). The HME-RhoC clones nearly recapitulated the invasive features of the IBC phenotype. Specifically, the cells grew under anchorage-independent conditions and produced tumors when orthotopically injected into athymic nude mice (12–14). The cells were highly motile and invasive and produced conditioned medium rich in pro-angiogenic cytokines *in vitro* (12–14). Taken together, these data demonstrate that overexpressed, active *RhoC GTPase* is a mammary oncogene leading to advanced disease.

Regulation of the GTPase activity of both the Ras and the Rho proteins is achieved through interactions of GAPs, GDIs, GDF, and GEFs (15, 16). RhoA, RhoC, and a fraction of RhoB

Received 1/17/02; revised 4/4/02; accepted 4/15/02.
[1] Supported by National Cancer Institute Grant R01 CA 77612 (to S. D. M.); Grant DAMD 17-00-1-0345, from The Department of Defense, United States Army Breast Cancer Program (to S. D. M.); and Grant 5T32 CA 09537 (to S. D. M.) and a postdoctoral fellowship (to K. L. v. G.) from the Susan G. Komen Breast Cancer Foundation.
[2] To whom requests for reprints should be addressed, at 7217 CCGC, 1500 East Medical Center Drive, Ann Arbor, MI 48109-0948. E-mail: smerajve@umich.edu.

[3] The abbreviations used are: IBC, inflammatory breast cancer; FTI, farnesyl transferase inhibitor; HME, human mammary epithelial (cells); FBS, fetal bovine serum; RT-PCR, reverse transcription-PCR; PI, propidium iodide; RhoB-GG, geranylgeranylated RhoB; GAPDH, glyceraldehyde-3-phosphate dehydrogenase; GST, glutathione *S*-transferase; PI3K, phosphatidylinositol 3′-kinase; β-gal, β-galactosidase; GAP, GTPase-activating proteins; GDI, GDP-dissociation inhibitor; GDF, GDI dissociation factor; GEF, guanine nucleotide exchange factor; SEM, scanning electron microscopy.

are geranylgeranylated, and the remaining portion of RhoB is farnesylated (17–19). For the Rho proteins to enter the GDP/GTP cycle they must be transported and localized to the membrane (19, 20). GTP binding produces a conformational change in the GTPase, thereby allowing interaction with downstream effector proteins (15, 21). Hydrolysis of GTP to GDP by the intrinsic Rho GTPase activity modulates the interaction with the effector protein (22, 23). The GTPase activity is greatly increased by activated GAPs, thus leading to increased hydrolysis of GTP (24). The entire process is balanced by the GDIs, which prevent GDP dissociation by binding to the prenylation group of the GTPase and sequestering the complex in the cytoplasm (25). The GTPase is subsequently liberated from the GDI by GDFs, closing the cycle (25).

In light of evidence demonstrating that FTIs can target non-Ras molecules, such as the RhoB protein, and recent work suggesting that RhoB alterations, specifically, the accumulation of RhoB-GG, may interfere with transforming Rho signals, we sought to test the effect of FTIs on RhoC-transformed breast cells.

Materials and Methods

Cell Culture. Cell lines were maintained under defined culture conditions for optimal growth in each case as described previously (26–28). E6/E7 immortalized HME cells (29) were grown in 5% FBS (Sigma Chemical Co., St. Louis, MO)-supplemented Ham's F-12 medium (JRH BioSciences, Lenexa, KS) containing insulin, hydrocortisone, epidermal growth factor, and cholera toxin (Sigma Chemical Co.). Stable HME transfectants containing either the human *RhoC GTPase* or control *β-gal* genes were maintained in the described medium supplemented with 100 μg/ml hygromycin (LifeScience Technologies; Gaithersburg, MD) as described previously (12, 13). The SUM149 IBC cell line was grown in 5% FBS-supplemented Ham's F-12 medium containing insulin and hydrocortisone. The HME cells were characterized as being keratin 19 positive, thus ensuring that they are from the same differentiation lineage as the SUM149 IBC tumor cell line. For FTI treatment, actively growing cells were treated with 25 μM FTI L-744,832 and harvested 48 h later. Cell viability was assessed prior to assays using a trypan blue exclusion assay. Harvested cells were washed in 10 ml of HBSS (LifeScience Technologies). A 100-μl aliquot was taken, diluted 1:1 with prediluted trypan blue (Sigma Chemical Co.), and counted on a hemacytometer.

Transient transfections were performed by growing cells in 100-mm plates until reaching 50% confluence. Expression constructs for wild-type RhoB, RhoB-GG, and a geranylgeranyl-deficient RhoB mutant were generated as described previously (30–32). The RhoB containing vectors or a vector control were introduced into the cells using FuGene6 transfection reagent (Roche, Indianapolis, IN) as described previously (12). Transient transfectants were used in biological assays 24 h after transfection.

Anchorage-independent Growth and Focus Formation. For anchorage-independent growth assays, a 2% stock of sterile low-melt agarose was diluted 1:1 with 2× MEM. Further dilution to 0.6% agarose was made using 10% FBS-supplemented Ham's F-12 medium complete with growth factors, and 1 ml was added to each well of a six-well plate as a base-layer. The cell layer was then prepared by diluting agarose to 0.3% and 0.6% with 10^3 cells (either untreated or 25 μM FTI L-744,832 for 24 h) in 2.5% FBS-supplemented Ham's F-12/1.5 ml/well. A 1-ml layer of medium was maintained on top of the agar to provide nutrients and, in the case of the treated cells, additional inhibitor. Colonies ≥100 μm in diameter were counted after a 2-week incubation at 37°C in a 10% CO_2 incubator.

A modified focus formation assay was performed by harvesting treated and untreated cells and plating at dilutions of 1000, 500, and 100 cells/35-mm dish. The cells were then cultured for 2 weeks at 37°C in a 10% CO_2 incubator. The plates were washed with 10 ml of PBS, fixed for 10 min with ice-cold methanol, and stained for 10 min with 2% methylene blue in 50% ethanol, and visible foci were counted.

Western Blot and RhoC Activation Analysis. Proteins were harvested from cell cultures using radioimmunoprecipitation assay buffer (1× PBS, 1% NP40, 0.5% sodium deoxycholate, 0.1% SDS, 0.1 mg/ml phenylmethylsulfonyl fluoride, 1 mM sodium orthovanadate, and 0.3 mg/ml aprotinin; Sigma Chemical Co.) Ten-μg aliquots were mixed with Laemmli buffer, heat-denatured for 3 min, separated by SDS-PAGE, and transferred to nitrocellulose. Nonspecific binding was blocked by overnight incubation with 2% powdered milk in Tris-buffered saline with 0.05% Tween 20 (Sigma Chemical Co.). Immobilized proteins were probed using antibodies specific for RhoC GTPase (33), or RhoB GTPase (Cytoskeleton Inc. Denver, CO). Protein bands were visualized by ECL (Amersham-Pharmacia Biotech, Piscataway, NJ).

A RhoC activation assay was performed as described previously (34, 35). Cells grown to 40% confluence were incubated in the presence or absence of 25 μM FTI L-744,832 for 24 h. Proteins were harvested using GST-FISH buffer (34) and were centrifuged. The supernatant was mixed with a slurry of GST-rhotekin fusion protein bound to glutathione-sepharose beads. Only GTP-bound Rho binds to the GST-rhotekin fusion protein. The mixture was centrifuged, separated by SDS-PAGE, transferred to nitrocellulose and probed using a RhoC-specific antibody (33). Protein bands were visualized by ECL and exposed to Hyperfilm (Amersham).

Semiquantitative RT-PCR. Total RNA was harvested from actively growing cells at 50% confluence using Trizol Reagent (Life Technologies), and cDNA was made using the AMV-reverse transcriptase kit (Promega, Madison, WI). RhoC and RhoB transcripts were PCR amplified from aliquots of cDNA using a 1:100 dilution of Rho-specific primers mixed with GAPDH primers. PCR products were then separated on a 1.2% TAE-agarose gel and were visualized by ethidium bromide. The relative intensity of the Rho and GAPDH bands was measured using an Alpha Imager 2200 (Alpha Innotech Co., San Leandro, CA).

Motility and Invasion Assays. Random motility was determined using a gold-colloid assay (36). Gold colloid was layered onto glass coverslips and placed into 6-well plates. Cells were seeded onto the coverslips and allowed to adhere for 1 h at 37°C in a CO_2 incubator (12,500 cells/3 ml in serum-free medium). To stimulate the cells, the serum-free

medium was replaced with 5% FBS containing Ham's F-12 supplemented with growth factors and allowed to incubate for 3 h at 37°C. The medium was aspirated and the cells fixed using 2% gluteraldehyde (Sigma Chemical Co.). The coverslips were then mounted onto glass microscope slides and areas of clearing in the gold colloid corresponding to phagokinetic cell tracks were counted.

The invasion assay was performed as described previously with minor modification (37). A 10-μl aliquot of 10 mg/ml Matrigel (BD Biosciences, Bedford, MA) was spread onto a 6.5-mm Transwell filter with 8 μm pores (Costar, Corning, NY) air-dried in a laminar flow hood, and reconstituted with a few drops of serum-free medium. The lower chamber of the Transwell was filled with either serum-free or serum-containing media. Cells were harvested and resuspended in serum-free medium with 0.1% BSA at a concentration of 3.75×10^5 cells/ml, and 0.5 ml was added to the top chamber. The chambers were incubated for 24 h at 37°C in a 10% CO_2 incubator. The cell suspension was aspirated, and excess Matrigel was removed from the filter using a cotton swab. The filters were then cut away from the Transwell assembly and fixed, gel side down, with methanol to a glass microscope slide, stained with H&E, and 20 random ×40 magnification fields were counted. The number of cells that had invaded into the serum-free medium-containing lower chambers were considered background and were subtracted from the number of invaded cells in the serum-containing samples.

Statistical analysis was performed using a two-tailed Student *t* test.

Apoptosis Assay. Cytofluorometric analysis of cell cycle distribution and apoptosis was performed by PI staining of nuclei as reported previously (38, 39). Briefly, cells were treated with 25 μM FTI L-744,832 (Merck) alone, 10 μM LY294002 (Calbiochem, San Diego, CA) alone, or a combination of both FTI L-744,832 and LY294002. Untreated and treated cells, 1×10^6, were harvested from 35-mm wells, washed once with ice-cold PBS (Fisher Scientific, Pittsburgh, PA) and pelleted; supernatants were removed and 500 μl of PI-hypotonic lysis buffer [0.1% sodium citrate, 0.1% Triton X, 100 μg/ml RNAse type I-A, 50 μg/ml PI (SIGMA)] were added. Samples were analyzed by flow cytometry after a 20-min incubation at 25°C.

Rhodamine-Phallodin Staining of Actin Filaments. Visualization of actin filaments was accomplished by staining the cells with a rhodamine-conjugated phallotoxin. Briefly, cells were grown on glass coverslips for 48 h and washed with PBS followed by fixation with 1:1 ice-cold acetone and methanol. After a 30-min incubation in PBS containing 1% BSA, 5 μl of methanolic rhodamine-phalloidin stock (Molecular Probes, Eugene, OR) were added to each coverslip and allowed to stain for 20 min at room temperature. After repeated washing with PBS, the coverslips were mounted onto glass microscope slides using Gel/Mount (Biomedia Co., Foster City, CA). Cells were visualized under a Zeiss scanning laser confocal microscope equipped with a 573-nm fluorescence filter.

SEM. Cells (12,000) were fixed with buffered 2.5% glutaraldehyde for 1 h, rinsed, and post-fixed for an additional hour with buffered osmium tetroxide. After dehydration in ascending strengths of ethanol, the cells were critical-point dried, mounted onto standard SEM stubs, and gold-sputter coated. They were viewed using an AMRAY 1000-B Scanning Electron Microscope.

Results

Effect of FTI Treatment on RhoC-overexpressing Breast Cells. The ability of cells to grow in soft agar is a hallmark of malignant transformation (40). Previously, we found that RhoC overexpression led to the growth of mammary epithelial cells under anchorage-independent conditions (12, 14). As demonstrated in Fig. 1*A*, treatment of RhoC-overexpressing HME cells and the SUM149 IBC cell line with 25 μM FTI L-744,832 resulted in a significant decrease in anchorage-independent growth. Although the HME-β-gal control-transfected cells did not readily grow under anchorage-independent conditions, they were slightly affected by FTI treatment. The 80% decrease in anchorage-independent growth of the Rho-expressing cells did not correlate with a decrease in monolayer growth rate as determined by a 3-(4,5-dimethylthiazol-2-yl)-2,5-diphenyltetrazolium bromide (MTT) assay (data not shown). It has been suggested that FTI treatment sensitizes cells to apoptotic death on treatment with the PI3K inhibitor LY294002 (31). However, in our system, we did not observe an increase in apoptosis in cells treated with FTI L-744,832 alone, LY294002 alone, or a combination of the two, as has been observed for Ras-transformed cells (data not shown).

To evaluate the effect of FTI treatment on RhoC-mediated cellular motility, we assessed the same treated cell lines in colloidal-gold random motility assay. Cells were seeded onto glass coverslips overlayed with a gold colloid and stimulated with serum to induce motility. Discernable and quantifiable tracks were left as the cells moved and phagocytized the gold colloid. At 24 h after stimulation, the SUM149 and HME-RhoC cells treated with FTI L-744,832 were 1.8- to 2-fold less motile than their untreated counterparts (Fig. 1*B*). Both the HME-β-gal control and the MCF10AT c1 (an MCF10A clone transfected with a constituitively active Ras; Ref. 41) were unaffected by FTI treatment. As determined by a trypan blue dye exclusion assay, the reduction in cell motility was not caused by a decrease in the number of viable cells (data not shown).

As shown in Fig. 1*C*, when the FTI-treated cells were tested for their ability to invade through a Matrigel-coated filter in response to a chemoattractant, it was found that the SUM149 and HME-RhoC cells were 2-fold less invasive than the untreated cells. Again, the control cell lines, HME-β-gal and MCF10AT c1, were unaffected by FTI treatment.

Taken together, these data suggest that treatment of RhoC-overexpressing cells with a FTI leads to the inhibition of RhoC-mediated anchorage-independent growth, motility, and invasion without significantly affecting cell growth or viability.

As demonstrated in Fig. 2, *C* and *E*, rhodamine-phallodin staining for actin filaments shows a highly organized and polarized cytoskeleton in the RhoC-overexpressing cells. These actin bundles are lost or diminished on treatment with

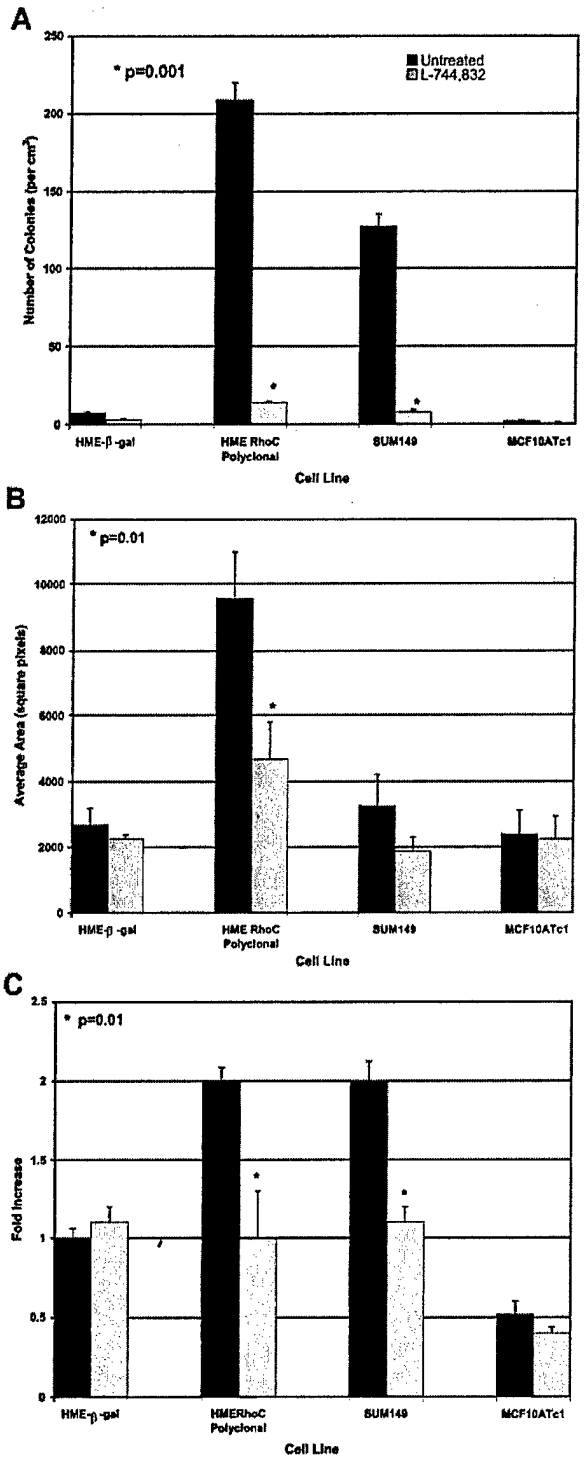

Fig. 1. *A*, comparison of anchorage-independent growth of untreated and FTI L-744,832 treated cell lines in 0.6% soft agar. The growth of RhoC overexpressing cell lines, HME-RhoC and SUM149, were significantly inhibited (P = 0.001) by FTI treatment, which suggests a reversion of malignant transformation. *B* demonstrates a significant reduction in the motility of FTI-treated HME-RhoC cells. A reduction in motility, although not significant, was also observed for the SUM149 cells. A significant reduction (P = 0.01) in the ability to invade through a Matrigel-coated filter was also observed for the HME-RhoC and SUM149 cells (*C*). None of the effects that resulted from treatment with FTI could be attributed to a decrease in viable cells, as determined by trypan blue dye-exclusion assays or by apoptosis assays.

FTI L-744,832 (Fig. 2, *D* and *F*). Numerous focal adhesions were visible on the periphery of the treated cells. However, loss of cytoskeletal polarity led to morphological changes towards a rounded shape, as demonstrated by laser scanning confocal microscopy and scanning electron microscopy (Fig. 2, *G–J*). The morphology of the control HME-β-gal cells was also similarly affected, albeit to a lesser degree, by FTI treatment, as these cells became dissociated and flattened (Fig. 2, *A* and *B*).

Rho Protein Levels Increase as a Result of FTI Treatment. To determine the effect of FTI treatment on RhoC expression, we performed semiquantitative RT-PCR and Western blot analysis. As shown in Fig. 3*A*, RhoC mRNA expression increased in all of the cell lines on FTI treatment. A concordant increase in RhoC protein levels was also observed, as determined by Western blot analysis using a RhoC-specific antibody developed in our laboratory (33). The activity of RhoC was assessed using a GST-pulldown assay (34, 35). This assay utilizes a GST-fusion protein of a Rho-binding domain motif found in a variety of Rho-effector proteins. GTP-bound Rho is in its active state and can bind the Rho-binding domain (35). Using this assay, we found that in the SUM149 and HME-RhoC cell, the levels of GTP-bound RhoC were not affected by FTI treatment, which indicated that RhoC activation itself was unaffected by RhoB and RhoC accumulation. As expected from the mRNA and protein levels, activated RhoC was elevated in all of the FTI-treated cells, including the HME-β-gal control cells.

Because previous studies suggested a role for RhoB in reverting the malignant phenotype of Ras-transformed cells treated with FTI (42), we performed semiquantitative RT-PCR and Western blot analysis for RhoB. As shown in Fig. 3*B*, RhoB mRNA levels markedly increased 24 h after treatment with FTI L-744,832 in all of the cell lines tested. Furthermore, RhoB protein levels were also significantly increased.

These results support earlier observations that the accumulation of RhoB, likely RhoB-GG but not farnesylated RhoB, leads to a reversion of the malignant phenotype by FTI (30, 42, 43). The mechanism of FTI inhibition of the RhoC-induced phenotype appears to be independent of direct action of the FTI on geranylgeranylated RhoC. This is demonstrated by an accumulation of RhoC protein and no change in its activity.

Expression of RhoB-GG Recapitulates the FTI-mediated Effects on RhoC-overexpressing Breast Cells. In light of the previous experiments, we hypothesized that the accumulation of RhoB protein, specifically the RhoB-GG isoform that accumulates in FTI-treated cells, would be sufficient to revert the RhoC-induced phenotype. To test this hypothesis, we transiently transfected breast cells with a RhoB-GG construct and performed a focus formation and random motility assay. As controls, we also transfected cells with a geranylgeranyl-deficient mutant RhoB construct. Transfection efficiency was assessed by cotransfection with a *β-gal* reporter gene and found to be ~30–50% for the SUM149 and HME-RhoC cells. This assay could not be performed for the HME-β-gal controls since these cells already express the *β-gal* gene. However, RT-PCR using

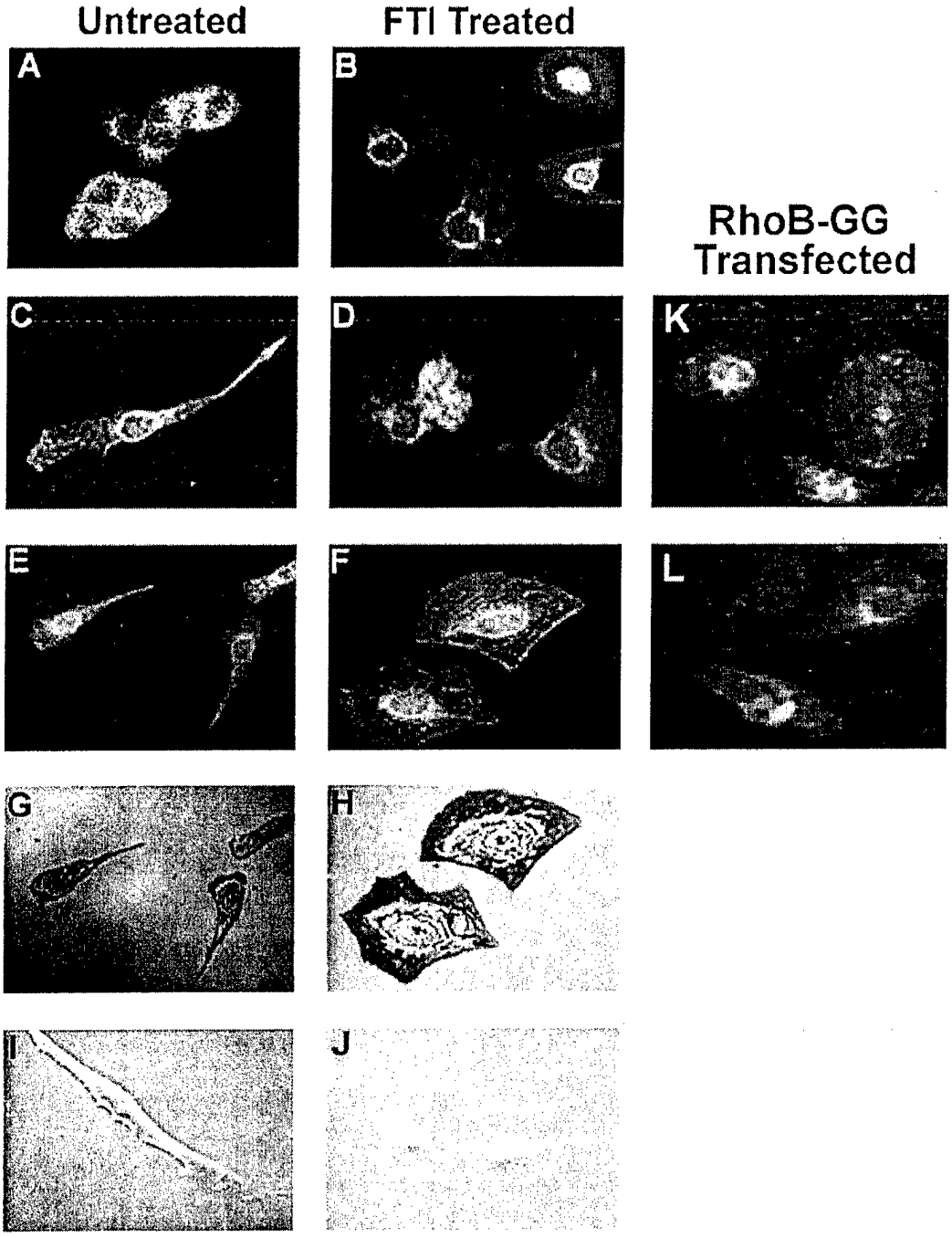

Fig. 2. Laser scanning confocal fluorescence microscopy (*A–F*) of untreated and L-744,832 treated cells after staining with a rhodamine-tagged phallotoxin that targets F-actin bundles. *A* and *B*, the HME-β-gal control cells untreated and FTI L-744,832-treated, respectively. *C* and *E* demonstrate a highly organized and polarized cytoskeleton in the SUM149 and HME-RhoC cells, respectively. *D* and *F* demonstrate dissociated actin bundles and decreased cellular polarity on FTI treatment. *G* and *H*, are laser scanning confocal microscopy images, and *I* and *J* are scanning electron microscopy images of untreated and FTI-treated HME-RhoC cells, respectively, showing the changes in cell morphology. *K* and *L* are RhoB-GG-transfected HME-RhoC and SUM149 cells, respectively.

vector-specific primers demonstrated mRNA expression in all of the cell lines tested.

Table 1 shows the results of a focus formation assay for the transfectants. The SUM149 and HME-RhoC cells, transiently transfected with RhoB-GG, formed significantly fewer foci than did the RhoB-GG-deficient mutant transfectants or the nontransfected cells. The morphology of the RhoB-GG-transfected cells were similar to their FTI-treated counter-

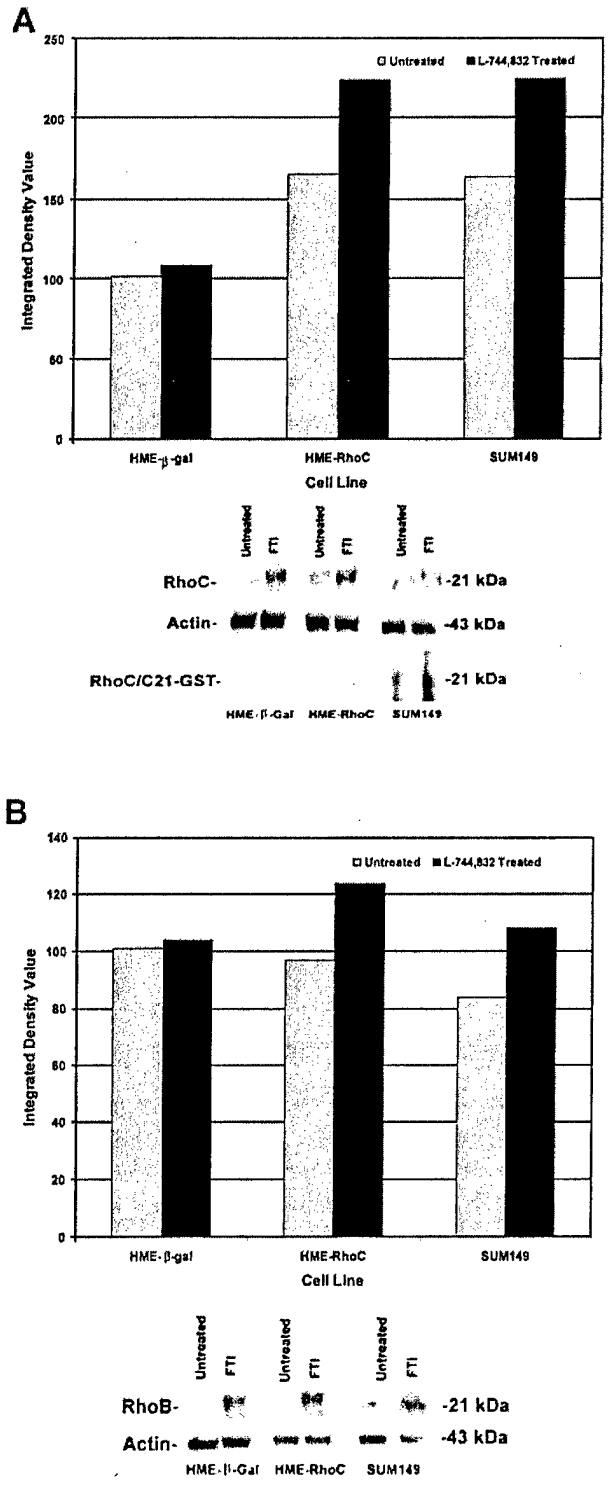

Fig. 3. Results of semiquantitative RT-PCR and Western blot analysis for RhoC GTPase (*A*) and RhoB GTPase (*B*). Densitometric comparison of the PCR products with a GAPDH internal standard demonstrated a modest increase in RhoC mRNA expression in all of the cell lines treated with FTI L-744,832 as compared with the untreated cell line. Similarly, an increase in RhoB mRNA expression was observed only for the HME-RhoC and SUM149 cell lines (*B*). A concurrent increase in RhoC protein levels was observed for the FTI-treated cell lines (*A*). This was accompanied by a slight increase in RhoC activity as determined by a C21-GST pulldown assay. As shown in *B*, RhoB protein levels increased in FTI-treated cells. *kDa*, M_r in thousands.

Table 1 Mean focus formation and SD after transient transfection with RhoB-GG, a geranylgeranyl-deficient RhoB (RhoB-A3), and vector alone

The number of foci were assessed in triplicate 35-mm plates. The data presented are from a seeding density of 100 cells/plate. However, similar trends were seen when cells were seeded at 1000 or 500 cells/plate. Focus formation was dramatically reduced in the RhoC-overexpressing HME-RhoC and SUM149 cells by expression of geranylgeranylated RhoB, but not an unprenylated mutant (RhoB-A3). Although a trend was noted, statistical analysis by a Kruskal-Wallis test did not demonstrate a significant difference between the groups.

Cell line	Vector alone	RhoB-GG	RhoB-A3
HME-β-gal	48.5 ± 5.5	24.5 ± 1	36.5 ± 2.5
HME-RhoC	85 ± 3	23.5 ± 1	69 ± 6.5
SUM149	19.5 ± 1.5	5 ± 0.5	20.5 ± 1
MCF10AT c1	53.5 ± 0.5	25.5 ± 6	46 ± 1.5

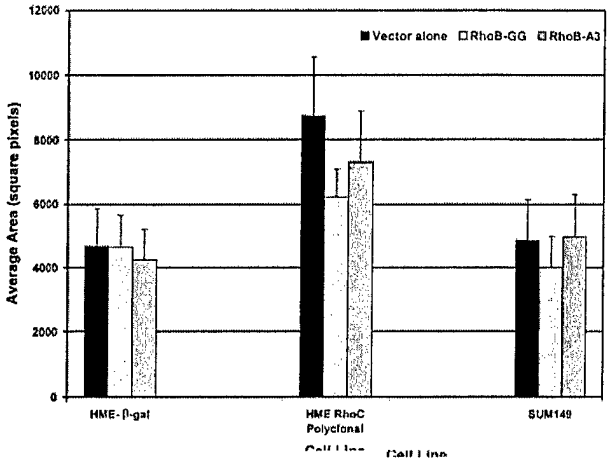

Fig. 4. Random motility assay of HME-β gal, HME-RhoC, and SUM149 cells transfected with either vector alone, RhoB-GG, or a geranylgeranyl mutant RhoB-A3. Although cell motility was not significantly altered, a trend was seen in the HME-RhoC and SUM149 cells transfected with RhoB-GG that resembled FTI treatment.

parts (Fig. 2, *K–L*). Similarly, the RhoB-GG transfectants were less motile when tested in the colloidal-gold assay (Fig. 4). Although statistical significance was not reached for the transfectants, the trends indicate that expression of RhoB-GG leads to decreased motility in RhoC-overexpressing breast cells. These data provide evidence for a role for RhoB-GG as a mechanism for inhibiting or reverting the RhoC-induced phenotype in these cells.

Discussion

The observation that H-Ras was inactive and not localized to its specific membrane compartment after FTI treatment led to the idea that these inhibitors could be used therapeutically (44–48). Like Ras, the Rho GTPases are posttranslationally modified to locate them to their distinct cellular compartment, so that they can carry out their specific function (17–19). Each Rho protein contains a COOH-terminal CAAX domain that determines prenylation and polybasic residues in the hypervariable domain, upstream of the CAAX domain, which dictate proper membrane localization (49).

Membrane localization and trafficking of the Rho GTPases are complex phenomena. Rho proteins are, in their inactive state, localized in the cytosol, sequestered there by specific RhoGD (25). On activation, the GTP-bound protein is prenylated and transported to its specific membrane compartment. The type of prenylation is dependent on the Rho protein (50–53). RhoC GTPase is geranylgeranylated, whereas RhoB is both geranylgeranylated and farnesylated (17–19, 50, 51).

It has been demonstrated that *in vitro*, Rho GTPases can self-aggregate (54). Cdc42 and Rac2 homodimer formation has been implicated in the negative regulation of the activity of those proteins (55). RhoB and RhoC GTPase have been found to exist, not as homodimers, but as either monomeric or oligomeric complexes. In addition, RhoC has been shown to have an arginine finger motif COOH-terminal to the CAAX domain, which imparts self-activated GTPase regulatory function (54). Specifically, GTP-bound RhoC, when in complex with itself, can self-convert to RhoC-GDP. In contrast, RhoB does not contain this arginine domain and, therefore, does not have intrinsic GAP activity. It is yet unknown whether RhoB and RhoC can form heterodimers either *in vitro* or *in vivo*. Because FTI cannot directly block geranylgeranyl RhoC function, one possible explanation for FTI suppression of RhoC function is that accumulation of RhoB-GG leads to the oligomerization of RhoC, which leads to increased intrinsic GAP activity and GTPase deactivation.

The promise of FTIs as a potent therapeutic reagent has been supported by *in vivo* studies. Mammary tumors that develop in K-*Ras* transgenic mice can be growth inhibited by FTI treatment (56). Lebowitz *et al.* (30) and Prendergast *et al.* (57–59) have provided have evidence that FTI suppression of Ras transformation was accomplished by interfering with Rho activity, because Rho was shown to be critical in Ras-induced transformation. Subsequent experiments demonstrated that a shift from farnesylated RhoB GTPase to RhoB-GG occurred on FTI treatment (30, 31, 60, 61). The shift in the specific forms of prenylated RhoB is accompanied by the accumulation and mislocalization of RhoB-GG, which is normally a short-lived protein (with a half-life of 2–4 h in cells; Refs. 30, 62). Our present data support these observations. In this study, we observed increased expression and accumulation of RhoB, presumably RhoB-GG, on treatment with FTI L-744,832. We also demonstrated that transient transfection of RhoC-overexpressing breast cells with RhoB-GG, recapitulated the effects of FTI treatment, inhibiting focus formation and random motility, whereas transfection with the RhoB GG-deficient mutant failed to mimic FTI effects.

In Ras-transformed cells, the effects of RhoB-GG may be attributable to a "gain-of-function" and relocalization of the protein (42, 43, 59, 63). Normally, RhoB GTPase is involved in vesicular and receptor trafficking (64). However, after FTI treatment, the inhibition of farnesylated RhoB and the accumulation of RhoB-GG, may lead to altered functions. The biosynthesis of geranylgeranyl PP_i is the next step after the synthesis of farnesyl PP_i in the acetyl-CoA pathway of cholesterol synthesis (reviewed by Cohen *et al.*; Ref. 48). Therefore, FTI treatment may provide more substrate for the geranylgeranyl PP_i synthase to produce geranylgeranyl PP_i and, ultimately, functionally geranylgeranylated Rho. Furthermore, several investigators suggest that a membrane receptor may exist that binds to the Rho prenyl-group, thereby helping to specifically localize it to a membrane compartment (51, 65–67). In this scenario, the accumulation of RhoB-GG may compete with RhoC, displacing it and possibly preventing it from interacting with downstream effector molecules.

In our experiments, we demonstrate that on FTI-treatment, RhoC levels also increase; however, the ratio of RhoB:RhoC remains increased over pretreatment levels. Furthermore, we speculate that RhoC may be accumulating in the cytoplasm, or, if it is reaching the inner membrane, its effect on the cell is attenuated by RhoB-GG. These ideas have yet to be tested. As demonstrated by labeling the actin cytoskeleton with a rhodamine-labeled phallotoxin, the polarized actin bundles associated with the motile RhoC cells are nearly lost on FTI treatment. Although focal adhesions are visible in both treated and untreated cells, they are located exclusively around the outside edges of the FTI-treated cells. Both laser confocal and scanning electron microscopy demonstrate that, as observed previously (57), the cells have lost their polarity and are flattened.

In contrast with Ras-transformed cells, the growth rate of the RhoC-overexpressing cells was only slightly affected by FTI treatment. Cell viability was also unaffected. Again, this is in contrast to previous experiments, which demonstrated that a combination of FTI and LY294002 (an inhibitor of P13K) led to increased apoptosis in Ras-transformed cells (31) but not in RhoC-overexpressing cells.

Taken together, these data suggest that FTIs may prove a potent novel therapeutic agent against tumors that overexpress RhoC GTPase. This is the first report of FTI inhibition of the cancer phenotype induced specifically by overexpression of RhoC GTPase. The mechanism of FTI action in RhoC-overexpressing IBC and HME transfectants may be similar to that previously described for Ras-transformed cells, namely, that the effect is mediated by the accumulation of RhoB-GG. However, as described above, there are notable differences in how FTI treatment affects cell growth in Ras-transformed *versus* RhoC-overexpressing cells. In addition to IBC, it has been demonstrated that aggressive noninflammatory, metastatic breast cancers, advanced pancreatic cancer, and metastatic melanoma overexpress RhoC GTPase, and this event significantly contributes to their clinical behavior; therefore, FTI treatment may be effective against these aggressive cancers (33, 68, 69). Our data support testing whether FTI treatment is efficacious in these aggressive RhoC-driven malignancies.

Acknowledgments

We thank Lisa Robbins for help in preparation of the manuscript and Satoru Hayasaka for performing statistical analysis. The reagents for the Rho-activation assay were kindly provided by Dr. John Collard of the Netherlands Cancer Institute (Amsterdam, the Netherlands).

References

1. Lee, B. J., and Tannenbaum, N. E. Inflammatory carcinoma of the breast: a report of twenty-eight cases from the breast clinic of Memorial Hospital. Surg. Gynecol. Obstet., *39:* 580–595, 1924.

2. Kleer, C. G., van Golen, K. L., and Merajver, S. D. Molecular biology of breast cancer metastasis. Inflammatory breast cancer: clinical syndrome and molecular determinants. Breast Cancer Res., *2:* 423–429, 2000.

3. Jaiyesimi, I. A., Buzdar, A. U., and Hortobagyi, G. Inflammatory breast cancer: a review. J. Clin. Oncol., *10:* 1014–1024, 1992.

4. Beahrs, O., Henson, D., and Hutter, R. Manual for Staging of Cancer, pp. 145–150. Philadelphia, PA: Lippincott, Williams, and Wilkins, 1988.

5. van Golen, K. L., Davies, S., Wu, Z. F., Wang, Y., Bucana, C. D., Root, H., Chandrasekharappa, S., Strawderman, M., Ethier, S. P., and Merajver, S. D. A novel putative low-affinity insulin-like growth factor-binding protein, LIBC (lost in inflammatory breast cancer), and RhoC GTPase correlate with the inflammatory breast cancer phenotype. Clin. Cancer Res., *5:* 2511–2519, 1999.

6. Ridley, A. J. The GTP-binding protein Rho. Int. J. Biochem. Cell Biol., *29:* 1225–1229, 1997.

7. Esteve, P., Embade, N., Perona, R., Jimenez, B., del Peso, L., Leon, J., Arends, M., Miki, T., and Lacal, J. C. Rho-regulated signals induce apoptosis *in vitro* and *in vivo* by a p53-independent, but Bc12 dependent pathway. Oncogene, *17:* 1855–1869, 1998.

8. Hall, A. Small GTP-binding proteins and the regulation of the cytoskeleton. Annu. Rev. Cell Biol., *10:* 31–54, 1994.

9. Apenstrom, P. Effectors for the Rho GTPases. Curr. Opin. Cell Biol., *11:* 95–102, 1999.

10. Nobes, C. D., and Hall, A. Rho, rac, and cdc42 GTPases regulate the assembly of multimolecular focal complexes associated with actin stress fibers, lamellipodia and filopodia. Cell, *81:* 53–62, 1995.

11. Takai, Y., Sasaki, T., and Matozaki, T. Small GTP-binding proteins. Physiol. Rev., *81:* 153–208, 2001.

12. van Golen, K. L., Wu, Z. F., Qiao, X. T., Bao, L. W., and Merajver, S. D. *RhoC GTPase*, a novel transforming oncogene for human mammary epithelial cells that partially recapitulates the inflammatory breast cancer phenotype. Cancer Res., *60:* 5832–5838, 2000.

13. van Golen, K. L., Wu, Z. F., Qiao, X. T., Bao, L. W., and Merajver, S. D. RhoC GTPase overexpression modulates induction of angiogenic factors in breast cells. Neoplasia (New York), *2:* 418–425, 2000.

14. van Golen, K. L., Wu, Z. F., Bao, L. W., and Merajver, S. D. RhoC GTPase induces a motile and invasive phenotype in inflammatory breast cancer. Clin. Exp. Metastasis, *17:* 745–745, 1999.

15. Geyer, M., and Wittinghofer, A. GEFs, GAPs, GDIs and effectors: taking a closer (3D) look at the regulation of Ras-related GTP-binding proteins. Curr. Opin. Struct. Biol., *7:* 786–792, 1997.

16. Prokopenko, S. N., Saint, R., and Bellen, H. J. Untying the Gordian knot of cytokinesis. Role of small G proteins and their regulators. J. Cell Biol., *148:* 843–848, 2000.

17. Seabra, M. C. Membrane association and targeting of prenylated Ras-like GTPases. Cell. Signalling, *10:* 167–172, 1998.

18. Kirschmeier, P. T., Whyte, D., Wilson, O., Bishop, W. R., and Pai, J. K. *In vivo* prenylation analysis of Ras and Rho proteins. Methods Enzymol., *332:* 115–127, 2001.

19. Adamson, P., Marshall, C. J., Hall, A., and Tilbrook, P. A. Post-translational modifications of p21rho proteins. J. Biol. Chem., *267:* 20033–20038, 1992.

20. Sinensky, M. Recent advances in the study of prenylated proteins. Biochim. Biophys. Acta., *1484:* 93–106, 2000.

21. Bishop, A. L., and Hall, A. Rho GTPases and their effector proteins. Biochem. J., *348 Pt 2:* 241–255, 2000.

22. Verbeke, G., and Molenberghs, G. Linear mixed models in practice: an SAS-oriented approach. New York, NY: Springer-Verlag, 1997.

23. Zohn, I. M., Campbell, S. L., Khosravi-Far, R., Rossman, K. L., and Der, C. J. Rho family proteins and Ras transformation: the RHOad less traveled gets congested. Oncogene, *17:* 1415–1438, 1998.

24. Gamblin, S. J., and Smerdon, S. J. GTPase-activating proteins and their complexes. Curr. Opin. Struct. Biol., *8:* 195–201, 1998.

25. Olofsson, B. Rho guanine dissociation inhibitors: pivotal molecules in cellular signalling. Cell. Signalling, *11:* 545–554, 1999.

26. Ethier, S. P., Kokeny, K. E., Ridings, J. W., and Dilts, C. A. erbB family receptor expression and growth regulation in a newly isolated human breast cancer cell line. Cancer Res., *56:* 899–907, 1996.

27. Ethier, S. P. Human breast cancer cell lines as models of growth regulation and disease progression. J. Mammary Gland Biol. Neoplasia, *1:* 111–121, 1996.

28. Sartor, C. I., Dziubinski, M. L., Yu, C. L., Jove, R., and Ethier, S. P. Role of epidermal growth factor receptor and STAT-3 activation in autonomous proliferation of SUM-102PT human breast cancer cells. Cancer Res., *57:* 978–987, 1997.

29. Band, V., Zajchowski, D., Kulesa, V., and Sager, R. Human papilloma virus DNAs immortalize normal human mammary epithelial cells and reduce their growth factor requirements. Proc. Natl. Acad. Sci. USA, *87:* 463–467, 1990.

30. Lebowitz, P. F., Davide, J. P., and Prendergast, G. C. Evidence that farnesyltransferase inhibitors suppress Ras transformation by interfering with Rho activity. Mol. Cell. Biol., *15:* 6613–6622, 1995.

31. Du, W., Liu, A., and Prendergast, G. C. Activation of the PI3'K-AKT pathway masks the proapoptotic effects of farnesyltransferase inhibitors. Cancer Res., *59:* 4208–4212, 1999.

32. Liu, A., Du, W., Liu, J. P., Jessell, T. M., and Prendergast, G. C. RhoB alteration is necessary for apoptotic and antineoplastic responses to farnesyltransferase inhibitors. Mol. Cell. Biol., *20:* 6105–6113, 2000.

33. Kleer, C. G., van Golen, K. L., Zhang, Y., Wu, Z. F., Rubin, M. A., and Merajver, S. D. Characterization of RhoC expression in benign and malignant breast disease: a potential new marker for small breast carcinomas with metastatic potential. Am. J. Pathol., *160:* 579–84, 2002.

34. Zondag, G. C. M., Evers, E. E., ten Klooster, J. P., Janssen, L., van der Kammen, R. A., and Collard, J. G. Oncogenic *Ras* downregulates Rac activity, which leads to increased Rho activity and epithelial-mesenchymal transition. J. Cell Biol., *149:* 775–782, 2000.

35. Evers, E. E., van der Kammen, R. A., ten Klooster, J. P., and Collard, J. G. Rho-like GTPases in tumor cell invasion. Methods Enzymol., *325:* 403–415, 2000.

36. Albrecht-Buehler, G. The phagokinetic tracks of 3T3 cells. Cell, *11:* 395–404, 1977.

37. van Golen, K. L., Risin, S., Staroselsky, A., Berger, D., Tainsky, M. A., Pathak, S., and Price, J. E. Predominance of the metastatic phenotype in hybrids formed by fusion of mouse and human melanoma clones. Clin. Exp. Metastasis, *14:* 95–106, 1996.

38. Darzynkiewicz, Z., Juan, G., Li, X., Gorczyca, W., Murakami, T., and Traganos, F. Cytometry in cell necrobiology: analysis of apoptosis and accidental cell death (necrosis). Cytometry, *27:* 1–20, 1997.

39. Sabourin, L. A., and Hawley, R. G. Suppression of programmed death and G_1 arrest in B-cell hybridomas by interleukin-6 is not accompanied by altered expression of immediate early response genes. J. Cell Physiol., *145:* 564–574, 1990.

40. MacPherson, I., and Montangnier, L. Agar suspension culture for the selective assay of cells transformed by polyoma virus. Virology, *23:* 291–294, 1964.

41. Santner, S. J., Dawson, P. J., Tait, L., Soule, H. D., Eliason, J., Mohamed, A. N., Wolman, S. R., Heppner, G. H., and Miller, F. R. Malignant MCF10CA1 cell lines derived from premalignant human breast epithelial MCF10AT cells. Breast Cancer Res. Treat., *65:* 101–110, 2001.

42. Du, W., Lebowitz, P. F., and Prendergast, G. C. Cell growth inhibition by farnesyltransferase inhibitors is mediated by gain of geranylgeranylated RhoB. Mol. Cell. Biol., *19:* 1831–1840, 1999.

43. Liu, A., and Prendergast, G. C. Geranylgeranylated RhoB is sufficient to mediate tissue-specific suppression of Akt kinase activity by farnesyltransferase inhibitors. FEBS Lett., *24114:* 1–4, 2000.

44. Garcia, A. M., Rowell, C., Ackermann, K., Kowalczyk, J. J., and Lewis, M. D. Peptidomimetic inhibitors of Ras farnesylation and function in whole cells. J. Biol. Chem., *268:* 18415–18418, 1993.

45. James, G. L., Goldstein, J. L., Brown, M. S., Rawson, T. E., Somers, T. C., McDowell, R. S., Crowley, C. W., Lucas, B. K., Levinson, A. D., and Marsters, J. C., Jr. Benzodiazepine peptidomimetics: potent inhibitors of Ras farnesylation in animal cells. Science (Wash. DC), *260:* 1937–1942, 1993.

46. Kohl, N. E., Mosser, S. D., deSolms, S. J., Giuliani, E. A., Pompliano, D. L., Graham, S. L., Smith, R. L., Scolnick, E. M., Oliff, A., and Gibbs, J. B. Selective inhibition of ras-dependent transformation by a farnesyltransferase inhibitor. Science (Wash. DC), *260:* 1934–1937, 1993.

47. Rowinsky, E. K., Windle, J. J., and Von Hoff, D. D. Ras protein farnesyltransferase: a strategic target for anticancer therapeutic development. J. Clin. Oncol., *17:* 3631–3652, 1999.

48. Cohen, L. H., Pieterman, E., van Leeuwen, R. E., Overhand, M., Burm, B. E., van der Marel, G. A., and van Boom, J. H. Inhibitors of prenylation of Ras and other G-proteins and their application as therapeutics. Biochem. Pharmacol., *60:* 1061–1068, 2000.

49. Mondal, M. S., Wang, Z., Seeds, A. M., and Rando, R. R. The specific binding of small molecule isoprenoids to rhoGDP dissociation inhibitor (rhoGDI). Biochemistry, *39:* 406–412, 2000.

50. Hancock, J. F., Magee, A. I., Childs, J. E., and Marshall, C. J. All ras proteins are polyisoprenylated but only some are palmitoylated. Cell, *57:* 1167–1177, 1989.

51. Hancock, J. F., Cadwallader, K., Paterson, H., and Marshall, C. J. A CAAX or a CAAL motif and a second signal are sufficient for plasma membrane targeting of ras proteins. EMBO J., *10:* 4033–4039, 1991.

52. Lai, R. K., Perez-Sala, D., Canada, F. J., and Rando, R. R. The γ subunit of transducin is farnesylated. Proc. Natl. Acad. Sci. USA, *87:* 7673–7677, 1990.

53. Rando, R. R. Chemical biology of protein isoprenylation/methylation. Biochim. Biophys. Acta, *1300:* 5–16, 1996.

54. Zhang, B., Zhang, Y., Collins, C. C., Johnson, D. I., and Zheng, Y. A built-in arginine finger triggers the self-stimulatory GTPase-activating activity of rho family GTPases. J. Biol. Chem., *274:* 2609–2612, 1999.

55. Zhang, B., and Zheng, Y. Negative regulation of Rho family GTPases Cdc42 and Rac2 by homodimer formation. J. Biol. Chem., *273:* 25728–25733, 1998.

56. Omer, C. A., Chen, Z., Diehl, R. E., Conner, M. W., Chen, H. Y., Trumbauer, M. E., Gopal-Truter, S., Seeburger, G., Bhimnathwala, H., Abrams, M. T., Davide, J. P., Ellis, M. S., Gibbs, J. B., Greenberg, I., Hamilton, K., Koblan, K. S., Kral, A. M., Liu, D., Lobell, R. B., Miller, P. J., Mosser, S. D., O'Neill, T. J., Rands, E., Schaber, M. D., Senderak, E. T., Oliff, A., and Kohl, N. E. Mouse mammary tumor virus-Ki-*ras*B transgenic mice develop mammary carcinomas that can be growth-inhibited by a farnesyl:protein transferase inhibitor. Cancer Res., *60:* 2680–2688, 2000.

57. Prendergast, G. C., Davide, J. P., deSolms, S. J., Giuliani, E. A., Graham, S. L., Gibbs, J. B., Oliff, A., and Kohl, N. E. Farnesyltransferase inhibition causes morphological reversion of ras-transformed cells by a complex mechanism that involves regulation of the actin cytoskeleton. Mol. Cell. Biol., *14:* 4193–4202, 1994.

58. Prendergast, G. C., Khosravi-Far, R., Solski, P. A., Kurzawa, H., Lebowitz, P. F., and Der, C. J. Critical role of Rho in cell transformation by oncogenic *Ras*. Oncogene, *10:* 2289–2296, 1995.

59. Prendergast, G. C., and Oliff, A. Farnesyltransferase inhibitors: antineoplastic properties, mechanisms of action, and clinical prospects. Semin. Cancer Biol., *10:* 443–452, 2000.

60. Lebowitz, P. F., Casey, P. J., Prendergast, G. C., and Thissen, J. A. Farnesyltransferase inhibitors alter the prenylation and growth-stimulating function of RhoB. J. Biol. Chem., *272:* 15591–15594, 1997.

61. Lebowitz, P. F., and Prendergast, G. C. Non-Ras targets of farnesyltransferase inhibitors: focus on Rho. Oncogene, *17:* 1439–1445, 1998.

62. Zalcman, G., Closson, V., Linares-Cruz, G., Lerebours, F., Honore, N., Tavitian, A., and Olofsson, B. Regulation of Ras-related RhoB protein expression during the cell cycle. Oncogene, *10:* 1935–1945, 1995.

63. Prendergast, G. C. Farnesyltransferase inhibitors define a role for RhoB in controlling neoplastic pathophysiology. Histol. Histopathol., *16:* 269–275, 2001.

64. Leung, T., Chen, X., Manser, E., and Lim, L. The p160 RhoA-binding kinase ROKα is a member of a kinase family and is involved in the reorganization of the cytoskeleton. Mol. Cell. Biol., *16:* 5313–5327, 1996.

65. Michaelson, D., Silletti, J., Murphy, G., D'Eustachio, P., Rush, M., and Philips, M. R. Differential localization of Rho GTPases in live cells: regulation by hypervariable regions and RhoGDI binding. J. Cell. Biol., *152:* 111–126, 2001.

66. Gelb, M. H. Protein prenylation, et cetera: signal transduction in two dimensions. Science (Wash. DC), *275:* 1750–1751, 1997.

67. Glomset, J. A., and Farnsworth, C. C. Role of protein modification reactions in programming interactions between ras-related GTPases and cell membranes. Annu. Rev. Cell Biol., *10:* 181–205, 1994.

68. Suwa, H., Ohshio, G., Imamura, T., Watanabe, G., Arii, S., Imamura, M., Narumiya, S., Hiai, H., and Fukumoto, M. Overexpression of the *rhoC* gene correlates with progression of ductal adenocarcinoma of the pancreas. Br. J. Cancer, *77:* 147–152, 1998.

69. Clark, E. A., Golub, T. R., Lander, E. S., and Hynes, R. O. Genomic analysis of metastasis reveals an essential role for RhoC. Nature (Lond.), *406:* 532–535, 2000.

Breast Cancer Research Vol 6 No 2 Kleer *et al.*

Research article

Open Access

WISP3 and RhoC guanosine triphosphatase cooperate in the development of inflammatory breast cancer

Celina G Kleer[1,3], Yanhong Zhang[1,3], Quintin Pan[2,3], Gary Gallagher[1,3], Mei Wu[1,2], Zhi-Fen Wu[2,3] and Sofia D Merajver[2,3]

[1]Department of Pathology, Univeristy of Michigan, Ann Arbor, MI, USA
[2]Department of Internal Medicine, Univeristy of Michigan, Ann Arbor, MI, USA
[3]Comprehensive Cancer Center, Univeristy of Michigan, Ann Arbor, MI, USA

Correspondence: Sofia D Merajver (e-mail: smerajve@umich.edu)

Received: 17 Jun 2003 Revisions requested: 28 Aug 2003 Revisions received: 4 Dec 2003 Accepted: 5 Dec 2003 Published: 19 Dec 2003

Breast Cancer Res 2004, 6:R110-R115 (DOI 10.1186/bcr755)

Abstract

Background: Inflammatory breast cancer (IBC) is the most lethal form of locally advanced breast cancer. We found concordant and consistent alterations of two genes in 90% of IBC tumors when compared with stage-matched non-IBC tumors: overexpression of RhoC guanosine triphosphatase and loss of WNT-1 induced secreted protein 3 (WISP3). Further work revealed that RhoC is a transforming oncogene for human mammary epithelial (HME) cells. Despite the aggressiveness of the RhoC-driven phenotype, it does not quantitatively reach that of the true IBC tumors. We have demonstrated that WISP3 has tumor growth and angiogenesis inhibitory functions in IBC. We proposed that RhoC and WISP3 cooperate in the development of IBC.

Methods: Using an antisense approach, we blocked WISP3 expression in HME cells. Cellular proliferation and growth were determined using the 3-[4,5-dimethylthiazol-2-yl]-2,5-diphenyltetrazolium bromide (MTT) assay and anchorage-independent growth in a soft agar assay. Vascular endothelial growth factor (VEGF) was measured in conditioned medium by enzyme-linked immunosorbent assay.

Results: Antisense inhibition of WISP3 in HME cells increased RhoC mRNA levels and resulted in an increase in cellular proliferation, anchorage-independent growth and VEGF levels in the conditioned medium. Conversely, restoration of WISP3 expression in the highly malignant IBC cell line SUM149 was able to decrease the expression of RhoC protein.

Conclusion: WISP3 modulates RhoC expression in HME cells and in the IBC cell line SUM149. This provides further evidence that these two genes act in concert to give rise to the highly aggressive IBC phenotype. We propose a model of this interaction as a starting point for further investigations.

Keywords: CCN proteins, motility, oncogene, tumor suppressor gene, vascular endothelial growth factor, WNT-pathway

Introduction

Inflammatory breast cancer (IBC) is the most lethal form of locally advanced breast cancer and accounts for approximately 6% of new breast cancer cases annually in the United States [1,2]. IBC has distinct clinical and pathological features. Patients present with erythema, skin nodules, dimpling of the skin (termed 'peau d'orange'), all features that develop rapidly, typically progressing within 6 months [1–4]. One salient feature of IBC that is observed in tissue sections is that cancer cells form emboli that spread through the dermal lymphatics. The dermatotropism of IBC is believed to be responsible for the clinical signs and symptoms and probably enables effective dissemination to distant sites [2]. These observations lead us to conclude that IBC is highly invasive and that it is capable of metastases from its inception. Indeed, at the time of diagnosis, most patients have locoregional and/or distant metastatic disease [3,4]. In spite of new advances in breast cancer

FBS = fetal bovine serum; GTPase = guanosine triphosphatase; HME = human mammary epithelial; IBC = inflammatory breast cancer; MTT = 3-[4,5-dimethylthiazol-2-yl]-2,5-diphenyltetrazolium bromide; PCR = polymerase chain reaction; RT–PCR = reverse transcriptase PCR; VEGF = vascular endothelial growth factor; WISP3 = WNT-1 induced secreted protein 3.

therapy including multimodality approaches, the 5-year disease-free survival rate is less than 45% [3,4].

Until recently, no biological markers defined the IBC phenotype. We proposed that a limited number of genetic alterations, occurring in rapid succession or concordantly, are responsible for the rapidly progressive and distinct clinical and pathological features of IBC. Using a modified version of the differential display technique and *in situ* hybridization of human tumors, we identified two genes that are consistently and concordantly altered in human IBC when compared with stage-matched non-IBC tumors: loss of WISP3 and overexpression of RhoC guanosine triphosphatase (GTPase) [5].

WNT-1 induced secreted protein 3 (WISP3) is a member of the CCN family of proteins, which have important biological functions in normal physiology as well as in carcinogenesis [6–8]. We found that WISP3 has growth and angiogenesis inhibitory functions in IBC *in vitro* and *in vivo* [9]. RhoC GTPase is a member of the Ras superfamily of small GTPases. Activation of Rho proteins leads to assembly of the actin–myosin contractile filaments into focal adhesion complexes that bring about cell polarity and facilitate motility [10–12]. Our laboratory has characterized RhoC as a transforming oncogene for human mammary epithelial (HME) cells; its overexpression results in a highly motile and invasive phenotype that recapitulates the IBC phenotype. Predicated on the high rate of concordance of RhoC and WISP3 changes in IBC, we propose that these two genes cooperate to determine this highly metastatic, unique breast cancer phenotype.

Materials and methods

Cell culture

The derivation of the SUM149 cell line has been described previously by Ethier et al [13]. This cell line was developed from a human primary IBC and has lost WISP3 expression [9]. HME cells were immortalized with human papilloma virus E6/E7 and were characterized as being keratin 19 positive, ensuring that they are from the same differentiation lineage as the SUM149 IBC tumor cell line [14,15]. MCF10A cells are spontaneously immortalized human mammary epithelial cells. Cells were cultured in Ham's F-12 medium supplemented with 5% fetal bovine serum (FBS), hydrocortisone (1 μg/ml), insulin (5 μg/ml), fungizone (2.5 μg/ml), gentamycin (5 μg/ml), penicillin (100 U/ml) and streptomycin (10 μg/ml) at 37°C under 10% CO_2.

Construction of expression vectors and stable transfections

Total RNAs were isolated from HME cells with a Trizol kit (Life Technologies, Inc, Gaithersburg, MD). First-strand cDNA synthesis was performed by using 1 μg of total RNA with AMV reverse transcriptase (Promega, Madison, WI) and oligo(dT) as a primer. A 2 μl portion of the reaction mixture was used for amplification by polymerase chain reaction (PCR). Human WISP3 cDNA was amplified by PCR with the forward and reverse primers 5′-ACGAATTCAATGAACAAGCGGCG-3′ and 3′-GCGAATTCTTTTACAGAATCTTG-5′, respectively, under the following conditions: denaturing for 1 min at 94°C, annealing for 1 min at 58°C, and elongation for 1 min at 72°C, for 35 cycles. PCR products were cloned into pGEM-T Easy vector (Promega). The 1.1 kb full-length cDNA encoding WISP3 was excised by *Eco*RI and subcloned into the *Eco*RI site of pFlag-CMV4 vector (Sigma, St Louis, MO). The insert was confirmed by DNA sequencing. The plasmids were purified. Subsequently, the SUM149 cells were transfected with pFlag-WISP3 sense (SUM149/WISP3), and HME cells were transfected with pFlag-WISP3 antisense (HME/AS WISP3). MCF10A cells were stably tranfected with full-length RhoC cDNA (MCF10A/RhoC). pFlag control vectors were used as controls (FuGene TM 6 transfection reagent; Roch–Boehringer-Mannheim, Germany). Transfectants were selected in the medium containing 150 μg/ml G418. The cells surviving during selection were expanded and maintained in the selected medium.

Reverse transcriptase PCR (RT–PCR) analysis

Total RNA (1 μg) from HME/AS WISP3 clones and empty vector controls were reverse-transcribed with Superscript reverse transcriptase (Invitrogen) using oligo(dT) and random hexanucleotide primer for first-strand cDNA synthesis. PCRs were performed directly on 1 μl of first-strand cDNA using 500 nmol of each of the following gene-specific primers: WISP3, 5′-ATGCAGGGGCTCCTCTTCTGC-3′ (forward primer) and 5′-ACTTTTCCCCCATTTGCTTG-3′ (reverse primer); RhoC , 5′-ATGGCTGCAATCCGAAAG-3′ (forward primer) and 5′-GATCTCAGAGAATGGGACAGC-3′ (reverse primer); GAPDH, 5′-CGGAGTCAACGGATTTGGTCGTAT-3′ (forward primer) and 5′-AGCCTTCTCCATGGTGGTGAAGAC-3′ (reverse primer). The 100 μl reaction volume consisted of 50 mM KCl, 10 mM Tris-HCl pH 8.3, 1.5 mM $MgCl_2$, and deoxynucleotide triphosphates (each at 200 μM). PCR was performed for initial denaturation at 94°C for 5 min, followed by 35 cycles of denaturation (94°C, 1 min), annealing (55°C, 1 min), and extension (72°C, 1 min) with 5 units of *Taq* polymerase (Invitrogen). This was followed by a final extension step at 72°C for 10 min. The products were analyzed on 1% agarose gels stained with ethidium bromide and detected with ultraviolet illumination.

Western immunoblots

Western immunoblots were performed with polyclonal anti-RhoC and anti-WISP3 antibodies. Cultured cells were washed in ice-cold phosphate-buffered saline, lysed in lysis buffer (10% glycerol, 50 mM Tris-HCl pH 7.4, 100 mM NaCl, 1% Nonidet P40, 2 mM $MgCl_2$, 1 μg/ml leupeptin, 1 μg/ml aprotinin, 1 mM phenylmethylsulphonyl

fluoride) on ice for 5 min, and then centrifuged for 5 min at 4°C. Cleared lysates (each containing 50 µg of protein) were subjected to SDS–polyacrylamide-gel electrophoresis and transferred to poly(vinylidene difluoride) membrane. Western blots were performed as described previously, with anti-RhoC rabbit polyclonal antibody and anti-β-actin goat antibody (Sigma) at dilutions of 1 : 1500 and 1 : 2000, respectively [16].

Anchorage-independent growth

For studies of anchorage-independent growth we performed soft agar assays on stable clones of HME/AS WISP3, HME/Flag, and SUM149 cells. Each well of a six-well plate was first layered with 0.6% agar diluted with 10% FBS-supplemented Ham's F-12 medium complete with growth factors. The cell layer was then prepared by diluting agarose to concentrations of 0.3% and 0.6% with 10^3 cells in 2.5% FBS-supplemented Ham's F-12/1.5 ml/well. Plates were maintained at 37°C under 10% CO_2 for 3 weeks. Colonies 100 µm or more in diameter were counted under the microscope with a grid.

Monolayer growth rate

Monolayer culture growth rate was determined by qualitative measurement of the conversion of 3-(4,5-dimethylthiazol-2-yl)-2,5-diphenyltetrazolium bromide (MTT; Sigma) to a water-insoluble formazan by viable cells. In all, 3000 cells obtained for HME/AS WISP3 clones, HME/Flag, and HME wild-type cells, suspended in 200 µl of culture medium, were plated in 96-well plates and grown under normal conditions. Cultures were assayed at 0, 2, 4, 6, and 8 days by the addition of MTT and incubation for 1 hour at 37°C. The MTT-containing medium was aspirated and 100 µl of dimethyl sulphoxide (Sigma) was added to lyse the cells and solubilize the formazan. Optical densities of the lysates were determined on a Dynatech MR 5000 microplate reader at 595 nm.

Analysis of vascular endothelial growth factor

Conditioned medium was generated by incubating HME/AS WISP3 cells, HME/Flag cells, and SUM149 cells in serum-free medium. After 3 days the medium was collected, cleared of cell debris by centrifugation, concentrated approximately 10-fold through a Centriplus YM-10 column (Millipore, Bedford, MA). The levels of vascular endothelial growth factor (VEGF), which is a factor known to be secreted by IBC, were measured in the cell culture supernatants by enzyme-linked immunosorbent assay, as described previously [9,17].

Results

Inhibition of WISP3 increases RhoC mRNA levels in immortalized HME cells and induces proliferation, anchorage-independent growth, and VEGF production

To study the effects of inhibition of WISP3 expression on the phenotype of HME cells, we established clones of HME cells stably transfected with antisense WISP3 constructs (HME/AS WISP3). Effective inhibition of WISP3 expression was confirmed by RT–PCR (Fig. 1). Inhibition of WISP3 expression in HME cells resulted in increased expression of RhoC transcript in comparison with HME cells transfected with the control empty vector (Fig. 1). After 14 days of growth in soft agar, inhibition of WISP3 expression in HME cells resulted in a significant increase in the number of colonies formed in comparison with the empty vector control (*t*-test, $P<0.05$ for both clones; Fig. 2a). Inhibition of WISP3 expression resulted in an increase in cellular proliferation (*t*-test, $P<0.05$; Fig. 2b).

Figure 1

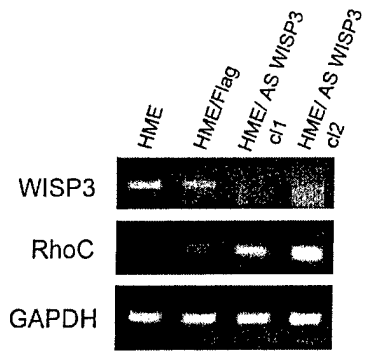

Inhibition of WISP3 in human mammary epithelial (HME) cells results in an increase in RhoC transcript levels. Reverse transcriptase polymerase chain reaction was conducted on vector and HME cells that have inhibition of WISP3 expression using full-length WISP3 antisense mRNA. HME/AS WISP3 cells showed increased levels of RhoC transcript in comparison with controls.

Previously, we had shown that restoration of WISP3 expression in an IBC cell line decreases the production of VEGF, a major pro-angiogenic factor secreted by IBC [9]. To determine the effect of WISP3 inhibition on the secretion of VEGF, we measured the concentration of VEGF in the conditioned medium of the stably transfected HME/AS WISP3 cells. Figure 2c shows that inhibition of WISP3 expression resulted in increased levels of VEGF in the conditioned medium (*t*-test, $P<0.05$ for all clones).

Restoration of WISP3 expression in SUM149 cells decreases RhoC expression

Because decreased expression of WISP3 in HME cells induced a significant increase in RhoC expression and some features of RhoC induced functional changes including anchorage-independent growth and production of VEGF, we sought to determine whether restoration of WISP3 expression in the SUM149 IBC cell line, which has lost WISP3 expression in the wild type, has an effect in RhoC expression. To test this, we stably transfected WISP3 in SUM149 cells and measured RhoC expression

Figure 2

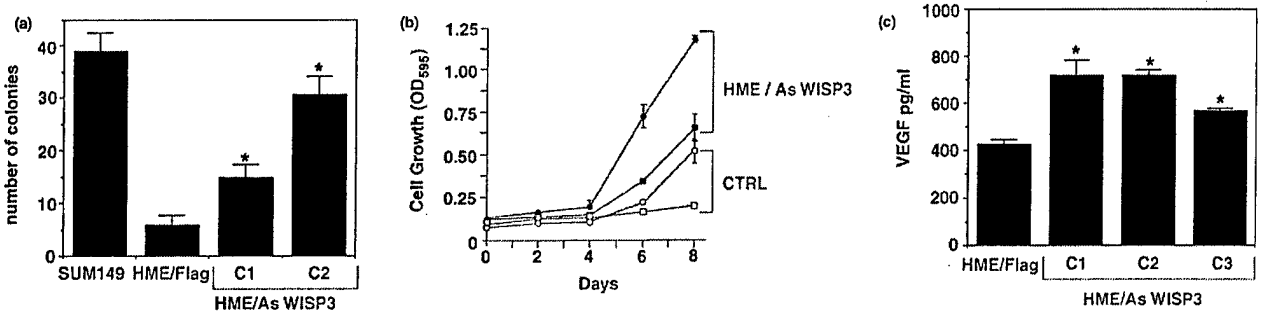

Inhibition of WISP3 induces anchorage-independent growth, proliferation and secretion of vascular endothelial growth factor (VEGF) in human mammary epithelial (HME) cells. **(a)** Inhibition of WISP3 expression in HME cells. HME cells greatly increased the number of colonies formed in soft agar in comparison with empty vector control (HME/Flag; *t*-test, $P<0.05$ for both clones). **(b)** Effect of inhibition of WISP3 expression on the proliferation of HME cells was studied with the 3-(4,5-dimethylthiazol-2-yl)-2,5-diphenyltetrazolium bromide (MTT) assay. The stable HME/AS WISP3 cells have a significant increase in the proliferation rate in comparison with the empty vector control. Results are expressed as means ± SEM of three independent experiments. In all, 3000 cells were assessed in each plate (*t*-test, $P<0.05$). **(c)** Increase in VEGF measured by enzyme-linked immunosorbent assay, as a result of inhibition of WISP3 expression in HME cells. Results are expressed as means ± SEM; *t*-test, $P<0.05$ for all clones.

Figure 3

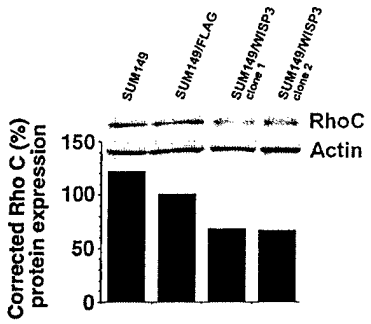

Restoration of WISP3 expression in SUM149 inflammatory breast cancer cells decreases RhoC protein expression. Western immunoblot of cell culture of SUM 149 cells, empty vector control (SUM149/Flag), and two WISP3-expressing clones with antibodies against RhoC and actin. Gels were scanned and pixel intensity values were obtained. Values for RhoC were corrected for loading by dividing the RhoC pixel intensity by the actin pixel intensity.

Figure 4

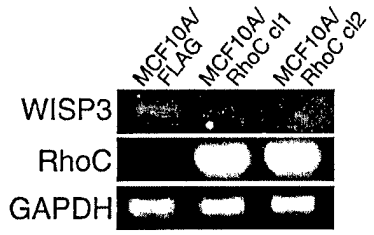

RhoC overexpression in MCF10A cells results in a decrease in WISP3 mRNA level. Reverse transcriptase polymerase chain reaction was conducted on vector and MCF10A cells stably overexpressing RhoC. RhoC-overexpressing cells had decreased levels of WISP3 mRNA.

by Western blotting. Restoration of WISP3 expression in SUM149 cells resulted in a decrease in RhoC protein expression in comparison with the empty vector control (Fig. 3). To investigate whether the relationship between WISP3 and RhoC expression is reciprocal, we developed MCF10A cells stably transfected with RhoC. These cells showed a 2.5-fold decrease in WISP3 mRNA expression (Fig. 4).

Discussion

Our previous work showed that the overexpression of RhoC GTPase and the loss of WISP3 expression are alterations that occur concordantly, more often in IBC than in slow-growing locally advanced breast cancers. WISP3 loss was found in concert with RhoC GTPase overexpression in 90% of archival patient samples of IBC, but rarely in stage-matched non-IBC tumors. Our laboratory further demonstrated that RhoC GTPase is a transforming oncogene for HME cells and that WISP3 has tumor inhibitory functions in IBC. However, neither alteration occurring in isolation seems to be sufficient to develop the full-blown, highly malignant IBC phenotype. Here we postulate that dysregulation of WISP3 might upregulate RhoC GTPase and thus enhance the aggressiveness of the phenotype that results when these two alterations are present.

We have shown that overexpression of RhoC GTPase in immortalized HME cells produced a striking tumorigenic effect that, for the most part, recapitulates the phenotype of the SUM149 IBC cell line. HME cells stably transfected with RhoC exhibited greatly increased growth under anchorage-independent conditions [15]. HME cells over-

expressing RhoC produced up to 100-fold more colonies than the controls, about 60% of the level of colony formation of the SUM149 IBC cell line. RhoC overexpression induced motility and invasion in HME cells, and markedly induced the production of angiogenic mediators including VEGF [17]. The HME/RhoC transfectants formed tumors when injected into the mammary fat pad of athymic nude mice [15].

Importantly, restoration of WISP3 in SUM149 cells ameliorated these features of the malignant phenotype. The SUM149/WISP3$^+$ cells exhibited decreased growth *in vitro* and *in vivo* in comparison with SUM149 cells transfected with the empty vector. The invasiveness of SUM149 cells was greatly decreased by restoring WISP3 expression. We also found that WISP3 markedly decreased the concentration of angiogenic mediators in the conditioned medium, especially VEGF, basic fibroblast growth factor, and interleukin-6 [9]. Given the high specificity of WISP3 and RhoC alterations in IBC and their interrelated functions in tumorigenesis, we propose that they cooperate in the development of IBC.

Using an antisense approach, inhibition of WISP3 expression in HME cells resulted in a threefold increase of RhoC GTPase transcript levels. The HME/AS WISP3 cells also exhibited increased cellular proliferation and anchorage-independent growth in soft agar. The HME/AS WISP3 cells produced significantly more colonies in soft agar in comparison with the control cells, an average of 58% of the level of colonies formed by the SUM149 IBC cells. HME/AS WISP3 cells also exhibited decreased production of VEGF in the conditioned medium.

The relationship between RhoC and WISP3 expression seems to be reciprocal. Restoration of WISP3 expression in SUM149 cells, which have lost WISP3 in the wild-type state, induced a 1.5-fold decrease in RhoC GTPase expression. These results are intriguing because changes in expression in Rho proteins by subtle factors such as 1.5–1.8 can be sufficient to modulate cellular behavior. Overexpression of RhoC in spontaneously immortalized HME cells, MCF10A, resulted in a 2.5-fold decrease in WISP3 mRNA expression.

In summary, overexpression of RhoC GTPase and loss of WISP3 are key genetic alterations in the development of IBC, and they have complementary functions. RhoC GTPase has a primary a role in motility, invasion, and angiogenesis [15,17]. WISP3 has a pivotal role in tumor growth, invasion, and angiogenesis [9]. Here we have further strengthened the evidence that these genes cooperate in the development of IBC, because WISP3 expression modulates the expression of RhoC GTPase and its functions.

Conclusion

IBC is the most lethal form of locally advanced breast cancer, with a 5-year disease-free survival of less than 45%. Our work focused on determining the genetic alterations that result in this aggressive breast cancer phenotype. Previously, we have found that RhoC and WISP3 are consistently and concordantly altered in IBC tissues. RhoC functions as an oncogene, and WISP3 as a tumor suppressor gene. Here we provide evidence supporting the hypothesis that these two genes act in concert to give rise to the highly aggressive IBC phenotype. We propose a model of this interaction as a starting point for further investigations.

Competing interests

None declared.

Acknowledgements

This work was supported in part by DOD grants DAMD17-02-1-0490 and DAMD17-02-1-0491 (CGK), DOD grants DAMD17-00-1-0345 and DAMD17-02-1-0492 (SDM), and NIH grants K08CA090876-01A2 (CGK), RO1CA77612 (SDM), P30CA46592 and M01-RR00042. We thank S Ethier for supplying the SUM149 and HME cell lines and R Kunkel for art work.

References

1. Jaiyesimi IA, Buzdar AU, Hortobagyi G: **Inflammatory breast cancer: a review.** *J Clin Oncol* 1992, **10**:1014-1024.
2. Lee BJ, Tannenbaum ND: **Inflammatory carcinoma of the breast: a report of twenty-eight cases from the breast clinic of Memorial Hospital.** *Surg Gynecol Obstet* 1924, **39**:580-595.
3. Merajver SD, Weber BL, Cody R, Zhang D, Strawderman M, Calzone KA, LeClaire V, Levin A, Irani J, Halvie M, August D, Wicha M, Lichter A, Pierce LJ: **Breast conservation and prolonged chemotherapy for locally advanced breast cancer: the University of Michigan experience.** *J Clin Oncol* 1997, **15**: 2873-2881.
4. Swain SM, Sorace RA, Bagley CS, Danforth DN Jr, Bader J, Wesley MN, Steinberg SM, Lippman ME: **Neoadjuvant chemotherapy in the combined modality approach of locally advanced nonmetastatic breast cancer.** *Cancer Res* 1987, **47**: 3889-3894.
5. van Golen KL, Davies S, Wu ZF, Wang Y, Bucana CD, Root H, Chandrasekharappa S, Strawderman M, Ethier SP, Merajver SD: **A novel putative low-affinity insulin-like growth factor-binding protein, LIBC (lost in inflammatory breast cancer), and RhoC GTPase correlate with the inflammatory breast cancer phenotype.** *Clin Cancer Res* 1999, **5**:2511-2519.
6. Perbal B: **NOV (nephroblastoma overexpressed) and the CCN family of genes: structural and functional issues.** *Mol Pathol* 2001, **54**:57-79.
7. Pennica D, Swanson TA, Welsh JW, Roy MA, Lawrence DA, Lee J, Brush J, Taneyhill LA, Deuel B, Lew M, Watanabe C, Cohen RL, Melhem MF, Finley GG, Quirke P, Goddard AD, Hillan KJ, Gurney AL, Botstein D, Levine AJ: **WISP genes are members of the connective tissue growth factor family that are up-regulated in wnt-1-transformed cells and aberrantly expressed in human colon tumors.** *Proc Natl Acad Sci USA* 1998, **95**:14717-14722.
8. Hurvitz JR, Suwairi WM, Van Hul W, El-Shanti H, Superti-Furga A, Roudier J, Holderbaum D, Pauli RM, Herd JK, Van Hul EV, Rezai-Delui H, Legius E, Le Merrer M, Al-Alami J, Bahabri SA, Warman ML: **Mutations in the CCN gene family member WISP3 cause progressive pseudorheumatoid dysplasia.** *Nat Genet* 1999, **23**:94-98.
9. Kleer CG, Zhang Y, Pan Q, van Golen KL, Wu ZF, Livant D, Merajver SD: **WISP3 is a novel tumor suppressor gene of inflammatory breast cancer.** *Oncogene* 2002, **21**:3172-3180.
10. Kimura K, Ito M, Amano M, Chihara K, Fukata Y, Nakafuku M, Yamamori B, Feng J, Nakano T, Okawa K, Iwamatsu A, Kaibuchi

K: **Regulation of myosin phosphatase by Rho and Rho-associated kinase (Rho-kinase).** *Science* 1996, **273**:245-248.
11. Leung T, Chen XQ, Manser E, Lim L: **The p160 RhoA-binding kinase ROK alpha is a member of a kinase family and is involved in the reorganization of the cytoskeleton.** *Mol Cell Biol* 1996, **16**:5313-5327.
12. Nobes CD, Hall A: **Rho, rac, and cdc42 GTPases regulate the assembly of multimolecular focal complexes associated with actin stress fibers, lamellipodia, and filopodia.** *Cell* 1995, **81**: 53-62.
13. Ethier SP, Mahacek ML, Gullick WJ, Frank TS, Weber BL: **Differential isolation of normal luminal mammary epithelial cells and breast cancer cells from primary and metastatic sites using selective media.** *Cancer Res* 1993, **53**:627-635.
14. Band V, Zajchowski D, Kulesa V, Sager R: **Human papilloma virus DNAs immortalize normal human mammary epithelial cells and reduce their growth factor requirements.** *Proc Natl Acad Sci USA* 1990, **87**:463-467.
15. van Golen KL, Wu ZF, Qiao XT, Bao LW, Merajver SD: **RhoC GTPase, a novel transforming oncogene for human mammary epithelial cells that partially recapitulates the inflammatory breast cancer phenotype.** *Cancer Res* 2000, **60**:5832-5838.
16. Kleer CG, van Golen KL, Zhang Y, Wu ZF, Rubin MA, Merajver SD: **Characterization of RhoC expression in benign and malignant breast disease : a potential new marker for small breast carcinomas with metastatic ability.** *Am J Pathol* 2002, **160**:579-584.
17. van Golen KL, Wu ZF, Qiao XT, Bao L, Merajver SD: **RhoC GTPase overexpression modulates induction of angiogenic factors in breast cells.** *Neoplasia* 2000, **2**:418-425.

Correspondence

Sofia D Merajver, 7217 CCGC, 1500 East Medical Center Drive, Ann Arbor, MI 48109-0948, USA. Tel: +1 734 936 6884; fax: +1 734 936 7376; e-mail: smerajve@umich.edu

RESEARCH ARTICLE

Neoplasia • Vol. 6, No. 2, March/April 2004, pp. 179–185 179

www.neoplasia.com

WISP3 (CCN6) Is a Secreted Tumor-Suppressor Protein that Modulates IGF Signaling in Inflammatory Breast Cancer[1]

Celina G. Kleer, Yanhong Zhang*, Quintin Pan† and Sofia D. Merajver†*

Departments of *Pathology and †Internal Medicine, Division of Hematology and Oncology, University of Michigan Medical Center, Ann Arbor, MI, USA

Abstract

Inflammatory breast cancer (IBC) is the most lethal form of locally advanced breast cancer. We have found that WISP3 is lost in 80% of human IBC tumors and that it has growth- and angiogenesis-inhibitory functions in breast cancer *in vitro* and *in vivo*. WISP3 is a cysteine-rich, putatively secreted protein that belongs to the CCN family. It contains a signal peptide at the N-terminus and four highly conserved motifs. Here, for the first time, we investigate the function of WISP3 protein in relationship to its structural features. We found that WISP3 is secreted into the conditioned media and into the lumens of normal breast ducts. Once secreted, WISP3 was able to decrease, directly or through induction of other molecule(s), the IGF-1–induced activation of the IGF-IR, and two of its main downstream signaling molecules, IRS1 and ERK-1/2, in SUM149 IBC cells. Furthermore, WISP3 containing conditioned media decreased the growth rate of SUM149 cells. This work sheds light into the mechanism of WISP3 function by demonstrating that it is secreted and that, once in the extracellular media, it induces a series of molecular events that leads to modulation of IGF-IR signaling pathways and cellular growth in IBC cells.

Neoplasia (2004) **6**, 179–185

Keywords: IGF-binding proteins, MAPK signaling, cell proliferation, cell cycle control, ERK-1/2 phosphorylation.

Introduction

Inflammatory breast cancer (IBC) is the most lethal form of locally advanced breast cancer [1,2]. It is also a very distinct clinical and pathological type of carcinoma. Clinically, patients present with what has been classically termed "peau d'orange," characterized by skin thickening and dimpling, also with nodularity, erythema, and, often, nipple retraction [1–4]. IBC is highly angiogenic and angioinvasive. Clusters of malignant cells invade the dermal lymphatics, forming tumor emboli that likely cause the clinical symptoms, and disseminate to distant sites [1].

In our previous work, we found that WISP3 is lost in 80% of human IBC tumors and is a key genetic determinant of the IBC phenotype [5]. WISP3 has growth-, invasion-, and angiogenesis-inhibitory functions in IBC *in vitro* and *in vivo* [6]. WISP3 is a member of the CCN family of proteins, which also includes connective tissue growth factor (CTGF), Cyr61, Nov, WISP1, and WISP2 [7,8]. A putatively secreted protein with a secretory signal peptide at the NH_2 terminus, WISP3 contains 36 conserved cysteine residues that are organized into four highly conserved modules: 1) a motif associated with insulin-like growth factor binding protein (IGFBP) (GCGCCXXC); 2) a von Willebrand type C–like motif; 3) a thrombospondin 1 module; and 4) a carboxyl-terminal domain putatively involved in dimerization [8,9]. The role of each of these conserved domains in the function of the CCN proteins, in general, and of WISP3, in particular, remains to be elucidated.

IGF-I and its major receptor, IGF-IR, play an important role in normal breast biology and in the development of breast cancer [10–13]. A large body of work implicates the IGF family in breast cancer progression. High concentrations of IGF-I in serum are associated with increased mammographic density (one of the strongest predictors of breast cancer risk), and also reliably predict increased breast cancer risk specifically in premenopausal women [14]. *In vitro*, IGF-I is a strong mitogen for human breast cancer cells and has been found in the epithelial and stromal component of breast cancers [13]. High expression of IGF-IR has been demonstrated in most primary human breast cancers when compared to normal or benign breast tissues, and hyperactivation of IGF-IR in breast cancer has been linked to increased radioresistance and cancer recurrence at the primary site [13,15,16]. High levels of IRS-1, a major signaling molecule downstream of the IGF-IR, correlate with tumor size and shorter disease-free survival in ER^+ breast cancer patients [17,18]. Based on the protein sequence of WISP3 and the important role of IGF signaling in breast cancer, we hypothesized that WISP3 is secreted into the extracellular medium and that the growth-inhibitory effect of

Address all correspondence to: Sofia D. Merajver, MD, PhD, and Celina G. Kleer, MD, Department of Internal Medicine, 7217 CCGC, 1500 East Medical Center Drive, Ann Arbor, MI 48108-0948, USA. E-mail: smerajve@umich.edu

[1]This work was supported, in part, by Army grants DAMD17-02-1-0490 (C.G.K.), DAMD17-02-1-491 (C.G.K.), and DAMD-17-00-1-0345 (S.D.M.); National Institutes of Health grants K08CAO9O876 (C.G.K.), RO1CA77612 (S.D.M.) and 1 P50-CADE97258 (S.D.M.); and a grant from the John and Suzanne Munn Endowed Research Fund of the University of Michigan Comprehensive Cancer Center (C.G.K.).

Received 5 September 2003; Revised 2 December 2003; Accepted 3 December 2003.

DOI 10.1593/neo.03316

WISP3 in IBC may be dependent, at least in part, on modulation of IGF-I signaling. To test this hypothesis, we investigated the downstream effects of WISP3 starting at the IGF-IR receptor and signaling pathway. Here, we demonstrate that WISP3 is a secreted protein and that, once in the conditioned media, it can effectively modulate IGF-IR activation and its signaling cascade and the cellular growth of IBC cells.

Materials and Methods

Cell Culture and Transfections

SUM149 cells derive from a primary IBC that has lost WISP3 expression [6,19]. SUM149 cells and their transfectants were cultured in Ham's F-12 media supplemented with 5% fetal bovine serum (FBS), hydrocortisone (1 μg/ml), insulin (5 μg/ml), fungizone (2.5 μg/ml), gentamycin (5 μg/ml), and penicillin/streptomycin (100 μ/ml each), at 37°C under 10% CO_2. HEK-293 cells derived from human embryonic kidney epithelial cells were grown in Dulbecco's modified Eagle's medium (DMEM) containing 10% FBS. SUM149 and HEK-293 cells were transfected with HIS^- tagged (pcDNA 3.1/V5-HIS TOPO TA expression vector; Invitrogen, Carlsbad, CA) and $Flag^-$ tagged (pFlag-CMV vector; Sigma, St. Louis, MO) full-length WISP3 cDNA, and clonal cell lines were established as described previously [6]. Control cell lines were generated by transfecting the SUM149 and HEK-293 cell lines with the empty vectors. The inserts were confirmed by sequencing. Cells were incubated in serum-free medium. WISP3 and control conditioned media were collected 3 days later. The conditioned media were cleared of cell debris by centrifugation, and concentrated 10-fold through a Centriplus YM-10 column (Millipore, Bedford, MA) before use.

IGF-I Stimulation

Seventy percent confluent SUM149 cells were shifted to serum-free medium. After 24 hours of starvation, the cells were cultured in WISP3 and control conditioned media for 24 hours. Subsequently, SUM149 cells were stimulated with 20 ng/ml human recombinant IGF-I (Upstate Biotechnology Inc., Lake Placid, NY) for 15 minutes.

Immunoprecipitation and Western Blotting

Cells were lysed in lysis buffer composed of 50 mM Tris–HCl (pH 7.4), 150 mM NaCl, 1% NP-40, 0.25% sodium deoxycholate, 1 mM EGTA, 1 mM Na_3VO_4, 1 mM PMSF, and 1 μg/ml aprotinin. The lysates were clarified by centrifugation at 14,000*g* for 10 minutes. A total of 500 μg of cell lysates was incubated with 1 μg/ml anti–IGF-IR mAb (Calbiochem, San Diego, CA) overnight at 4°C. Immune complexes were precipitated by adding 50 μl of protein A/G plus agarose bead slurry for 2 hours. The agarose beads were collected and washed three times with ice-cold lysis buffer, and resuspended in 25 μl of 2 × Laemmli sample buffer for sodium dodecyl sulfate polyacrylamide gel electrophoresis (SDS-PAGE). Fifty micrograms of protein extract was separated by SDS-PAGE and transferred onto a PVDF membrane (Amersham Pharmacia Biotech). The precipitated IGF-IR was detected with anti–IGF-IR β subunit polyclonal Ab (Santa Cruz Biotechnology, Santa Cruz, CA). Tyrosine phosphorylation of immunoprecipitated IGF-IR was assessed with anti–phosphotyrosine mAB PY20 (Transduction Laboratories, Lexington, KY). Total IGF-IR, phosphorylated and total IRS1, and ERK-1/2 were measured with appropriate antibodies (Transduction Laboratories; Upstate Biotechnology Inc.). WISP3 expression was confirmed by Western blot using a polyclonal anti–WISP3 antibody (gift from Dr. Warman) and an antibody against the HIS tag (Invitrogen). The protein bands were visualized using enhanced chemiluminescence (Amersham Pharmacia Biotech, Piscataway, NJ). All experiments were repeated at least three times and the optical density of the bands was quantified by densitometry (Scio Image software for Win 95/98, version 0.4). Statistical analysis was performed using 95% confidence intervals for the estimates of the means. A P value of $< .05$ was considered statistically significant.

Effect of WISP3 in the Proliferation of SUM149 cells

SUM149 cells were plated in 96-well tissue culture plates at a density of 5×10^4 cells/ml in Ham's F-12 media with 5% FBS. One hundred microliters of serum-free medium was added for 24 hours. Ten-fold concentrated WISP3 and control conditioned media were added in the presence and absence of IGF-I simulation as described above. MTT reagents were added 24 hours later according to the manufacturer's protocol (Sigma), and the plate was read at a wavelength of 595 nm. The experiment was performed in triplicate.

Human Breast Tissues and Immunohistochemistry

WISP3 protein expression was studied by immunohistochemistry in normal human breast tissues obtained from 10 reduction mammoplasty procedures. Immunohistochemical analysis was performed by using a polyclonal anti–WISP3 antibody at 1:500 dilution with overnight incubation and microwave antigen retrieval [20]. The detection reaction followed the Dako Envision$^+$ System Peroxidase kit protocol (Dako, Carpinteria, CA). Diaminobenzidine was used as chromogen and hematoxylin was used as counterstain. Positive and negative controls were tumor xenografts derived from cell lines shown to express high levels of WISP3 (SUM149 cell line stably transfected with WISP3) and from a cell line that does not express WISP3 (SUM149 wild type), respectively.

Results

WISP3 Protein Is Secreted by Human Breast Epithelial Cells

WISP3 protein contains a multimodular structure with a secretory signal peptide at the N-terminus. To investigate whether WISP3 is secreted by breast epithelial cells, SUM149 IBC cells previously characterized with a loss in WISP3 expression were stably transfected to express full-length WISP3. Conditioned media from SUM149/WISP3–overexpressing clones were collected and

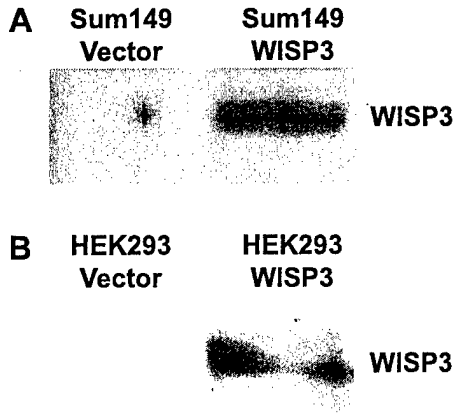

Figure 1. *WISP3 protein is secreted and detected in the conditioned media. (A) Western immunoblot using anti–WISP3 polyclonal antibody detects WISP3 protein in the conditioned media of SUM149 cells transfected with WISP3 full-length cDNA. WISP3 protein is not detected in the conditioned media of SUM149 cells transfected with the empty vector. (B) Western immunoblot of the conditioned media of HEK-293 cells transfected with WISP3, detected using an anti–HIS antibody. WISP3 is not detected in the conditioned media of the control cells.*

detected for WISP3 by Western blot analysis using a polyclonal anti–WISP3 antibody. WISP3 protein was detected in the media of SUM149-expressing WISP3 (SUM149/WISP3), and not in the media of empty vector–transfected SUM149 cells (SUM149/Flag) (Figure 1*A*). In order to explore these results from a different perspective, we performed transient transfections of WISP3 in SUM149 cells using a HIS^- tagged full-length WISP3 expression vector. In this case, WISP3 protein was detected in the conditioned media using both anti–WISP3 antibody and anti–HIS antibody (data not shown). To specifically address whether WISP3 would be detected in the conditioned media of a nonmammary cell, we repeated these experiments with the HEK293 cell line, derived from human embryonic kidney epithelial cells. WISP3 was detected in the conditioned media of these cells and not in the conditioned media of the empty vector controls (Figure 1*B*).

In situ expression of WISP3 protein was determined by immunohistochemical analysis of normal breast tissues derived from reduction mammoplasty procedures. In all 10 tissues examined, WISP3 protein was expressed at low levels in the cytoplasm of normal epithelial cells from ducts and acini and, interestingly, was present in the luminal secretions of ducts and lobules (Figure 2*A*). Xenografts derived from wild-type SUM149 cells ($WISP3^-$) and from SUM149/$WISP3^+$ cells were used as negative and positive controls, respectively (Figure 2, *B* and *C*).

WISP3 Containing Conditioned Media Reduces IGF-I–Induced IGF-IR Activation and Signaling Pathways

The effect of WISP3 on the activation of the IGF-I signaling pathway was studied in SUM149 cells derived from a primary IBC [5,6,19,21]. The activation of the IGF signaling

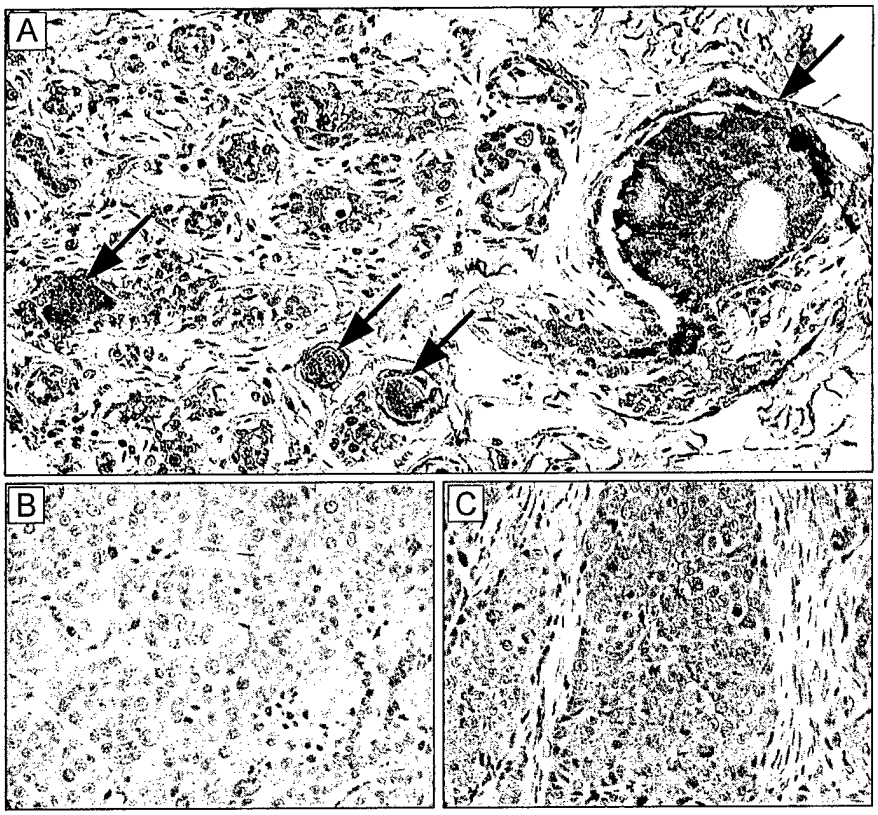

Figure 2. *In situ expression of WISP3 protein in normal breast tissues. (A) Immunohistochemical analysis of normal breast tissues using a polyclonal anti–WISP3 antibody shows that WISP3 protein is expressed at low levels in the cytoplasm of normal epithelial cells and in the luminal secretions of ducts and acini (arrows) (× 200). (B and C) Xenografts derived from wild-type SUM149 and SUM149/WISP3 cells were used as negative and positive controls, respectively (× 400).*

cascade plays a central role in breast cancer development and progression. To investigate whether the presence of WISP3 in the conditioned media has an effect on IGF-IR signaling pathways in IBC cells, phosphorylation of IGF-IR, IRS1, and ERK-1/2 was determined in wild-type SUM149 cells in the presence or absence of WISP3 in the conditioned media. Experiments were carried out under baseline conditions without addition of IGF-I and after stimulation with IGF-I. In the presence of WISP3 in the conditioned media, SUM149 cells exhibited decreased IGF-IR phosphorylation (Figure 3). The effect of WISP3 in the phosphorylation of the IGF-IR was evident in the presence of IGF-I stimulation because WISP3 was able to ameliorate the effect of IGF-I stimulation on the activation of the IGF-IR (Figure 3). Similarly, WISP3 conditioned media decreased the IGF-I–induced IRS1 and ERK-1/2 phosphorylation (Figures 4 and 5).

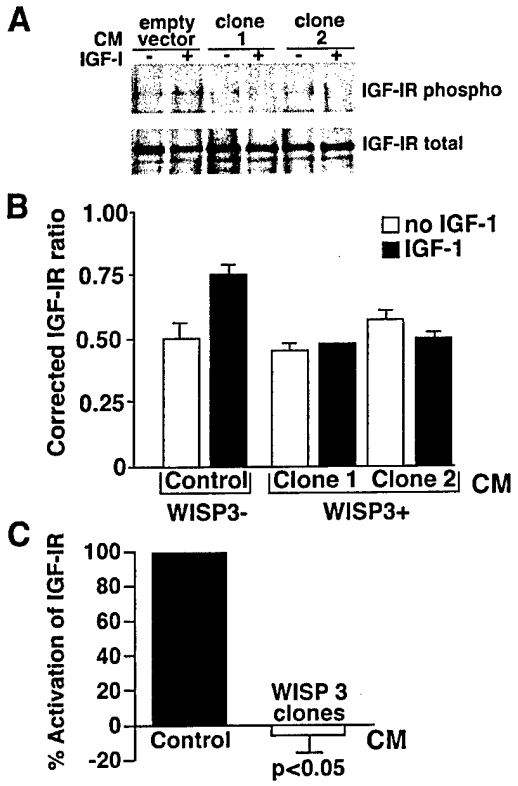

Figure 3. *WISP3 decreases IGF-I–induced phosphorylation of the IGF-IR. (A) Western blot analysis of SUM149 cell lines bathed in WISP3⁺ and control (WISP3⁻) conditioned media. The experiment was carried out under baseline conditions (without IGF-I) and after stimulation with 20 ng/ml IGF-I. The IGF-IR was precipitated from 500 μg of protein lysate with an anti–IGF-IR mAb and subsequently detected by immunoblot with an anti–IGF-IR β subunit polyclonal Ab. Tyrosine phosphorylation of immunoprecipitated IGF-IR was assessed with an anti–phosphotyrosine mAb PY20. (B) Relative protein levels of IGF-IR phosphorylation normalized for total IGF-IR. Blots were scanned and the pixel intensity measured using Scn Image program. Results are expressed as mean ± SEM of three independent experiments. (C) Quantitation of the differences in the percent activation of the IGF-IR. The difference in normalized IGF-IR phosphorylation under baseline conditions and after IGF-I stimulation was calculated for each cell line. Results were corrected using the difference in IGF-IR phosphorylation in the absence of IGF-I stimulation as reference. WISP3 was able to decrease the IGF-I–induced activation of the IGF-IR (t test, P < .05).*

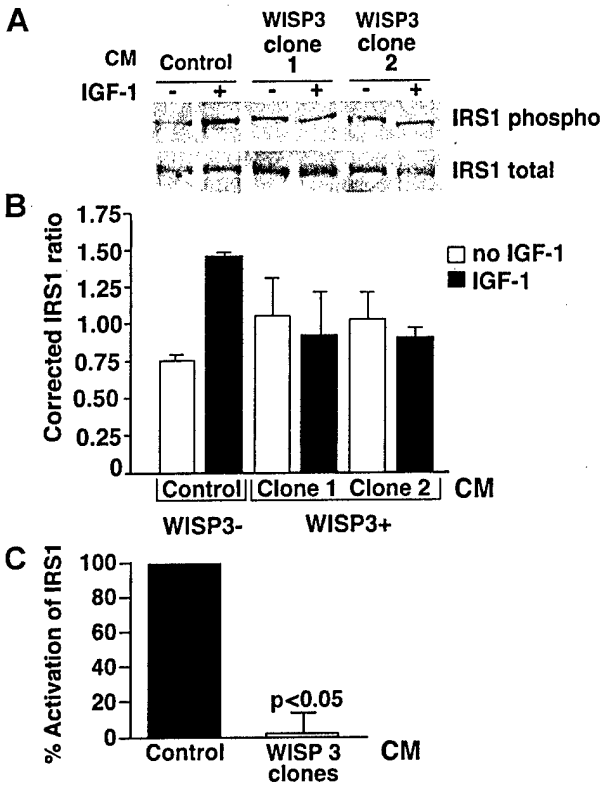

Figure 4. *WISP3 decreases IGF-I–induced phosphorylation of IRS1. (A) Western blot analysis of SUM149 cell lines bathed in WISP3⁺ and control WISP3-conditioned media. The experiment was carried out under baseline conditions (without IGF-I) and after stimulation with IGF-I. The expression of phosphorylated IRS1 was detected by Western blot using a polyclonal antibody against phosphorylated IRS1. The Western blot was stripped and probed with an antibody against total IRS1. (B) Relative protein levels of IRS1 phosphorylation normalized for total IRS1. Blots were scanned and the pixel intensity measured. Results are expressed as mean ± SEM of three independent experiments. (C) The differences in the percent activation of IRS-1 were quantitated. The difference in the corrected IRS1 phosphorylation under baseline conditions and after IGF-I stimulation was calculated for each cell line and results were normalized using the difference in IRS1 phosphorylation in the absence of IGF-I stimulation as reference. WISP3-rich conditioned media was able to decrease the phosphorylation of IRS-1 triggered by IGF-I (t test, P < .05).*

WISP3 Containing Conditioned Media Reduces the Growth of IBC Cell Lines

After establishing that the presence of WISP3 in the conditioned media was able to modulate IGF-I signaling pathways, its effect on cellular proliferation was determined in the presence and absence of IGF-I stimulation. SUM149 cells bathed in the WISP3 conditioned media had significantly lower growth rates than the control SUM149 cells bathed in control (WISP3-deficient) conditioned media, both in the presence and absence of IGF-I stimulation (*t* test, $P < .05$; Figure 6).

Discussion

We have previously demonstrated that WISP3 is lost in 80% of IBC tumors and that it has tumor-suppressor functions in IBC [5,6]. Studies on the SUM149 IBC cell line showed that restoration of WISP3 expression has potent growth- and

angiogenesis-inhibitory functions *in vitro* and *in vivo* [6]. Restoration of WISP3 resulted in a significant decrease in anchorage-independent growth in soft agar and cellular proliferation, as well as a drastic decrease in the invasive capabilities of the SUM149 cells, which are highly invasive in their wild-type state. Furthermore, restoration of WISP3 expression in SUM149 cells resulted in a biologically relevant decrease in the level of angiogenic factors (VEGF, bFGF, and IL-6) in the conditioned media of the cells. *In vivo*, restoration of WISP3 expression in SUM149 cells caused a drastic decrease in tumor volume and rate of tumor growth when injected in nude mice [6]. Taken together, this body of work had strongly supported a tumor-suppressor role for WISP3 in mammary tumor progression. In the present study, we sought to discover the molecular mechanisms underlying the tumor-suppressor function of WISP3.

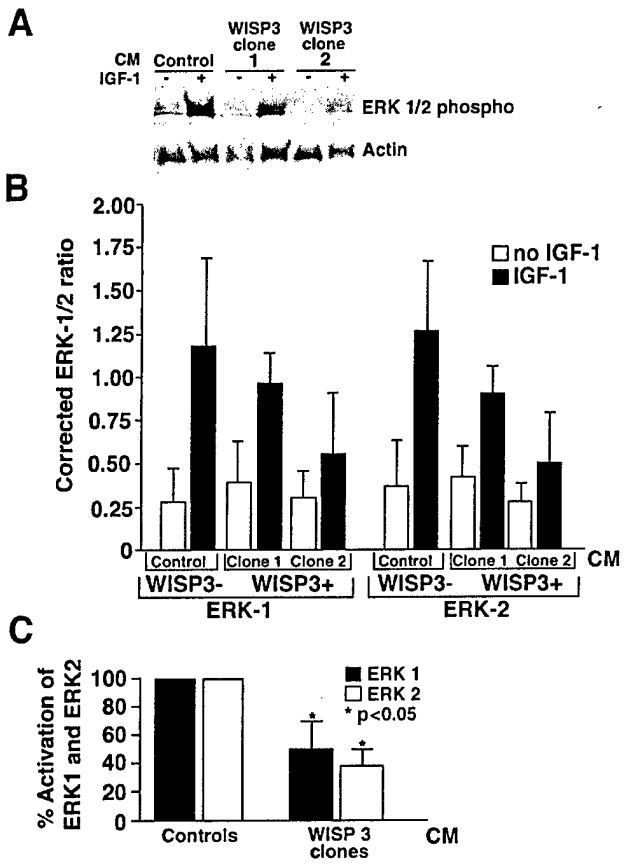

Figure 5. *WISP3 decreases IGF-I–induced phosphorylation of ERK-1/2. (A) Western blot analysis of SUM149 cell lines bathed in WISP3⁺ and control (WISP3⁻) conditioned media, under baseline conditions (without IGF-I) and after stimulation with IGF-I. The expression of ERK-1/2 was detected by Western blot using a polyclonal antibody against phosphorylated ERK-1/2. The blot was stripped and probed with an antibody against β-actin. (B) Relative protein levels of ERK-1/2 phosphorylation normalized using actin. Blots were scanned and the pixel intensity measured. Results are expressed as mean ± SEM of three independent experiments. (C) Quantitation of the differences in the percent activation of ERK-1/2. The difference in the corrected ERK-1/2 phosphorylation under baseline conditions and after IGF-I stimulation was calculated for each cell line. Results were normalized using the difference in ERK-1/2 phosphorylation in the absence of IGF-I stimulation as reference. WISP3-rich conditioned media ameliorated the phosphorylation of ERK 1 and ERK 2 induced by IGF-I stimulation (t test, P < .05).*

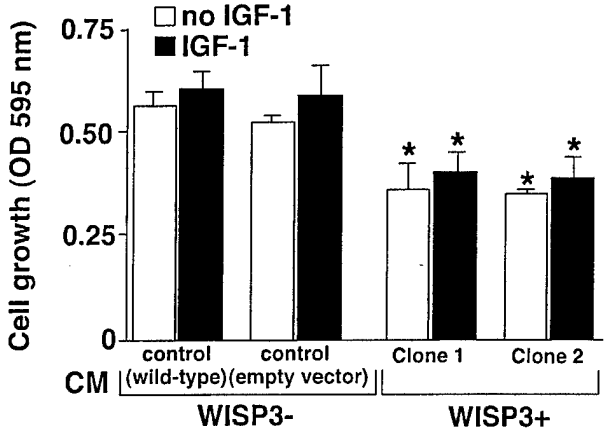

Figure 6. *WISP3 decreases the growth of IBC cells. The growth of SUM149 cells was measured in the absence (WISP3⁻) and presence of WISP3 (WISP3⁺) in the conditioned media under baseline conditions (no IGF-I) and after IGF-I stimulation by an MTT assay. SUM149 cells were grown in 96-well plates at a density of 5 × 10⁴ cells/ml. Serum-starved cells were incubated for 24 hours in the WISP3 and control conditioned media, with or without IGF-I stimulation. Results are expressed as mean ± SEM of three independent experiments. WISP3⁺ conditioned media decreases significantly the growth of SUM149 cells (t test, P < .05 for both clones).*

WISP3 belongs to the CCN family of proteins, which are highly conserved, putatively secreted proteins with important roles in development during chondrogenesis and skeletogenesis [7]. The CCN proteins have been recently also implicated in carcinogenesis [7,22–26]. It is not well understood, however, how the functions of the CCN proteins in development relate to their role in cancer. Moreover, their expression during tumorigenesis cannot be generalized across different tissue types. This may be due to tissue-specific functions of the CCN proteins, perhaps mediated by their multimodular structure and the presence of different affinities for binding partners and ligands in different tissues [7]. The presence of different receptors and differential processing of the CCN proteins (e.g., cleavage by proteases) may account also for their diverse functions in different tissues. In this paper, we focused on determining whether WISP3 is secreted into the conditioned media and its relationship to IGF signaling pathways.

Analysis of the protein sequence of WISP3 revealed that it contains a signal peptide at the N-terminal region that may participate in the secretion of the protein into the extracellular media [7–9]. Indeed, by Western blot, using two different specific antibodies, we were able to detect WISP3 protein in the conditioned media of SUM149 and HEK293 cells transfected with WISP3. Furthermore, consistent with these results, by immunohistochemical analysis, WISP3 protein was detected in the secretions accumulated in the lumens of ducts and lobules in normal breast tissues. The fact that WISP3 is secreted and present in the conditioned media (thereby alluding to its stability in solution) led us to the hypothesis that it may directly or indirectly regulate IGF signaling.

Although the signaling pathways that are required for the effects of IGF-I in breast cancer have not been completely elucidated, the contribution of IGF-I–induced IGF-IR

activation appears to be critical in hormone-dependent and -independent breast cancer [27–30]. IGF-I is locally released by breast cancer cells and stromal fibroblasts, and it is involved in autocrine and paracrine stimulation of the mammary epithelium [31]. In breast cancer cells, when IGF-I binds IGF-IR, signaling occurs mainly through activation of IRS-1 and RAS-dependent phosphorylation of MAP kinase with subsequent activation of nuclear transcription factors [32,33]. IGF-I signaling promotes cell growth, survival, and motility of breast cancer cells, as well as resistance to therapeutic interventions [10–12,14–18]. We hypothesized that expression of WISP3 could result in a series of molecular events that leads to the modulation of IGF-IR activation and downstream signaling. Contributing to this hypothesis is the fact that we have shown that WISP3 is secreted into the media where it has the opportunity to directly or indirectly modulate the strength of IGF signaling. Indeed, in the presence of IGF-I, WISP3 containing conditioned media decreased IGF-IR phosphorylation and the phosphorylation of two main downstream IGF-IR signaling molecules, IRS1 and ERK-1/2. This inhibition was not evident under baseline conditions, without stimulation with IGF-I. Our experiments thus show that even relatively small concentrations of WISP3 secreted by WISP3-transfected cells are able to modulate, directly or indirectly, IGF-I signaling in the setting of IGF-I stimulation.

A major growth-regulatory IGF-IR downstream pathway that regulates breast cancer growth and survival converges on ERK-1/2 cascade [34]. We observed a decrease in ERK-1/2 phosphorylation by addition of WISP3 containing conditioned media in the presence of IGF-I stimulation. ERK-1/2 influence chromatin remodeling and activation of gene expression, leading to enhanced cellular proliferation and decreased apoptosis [35–37]. Specifically, ERK-1/2 have been shown to activate the transcription of key genes involved in cell cycle progression including cyclin D1 and cyclin E. We have shown previously that restoration of WISP3 expression in the highly malignant SUM149 IBC cell line markedly decreased the levels of cyclin E and PCNA, a reliable marker of cellular proliferation [6].

The mechanism whereby WISP3 may modulate IGF-IR activation in the presence of IGF-I remains to be elucidated. WISP3 contains a highly conserved motif (GCGCCXXC) characteristic of IGFBPs, which may provide the proper protein folding to interact with IGF-like ligands, thereby enabling interference with IGF signaling. Although initial studies reported that two other CCN proteins, CTGF (CTGF) and Nov, specifically bind to IGF-I [38,39], these results have not been subsequently built on and they remain to be duplicated by other investigators. Whether WISP3 physically binds to IGF-I warrants further investigation, in light of out data.

Another mechanism that may explain the modulation of IGF-IR phosphorylation by WISP3-containing conditioned media is the formation of a WISP3/IGF-I complex that may bind to the IGF-IR and occupy IGF binding sites, but the complex may be either inhibitory or may be only a weak agonist of the receptor. In another system [40], this hypothesis is supported by recent data showing that IGF-I can still freely bind to the receptor even when complexed to a truncated N-terminal fragment of IGF-binding protein 5 (mini-IGFBP5); interestingly, the N-terminal portion of IGFBP5 has high homology to the N-terminal portion of WISP3. Mini-IGFBP5 binding to IGF-I resulted in incomplete inhibition of receptor binding [40]. In a similar manner, a WISP3/IGF-I complex might still bind to the IGF-IR but exert only a weak agonist effect, effectively resulting in physiologic antagonism of IGF-I action under conditions of high IGF-I stimulation. WISP3-rich conditioned media was able to significantly decrease the proliferation rate of IBC cells. The fact that this effect was seen both in the presence and absence of IGF-I simulation suggests that, in addition to interfering with IGF-I signaling pathways, WISP3 may have IGF-independent functions in IBC. In sum, we show that WISP3 is a secreted protein that modulates IGF-I signaling pathways, leading to a decrease in the growth of IBC cells.

Acknowledgements

We thank Robin Kunkel and Elizabeth Horn for artwork; S. Ethier for the SUM149 and HME cell lines; Wendy Kutz and Matthew Warman from Case Western Reserve University for providing anti–WISP3 antibody; and Michelle LeBlanc and the Immunohistochemistry Core of the University of Michigan Cancer Center for tissue processing and immunohistochemistry.

References

[1] Lee BJ (1924). Inflammatory carcinoma of the breast: a report of twenty-eight cases from the breast clinic of Memorial Hospital. *Surg Gynecol Obstet* **39,** 580–595.

[2] Jaiyesimi IA, Buzdar AU, and Hortobagyi G (1992). Inflammatory breast cancer: a review. *J Clin Oncol* **10,** 1014–1024.

[3] Merajver SD, Weber BL, Cody R, Zhang D, Strawderman M, Calzone KA, LeClaire V, Levin A, Irani J, Helvie M, August D, Wicha M, Lichter A, and Pierce LJ (1997). Breast conservation and prolonged chemotherapy for locally advanced breast cancer: the University of Michigan experience. *J Clin Oncol* **15,** 2873–2881.

[4] Swain SM, Sorace RA, Bagley CS, Danforth Jr, DN, Bader J, Wesley MN, Steinberg SM, and Lippman ME (1987). Neoadjuvant chemotherapy in the combined modality approach of locally advanced nonmetastatic breast cancer. *Cancer Res* **47,** 3889–3894.

[5] van Golen KL, Davies S, Wu ZF, Wang Y, Bucana CD, Root H, Chandrasekharappa S, Strawderman M, Ethier SP, and Merajver SD (1999). A novel putative low-affinity insulin-like growth factor–binding protein, LIBC (lost in inflammatory breast cancer), and RhoC GTPase correlate with the inflammatory breast cancer phenotype. *Clin Cancer Res* **5,** 2511–2519.

[6] Kleer CG, Zhang Y, Pan Q, van Golen KL, Wu ZF, Livant D, and Merajver SD (2002). *WISP3* is a novel tumor suppressor gene of inflammatory breast cancer. *Oncogene* **21,** 3172–3180.

[7] Perbal B (2001). *NOV* (nephroblastoma overexpressed) and the *CCN* family of genes: structural and functional issues. *Mol Pathol* **54,** 57–79.

[8] Pennica D, Swanson TA, Welsh JW, Roy MA, Lawrence DA, Lee J, Brush J, Taneyhill LA, Deuel B, Lew M, Watanabe C, Cohen RL, Melhem MF, Finley GG, Quirke P, Goddard AD, Hillan KJ, Gurney AL, Botstein D, and Levine AJ (1998). *WISP* genes are members of the connective tissue growth factor family that are up-regulated in wnt-1–transformed cells and aberrantly expressed in human colon tumors. *Proc Natl Acad Sci USA* **95,** 14717–14722.

[9] Hurvitz JR, Suwairi WM, Van Hul W, El-Shanti H, Superti-Furga A, Roudier J, Holderbaum D, Pauli RM, Herd JK, Van Hul EV, Rezai-Delui

H, Legius E, Le Merrer M, Al-Alami J, Bahabri SA, and Warman ML (1999). Mutations in the *CCN* gene family member *WISP3* cause progressive pseudorheumatoid dysplasia. *Nat Genet* **23,** 94–98.

[10] Bartucci M, Morelli C, Mauro L, Ando S, and Surmacz E (2001). Differential insulin-like growth factor I receptor signaling and function in estrogen receptor (ER)–positive MCF-7 and ER-negative MDA-MB-231 breast cancer cells. *Cancer Res* **61,** 6747–6754.

[11] Furstenberger G, and Senn HJ (2002). Insulin-like growth factors and cancer. *Lancet Oncol* **3,** 298–302.

[12] Kleinberg DL, Feldman M, and Ruan W (2000). IGF-I: an essential factor in terminal end bud formation and ductal morphogenesis. *J Mammary Gland Biol Neoplasia* **5,** 7–17.

[13] Surmacz E (2000). Function of the IGF-I receptor in breast cancer. *J Mammary Gland Biol Neoplasia* **5,** 95–105.

[14] Byrne C, Colditz GA, Willett WC, Speizer FE, Pollak M, and Hankinson SE (2000). Plasma insulin–like growth factor (IGF) I, IGF-binding protein 3, and mammographic density. *Cancer Res* **60,** 3744–3748.

[15] Turner BC, Haffty BG, Narayanan L, Yuan J, Havre PA, Gumbs AA, Kaplan L, Burgaud JL, Carter D, Baserga R, and Glazer PM (1997). Insulin-like growth factor-I receptor overexpression mediates cellular radioresistance and local breast cancer recurrence after lumpectomy and radiation. *Cancer Res* **57,** 3079–3083.

[16] Resnik JL, Reichart DB, Huey K, Webster NJ, and Seely BL (1998). Elevated insulin-like growth factor I receptor autophosphorylation and kinase activity in human breast cancer. *Cancer Res* **58,** 1159–1164.

[17] Rocha RL, Hilsenbeck SG, Jackson JG, VanDenBerg CL, Weng C, Lee AV, and Yee D (1997). Insulin-like growth factor binding protein-3 and insulin receptor substrate-1 in breast cancer: correlation with clinical parameters and disease-free survival. *Clin Cancer Res* **3,** 103–109.

[18] Lee AV, Jackson JG, Gooch JL, Hilsenbeck SG, Coronado-Heinsohn E, Osborne CK, and Yee D (1999). Enhancement of insulin-like growth factor signaling in human breast cancer: estrogen regulation of insulin receptor substrate-1 expression *in vitro* and *in vivo. Mol Endocrinol* **13,** 787–796.

[19] Ethier SP, Mahacek ML, Gullick WJ, Frank TS, and Weber BL (1993). Differential isolation of normal luminal mammary epithelial cells and breast cancer cells from primary and metastatic sites using selective media. *Cancer Res* **53,** 627–635.

[20] Shi SR, Key ME, and Kalra KL (1991). Antigen retrieval in formalin-fixed, paraffin-embedded tissues: an enhancement method for immunohistochemical staining based on microwave oven heating of tissue sections. *J Histochem Cytochem* **39,** 741–748.

[21] van Golen KL, Wu ZF, Qiao XT, Bao LW, and Merajver SD (2000). RhoC GTPase, a novel transforming oncogene for human mammary epithelial cells that partially recapitulates the inflammatory breast cancer phenotype. *Cancer Res* **60,** 5832–5838.

[22] Soon LL, Yie TA, Shvarts A, Levine AJ, Su F, and Tchou-Wong KM (2003). Overexpression of WISP-1 down-regulated motility and invasion of lung cancer cells through inhibition of Rac activation. *J Biol Chem* **278,** 11465–11470.

[23] Vilmos P, Gaudenz K, Hegedus Z, and Marsh JL (2001). The Twisted gastrulation family of proteins, together with the IGFBP and CCN families, comprise the TIC superfamily of cysteine rich secreted factors. *Mol Pathol* **54,** 317–323.

[24] Kireeva ML, Mo FE, Yang GP, and Lau LF (1996). Cyr61, a product of a growth factor–inducible immediate-early gene, promotes cell proliferation, migration, and adhesion. *Mol Cell Biol* **16,** 1326–1334.

[25] Tong X, Xie D, O'Kelly J, Miller CW, Muller-Tidow C, and Koeffler HP (2001). Cyr61, a member of CCN family, is a tumor suppressor in non-small cell lung cancer. *J Biol Chem* **276,** 47709–47714.

[26] Xie D, Nakachi K, Wang H, Elashoff R, and Koeffler HP (2001). Elevated levels of connective tissue growth factor, WISP-1, and CYR61 in primary breast cancers associated with more advanced features. *Cancer Res* **61,** 8917–8923.

[27] Godden J, Leake R, and Kerr DJ (1992). The response of breast cancer cells to steroid and peptide growth factors. *Anticancer Res* **12,** 1683–1688.

[28] Jackson JG, White MF, and Yee D (1998). Insulin receptor substrate-1 is the predominant signaling molecule activated by insulin-like growth factor-I, insulin, and interleukin-4 in estrogen receptor–positive human breast cancer cells. *J Biol Chem* **273,** 9994–10003.

[29] Jackson JG, and Yee D (1999). IRS-1 expression and activation are not sufficient to activate downstream pathways and enable IGF-I growth response in estrogen receptor negative breast cancer cells. *Growth Horm IGF Res* **9,** 280–289.

[30] Peyrat JP, Bonneterre J, Dusanter-Fourt I, Leroy-Martin B, Djiane J, and Demaille A (1989). Characterization of insulin-like growth factor 1 receptors (IGF1-R) in human breast cancer cell lines. *Bull Cancer* **76,** 311–319.

[31] Satyamoorthy K, Li G, Vaidya B, Patel D, and Herlyn M (2001). Insulin-like growth factor-1 induces survival and growth of biologically early melanoma cells through both the mitogen-activated protein kinase and beta-catenin pathways. *Cancer Res* **61,** 7318–7324.

[32] Resnicoff M, and Baserga R (1998). The role of the insulin-like growth factor I receptor in transformation and apoptosis. *Ann NY Acad Sci* **842,** 76–81.

[33] Baserga R (1999). The IGF-I receptor in cancer research. *Exp Cell Res* **253,** 1–6.

[34] Santen RJ, Song RX, McPherson R, Kumar R, Adam L, Jeng MH, and Yue W (2002). The role of mitogen-activated protein (MAP) kinase in breast cancer. *J Steroid Biochem Mol Biol* **80,** 239–256.

[35] Murphy LO, Smith S, Chen RH, Fingar DC, and Blenis J (2002). Molecular interpretation of ERK signal duration by immediate early gene products. *Nat Cell Biol* **4,** 556–564.

[36] Volmat V, Camps M, Arkinstall S, Pouyssegur J, and Lenormand P (2001). The nucleus, a site for signal termination by sequestration and inactivation of p42/p44 MAP kinases. *J Cell Sci* **114,** 3433–3443.

[37] Volmat V, and Pouyssegur J (2001). Spatiotemporal regulation of the p42/p44 MAPK pathway. *Biol Cell* **93,** 71–79.

[38] Kim HS, Nagalla SR, Oh Y, Wilson E, Roberts CT Jr, and Rosenfeld RG (1997). Identification of a family of low-affinity insulin-like growth factor binding proteins (IGFBPs): characterization of connective tissue growth factor as a member of the IGFBP superfamily. *Proc Natl Acad Sci USA* **94,** 12981–12986.

[39] Burren CP, Wilson EM, Hwa V, Oh Y, and Rosenfeld RG (1999). Binding properties and distribution of insulin-like growth factor binding protein–related protein 3 (IGFBP-rP3/NovH), an additional member of the IGFBP superfamily. *J Clin Endocrinol Metab* **84,** 1096–1103.

[40] Zeslawski W, Beisel HG, Kamionka M, Kalus W, Engh RA, Huber R, Lang K, and Holak TA (2001). The interaction of insulin-like growth factor-I with the N-terminal domain of IGFBP-5. *EMBO J* **20,** 3638–3644.